

Analyzing the molecular mechanism of Bucky ball localization during germ cell specification in zebrafish

Doctoral Thesis

Dissertation for the award of the degree

“Doctor rerum naturalium (Dr. rer. nat)”

in the GGNB program: “Genes and Development”

at the Georg August University Göttingen

Faculty of Biology

submitted by

Stephan Riemer

born in Kirchheim unter Teck, Germany

Göttingen, October 2014

Members of the Thesis Committee:

Supervisor:

Dr. Roland Dosch (Reviewer)

Department of Developmental Biochemistry, Georg August University Göttingen

Second member of the thesis committee:

Prof. Dr. Gregor Bucher (Reviewer)

Department of Developmental Biology, Georg August University Göttingen

Third member of the thesis committee:

PD Dr. Halyna Shcherbata

Gene expression and signaling, Max Planck Institute for Biophysical Chemistry, Göttingen

Date of the oral examination:

Affidavit

Herewith, I declare that I prepared the PhD thesis “Analyzing the molecular mechanism of Bucky ball localization during germ cell specification in zebrafish” on my own and with no other sources and aids than quoted.

Göttingen, 15.10.2014

Stephan Riemer

Table of Contents

Acknowledgements	8
List of Abbreviations	9
Abstract	12
1 Introduction	13
1.1 Mechanisms of germ cell specification	14
1.2 Germ plasm and its role in germ cell specification	15
1.2.1 Germ plasm localizes to the Balbiani body during early oogenesis	15
1.2.2 Germ plasm localization during early embryogenesis	16
1.2.3 Characteristics of primordial germ cells	18
1.3 Germline development in zebrafish	19
1.3.1 Germ plasm localization during oogenesis	19
1.3.2 Germ plasm localization during early embryogenesis	20
1.4 Molecular composition of germ plasm	22
1.4.1 RNA helicase Vasa is required for germ cell development	22
1.4.2 RNA-binding protein Nanos is essential for primordial germ cell maintenance.....	24
1.4.3 RNA-binding protein Dazl is involved in translational regulation in primordial germ cells	25
1.5 Molecular mechanism of germ plasm localization in zebrafish	26
1.5.1 Germ plasm localization mechanisms in oocytes	26
1.5.2 Germ plasm localization mechanisms in embryos.....	26
1.6 Bucky ball in zebrafish germ cell specification	28
1.6.1 Bucky ball is necessary and sufficient for germ plasm formation.....	29
1.6.2 A <i>buc-gfp</i> transgene rescues the mutant phenotype.....	30
1.6.3 Oskar organizes germ plasm formation in <i>Drosophila</i>	30
1.6.4 Similarities and differences between Buc and Osk.....	31
1.7 Aims	32
2 Materials and Methods	33
2.1 Zebrafish handling and maintenance	33
2.1.1 DNA extraction from zebrafish fins.....	33
2.1.2 Genotyping based on short tandem repeats.....	33
2.1.3 KASP genotyping.....	34
2.2 Manipulation of zebrafish embryos	34
2.2.1 Microinjection	34
2.2.2 Dechoriation	34
2.2.3 Deyolking	34

2.2.4	Preparation of embryo lysates	34
2.3	<i>Drosophila</i> handling and manipulation.....	35
2.3.1	Breeding and crossing	35
2.3.2	Microinjections.....	35
2.3.3	Germline transformation	35
2.3.4	Cuticle preparation	36
2.4	Chemicals	36
2.5	Plasmid vectors and constructs.....	36
2.5.1	Plasmid Vectors.....	36
2.5.2	Cloned vector and expression constructs	36
2.6	Molecular biology methods	40
2.6.1	PCR	40
2.6.2	Agarose gel electrophoresis	42
2.6.3	Purification of DNA	43
2.6.4	Restriction enzyme cloning.....	43
2.6.5	Gateway cloning.....	43
2.6.6	Chemical transformation	44
2.6.7	Plasmid DNA preparation	44
2.6.8	DNA sequencing analysis	44
2.6.9	cDNA synthesis.....	46
2.6.10	<i>In vitro</i> transcription.....	46
2.7	Biochemical methods	46
2.7.1	Generation of Buc antibody	46
2.7.2	SDS-polyacrylamide gel electrophoresis	47
2.7.3	Coomassie staining.....	47
2.7.4	Western blotting	47
2.7.5	Co-Immunoprecipitation	48
2.7.6	Fixation of zebrafish oocytes	48
2.7.7	Fixation of zebrafish embryos.....	48
2.7.8	Immunostaining of zebrafish embryos and oocytes.....	48
2.8	Cell biology methods	49
2.8.1	Live-Cell Imaging	49
2.9	Bioinformatics methods	49
2.9.1	Pairwise sequence alignment	49
2.9.2	Multiple sequence alignments.....	50
2.9.3	Hidden Markov models analysis	50
2.9.4	Protein sequence analysis.....	50
2.9.5	Analysis mass spectrometry data	50
2.10	Statistical methods	50

3 Results.....	51
3.1 Buc is a permanent germ plasm component.....	51
3.1.1 Buc is continuously localized to the germ plasm during oogenesis.....	51
3.1.2 Buc is localized to the germ plasm during early embryogenesis	54
3.1.3 Buc is a germ plasm component in primordial germ cells.....	57
3.2 BucLoc is essential for Buc localization	59
3.2.1 Cross-species approach indicates distinct localization mechanisms of Buc and Osk	59
3.2.2 Proline-rich localization domain BucLoc is essential for Buc localization	63
3.3 BucLoc interacts with non-muscle myosin II	68
3.3.1 Identification of the BucLoc interactome.....	68
3.3.2 Endogenous Exosc9 co-localizes with Buc in oocytes	73
3.3.3 Endogenous p-Myl12.2 co-localizes continuously with Buc.....	74
4 Discussion.....	78
4.1 Localization of endogenous Buc to the germ plasm and its functional relevance.	78
4.1.1 Buc is localizes to the germ plasm during germ plasm aggregation and localization in oogenesis	78
4.1.2 Buc is a stable germ plasm component during germ cell specification in early embryogenesis	79
4.1.3 Buc localizes to germinal granules in primordial germ cells	81
4.2 Transgenic Buc-GFP marks the germ plasm <i>in vivo</i>	82
4.3 Buc and Osk have distinct localization mechanisms.....	84
4.4 Identification of BucLoc and other conserved domains in Buc protein.....	85
4.4.1 BucLoc identified as the first protein germ plasm localization domain	85
4.4.2 Additional protein domains in Buc	86
4.5 Analysis of the BucLoc interactome	87
4.5.1 Identification of BucLoc interacting proteins by Co-IP and mass spectrometry analysis	87
4.5.2 Further promising proteins among the 213 BucLoc interaction candidates.....	88
4.6 Exosome complex newly identified in germ plasm	89
4.7 Potential role of non-muscle myosin II in germ plasm localization.....	90
4.7.1 Buc co-localizes with p-Myl12.2 throughout oogenesis and early embryogenesis	90
4.7.2 Mechanistic trailer truck model of Buc localization and function during germ cell specification.....	91
5 Conclusion.....	94
6 Bibliography	95
List of Figures	107

List of Tables.....	109
7 Appendix	110
7.1 Hidden Markov model analysis of Buc and Osk.....	110
7.2 Further proteins of the BucLoc interactome	111
7.3 213 BucLoc interaction candidates.....	112
7.4 Digital appendix	120
Curriculum Vitae	121

Acknowledgements

First of all, I thank my supervisor Dr. Roland Dosch for giving me the opportunity to work on this interesting project. I am grateful for his support, his guidance and advice during the last years.

I thank the members of my thesis committee, Prof. Dr. Gregor Bucher and Dr. Halyna Shcherbata for ideas and helpful discussions.

Furthermore, I thank Prof. Dr. Tomas Pieler for supporting my work in his department and Prof. Dr. Jörg Großhans for giving me the opportunity to do the fly work in his laboratory. In this respect, I am grateful to the members of his group for help and support. Special thanks go to Dr. Philip Laupsien and Dr. Hung-wei Sung for their time and their support.

Moreover, I thank Dr. Thomas Lingner for the fruitful collaboration and the help with bioinformatics.

I am grateful to my colleagues in the zebrafish group Gudrun Kracht, Palsamy Kanagaraj, Pritesh Krishnakumar for helpful discussions and a great, encouraging working atmosphere.

I am likewise thankful to all colleagues at the Department of Developmental Biochemistry for their help and for creating a friendly atmosphere.

I also thank the GGNB for financial support and the GGNB team for their help.

Special thanks go to my parents, my sister and my brother for their lifelong encouragement and support.

Finally, I thank Vanessa Eckert for her love, her support and her patience.

List of Abbreviations

°C	Degrees Celsius
A	Adenine
aa	Amino acids
amol	Attomolar
bp	Base pairs
BSA	Bovine serum albumin
C	Cytosine
<i>C. elegans</i>	<i>Caenorhabditis elegans</i>
cDNA	Complementary DNA
CMV	Cytomegalovirus
Co-IP	Co-immunoprecipitation
C-terminus	Carboxy-terminus
DAPI	4',6-diamidino-2-phenylindole
<i>DAZ</i>	Deleted in azoospermia
dH ₂ O	Distilled water
Dm	<i>Drosophila melanogaster</i>
DNA	Deoxyribonucleic acid
dNTP	Deoxynucleotide triphosphate
dpf	Days post fertilization
<i>E. coli</i>	<i>Escherichia coli</i>
<i>e.g.</i>	<i>Exempli gratia</i>
EDTA	Ethylenediaminetetraacetic acid
eGFP	Enhanced green fluorescent protein
EGTA	Ethylene glycol tetraacetic acid
<i>et al.</i>	<i>Et alii</i>
FMA	Furrow microtubule array
fw	Forward
g	Gram
G	Guanine
GFP	Green fluorescent protein
h	Hour
HMM	Hidden Markov models

HMM	Hidden Markov models
hpf	Hours post fertilization
IP	Immunoprecipitation
kb	Kilo base pairs
kDa	Kilodalton
LB	Lysogeny broth
M	Molar
MEMFA	MOPS-EGTA-MgSO ₄ -formaldehyde buffer
mg	Milligram
min	Minute
miRNA	Micro RNA
ml	Millilitre
mM	Millimolar
MPI-BPC	Max Planck Institute for Biophysical Chemistry
mRNA	Messenger RNA
n	Number
ng	Nanogram
nl	Nanolitre
NMII	Non-muscle myosin II
p-NMII	Phospho-myosin light chain II
N-terminus	Amino-terminus
ORF	Open reading frame
PAGE	Polyacrylamide gel electrophoresis
PBS	Phosphate-buffered saline
PBT	Phosphate-buffered saline Triton X-100
PCR	Polymerase chain reaction
pg	Picogram
PGC	Primordial germ cell
pH	<i>Potassium hydrogenium</i>
piRNA	Piwi-interacting RNA
p-NMII	Phosphorylated non-muscle myosin II
RNA	Ribonucleic acid
RNase	Ribonuclease
rpm	Rounds per minute
RRM	RNA recognition motif
RT-qPCR	Reverse transcription quantitative real-time PCR

rv	Reverse
s	Second
SDS	Sodium dodecyl sulfate
SH3	SRC Homology 3
T	Thymine
TAE	Tris-Acetate-EDTA
Taq	<i>Thermus aquaticus</i>
TBE	Tris-Borate-EDTA
Tris	Tris(hydroxymethyl)aminomethane
U	Units
UAS	Upstream activation sequence
UMG	University Medical Center Göttingen
UTR	Untranslated region
UV	Ultraviolet
V	Volt
Zf	Zebrafish
µg	Microgram
µl	Microlitre
µm	Micrometer
µM	Micromolar

Abstract

Sexual reproducing animals depend on the proper establishment of the germline to ensure the survival of the species by generating fertile progeny. Therefore, many vertebrate and invertebrate species specify their germline already during embryogenesis by inheritance of maternal factors aggregated in the germ plasm. Only cells that inherit germ plasm during early embryogenesis are determined to become germ cells, whereas all other cells are liberated to pursue somatic fates and will form the body that transfers the germ cells to the next generation. Hence, proper localization of germ plasm is essential for germ cell specification. Recently, zebrafish Bucky ball has been identified as the first protein in vertebrates to be necessary for germ plasm aggregation and sufficient for specification of primordial germ cells. However, Buc protein localization and the underlying localization mechanism, essential for proper spatial germ plasm aggregation, were not known.

In this study, Buc localization was analyzed by immunostaining with a newly generated antibody and by live-cell imaging of a transgenic *buc-gfp* line. Furthermore, Buc localization was analyzed in comparison to the germ plasm regulator *Drosophila* Osk and the domain responsible for Buc localization was mapped in a systematic deletion approach. Additionally, proteins, interacting with the Buc localization domain, were identified via Co-IP followed by mass spectrometry analysis and were verified by *in vivo* co-localization analysis. This study shows that Buc protein continuously localizes to the germ plasm throughout zebrafish oogenesis and embryogenesis on the endogenous level as well as in the transgenic *buc-gfp* line. This specific localization pattern depends on the conserved N-terminal amino acids 11-88. Moreover, the localization domain BucLoc interacts with non-muscle myosin II and persistently co-localizes with the non-muscle myosin II regulatory chain Myl12.2.

With the localization of Buc, permanent protein localization to the germ plasm was described for the first time in zebrafish. This indicates that germ plasm aggregating function of Buc is required throughout the process of germ cell specification and beyond. Furthermore, BucLoc is the first protein localization domain being necessary and sufficient for localization to the germ plasm in a metazoan. Thus, BucLoc provides the first protein based reporter for germ plasm as well as primordial germ cells. In addition, the interaction and co-localization of Buc with non-muscle myosin II links Buc to the actin cytoskeleton. This would be in line with a previously suggested mechanism, stating that germ plasm granules associated with actin filaments are recruited to the germ plasm. Hence, functional investigations of the interaction between Buc and non-muscle myosin II can give insight into the localization of germ plasm to the presumptive primordial germ cells during early embryogenesis in zebrafish. Further insight into this mechanism will help to better understand the process of germ cell formation and might lead to the identification of new drug targets and therapies against infertility.

1 Introduction

Reproduction is the biological process of producing independent homogeneous offspring. Every species' survival is ensured by reproduction, thus making it the most important process in the lifetime of a living organism.

During biological evolution, two different types of reproduction were established: asexual and sexual reproduction. In asexual reproduction, offspring arises from a single organism. Hence, genes solely of one parent are transmitted to the next generation, making it genetically identical to its parent. This asexual reproduction is the main form of reproduction in single-cell organisms such as archaeobacteria, eubacteria and protists. Furthermore, many plants and fungi use this cost-efficient mechanism of reproduction since no energy has to be spent on meiosis, syngamy and the formation of male organisms (Crow, 1994).

In sexual reproduction, a female and a male gamete fuse, thereby giving rise to offspring, which is a genetic combination of the female and the male parent. This is the main form of reproduction in almost all animals and plants and has advantages when it comes to the incorporation of favorable mutations, the adaption to environmental changes and the elimination of harmful mutations (Crow, 1994). However, these advantages are acquired with a high effort and energy cost of meiosis, syngamy and the formation of male organisms. In addition, sexual reproduction in highly developed eukaryotes has a high cost from a developmental point of view. In the developmental context, sexual reproduction comprises that, at one point, cells designated for the single purpose of reproduction have to be specified, formed and separated from other cells of the body. As this process of germline development is essential for the survival of any species, the cells that will give rise to gametes are often set aside already during early embryonic development in 'higher' animals, such as bilateria. During further embryonic development, these specified cells will differentiate into primordial germ cells, migrate to the gonad region and establish the germline. The whole germline development, beginning with germ cell specification and ending with the establishment of the germline in the gonads, has to be tightly regulated and controlled to ensure the development of a fertile adult organism.

Despite the crucial importance of germ cell specification, little is known about this first critical step of germ cell development in the early embryo. Gaining insight into the mechanism of specifying a definite population of cells to pursue a specific fate will help to better understand numerous other cell specification processes during development of multicellular organisms. Furthermore, a better understanding of the process of germ cell formation will help to identify causes for infertility and might lead the way to the identification of new drug targets for future therapy.

1.1 Mechanisms of germ cell specification

In the process of germ cell specification, certain cells of the early embryo are designated to ensure proper development of the germline. These primordial germ cells carry the genetic information from one generation to the next and thus ensure the survival of the species. Germ cell specification takes place in all 'higher' animals, while the mode, by which the germ cells are specified, is not conserved. Two different modes of germ cell specification have been described.

On the one hand, there is induction of the germ cell fate through external signals from surrounding somatic cells. This mode of germ cell specification is supposed to be the more ancestral and prevalent one among metazoans and has been identified in vertebrates including mammals, reptiles and urodeles (Extavour and Akam, 2003). This mechanism was suggested for the first time in axolotl embryos as their primordial germ cells did not contain germ plasm, which is necessary for primordial germ cell formation in other organisms (Ikenishi and Nieuwkoop, 1978). The inductive mechanism is studied best in mice, in which primordial germ cells are induced in the proximal epiblast by BMP4 that signals from the extraembryonic ectoderm (Lawson et al., 1999). BMP4 triggers the expression of BLIMP1, a key regulator of primordial germ cell specification (Ohinata et al., 2005). Hence, BLIMP1 inhibits the expression of somatic genes and promoting the progression towards the germ cell fate (Hayashi et al., 2007).

On the other hand, germ cells are specified cell-autonomously by the inheritance of cytoplasmic determinants. This mode of germ cell specification is described amongst others in dipteran insects (*e.g. Drosophila*), nematodes (*e.g. C. elegans*) anuran amphibians (*e.g. Xenopus*) and zebrafish (Extavour and Akam, 2003). The theory of determinants specifying the germline, and thus setting it apart from the somatic cells, was already established at the end of the 19th century (Weismann, 1893). Weismann also stated for the first time that inheritance depends specifically on germ cells, whereas the somatic cells are not involved in heredity (1893). In contrast to Weismann, who thought the determinants are nuclear, Boveri found in vertebrates that these determinants are cytoplasmic (1910). This cytoplasmic germ plasm was visualized for the first time at the vegetal cortex of frog eggs (Bounoure, 1934). Functional experiments in frogs showed the importance of germ plasm in primordial germ cell formation. Physical removal or irradiation with ultraviolet (UV) light of vegetal cytoplasm in eggs resulted a reduction in the number of primordial germ cells or in sterile embryos (Buehr and Blackler, 1970; Smith, 1966). In corresponding gain-of-function experiments, fertility was restored by injection of vegetal cytoplasm in the vegetal pole of UV light-irradiated embryos (Smith, 1966; Wakahara, 1977). Hence, the vegetal cytoplasm, containing germ plasm in anuran amphibians, is necessary for the formation of primordial germ cells. Correspondingly, mechanical removal of germ plasm results in a severe reduction of primordial germ cells in zebrafish (Hashimoto et al., 2004). In *Drosophila*, germ plasm is sufficient for the formation of functional primordial germ cells, when ectopically localized (Illmensee and Mahowald, 1974). Recently, it was reported that transplantation of germ plasm to the animal pole of *Xenopus* embryos resulted in formation of ectopic primordial germ cells (Tada et al., 2012). Thus, similar to insects, vertebrate germ plasm is a direct germ cell determinant and is sufficient for germ cell determination.

The intriguing question why two different germ cell specification mechanisms evolved is still

in discussion. Despite induction being supposedly the more ancestral mode of germ cell specification, specification by inheritance of germ plasm is not restricted to any taxa. This indicates that germ plasm has convergently evolved (Johnson et al., 2011). Comparison of both germ cell specification mechanisms reveals that in species specifying their germ cells by inheritance of germ plasm, genes evolve more rapidly, leading to enhanced speciation (Evans et al., 2014). This finding supports the hypothesis that the evolution of germ plasm liberates restrictions on the development of somatic gene regulatory networks, since germ cell specification becomes independent of signals from somatic tissue (Johnson et al., 2011). Thus, germ cell specification by inheritance of germ plasm is a general and important process to study in vertebrates.

1.2 Germ plasm and its role in germ cell specification

Like many other processes in early development of ‘higher’ animals, germ cell specification by inheritance of germ plasm is controlled by maternal factors (Pelegri, 2003). Hence, germ plasm formation already begins in oogenesis until it starts exerting its effects during early embryogenesis.

1.2.1 Germ plasm localizes to the Balbiani body during early oogenesis

Germ plasm is formed by maternally provided molecules and is localized in the early oocyte within a distinct cytoplasmic structure named Balbiani body, also known as mitochondrial cloud in *Xenopus* (Cox and Spradling, 2003; Heasman et al., 1984). The macroscopic structure of the Balbiani body was first identified in spiders and is present in almost all animal oocytes of invertebrates (*e.g.* spiders, insects and mollusks) and vertebrates (*e.g.* frogs, birds, teleosts and mammals) (Guraya, 1979; Kloc et al., 2004; von Wittich, 1845). Even in mammals, such as mice or humans, which are supposed to specify germ cells by inductive mechanisms, a Balbiani body is present in the early oocyte (Albamonte et al., 2013; Pepling et al., 2007). The Balbiani body is composed of electron-dense granular/fibrous material, mitochondria, golgi, endoplasmic reticulum and various RNAs and proteins (Heasman et al., 1984). Studies in *Xenopus* and *Drosophila* suggest that one function of the Balbiani body is to accumulate a subset of mitochondria, which are designated to be delivered to the germ plasm and ultimately to the primordial germ cells (Cox and Spradling, 2003; Kloc et al., 2004; Marinos and Billett, 1981). In *Xenopus* these mitochondria accumulate together with other germ plasm components in the perinuclear region forming the Balbiani body (Figure 1). During late stages of *Xenopus* oogenesis, the Balbiani body disaggregates into islands that move towards and are anchored at the vegetal cortex (Kloc et al., 2004). This localization of the Balbiani body to the vegetal cortex is the so-called early, microtubule independent pathway of germ plasm localization. A second, late pathway in *Xenopus* is microtubule-dependent and localizes another population of RNAs to the vegetal cortex (King et al., 1999). Therefore, the maternally provided germ plasm components already aggregate in the oocyte, before the germ plasm localizes to a specific subset of cells during embryogenesis.

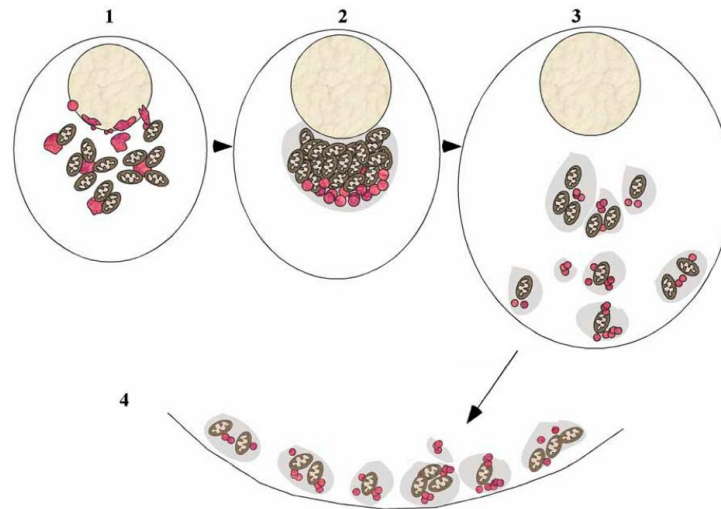


Figure 1: Formation of the Balbiani body and distribution along the vegetal cortex during *Xenopus* oogenesis. (1) Mitochondria (brown organelles) and other components of the Balbiani body (pink) start to aggregate in the perinuclear region at prestage I and early stage I oocytes. (2) The Balbiani body forms in the perinuclear region at stage I oocytes with germ plasm components concentrated at the vegetal apex of the Balbiani body (germinal vesicles, pink). (3) The Balbiani body disassembles into islands that move to the vegetal cortex between stages II and IV of oogenesis. (4) The germ plasm islands anchor at the vegetal cortex of stage IV-VI oocytes. Figure modified from Kloc et al. (2004).

1.2.2 Germ plasm localization during early embryogenesis

The formation of a Balbiani body in the oocyte and the recruitment of germ plasm components is a common pattern in various animals. At the same time, the localization of germ plasm in embryos is adapted to the individual developmental master plan of the respective animal.

In *Drosophila*, germ plasm, also known as pole plasm, is localized to the posterior pole during late oogenesis. Since *Drosophila* embryos develop as a syncytium, germ plasm is taken up into the future primordial germ cells, also known as pole cells, that bud off as the first cells at the posterior pole (Figure 2a). At this point, primordial germ cells stop dividing and are committed to germ cell fate after cellularization. They are then passively transported into the embryo by germ band extension movements. From there, the primordial germ cells migrate into the body cavity to form the embryonic gonads together with somatic precursors (Santos and Lehmann, 2004).

In early embryogenesis of *C. elegans*, cytoplasmic germ granules, also called P-granules, are asymmetrically distributed to one daughter cell during the first four cell cleavages (Figure 2b). The asymmetric division is achieved by displacement of the spindle towards one side of the cell, to which the germ granules accumulate. This process results in the separation of the sole founder cell of the germline (P_4) from other somatic cells (Strome, 2005). At 88-cell stage, P_4 divides once symmetrically into the primordial germ cells Z2 and Z3. These do not divide further and are subsequently moved inside the embryo through gastrulation in order to join somatic gonadal precursor cells (Wang and Seydoux, 2013).

In *Xenopus*, the germ plasm is localized at the vegetal pole of the embryo (Figure 2c). It is segregated to the first four blastomeres during the formation of the first two cleavage planes. At this stage, the germ plasm aggregates move towards the cleavage furrows and are

asymmetrically distributed during subsequent cell cleavages, leading to a constant number of germ plasm-containing cells. Later on, the germ plasm moves to the perinuclear region and the cluster of primordial germ cells is brought inside the embryo through gastrulation. (Whittington and Dixon, 1975). From there, the primordial germ cells migrate dorsally within the endoderm to finally reach the genital ridges (Wylie and Heasman, 1976).

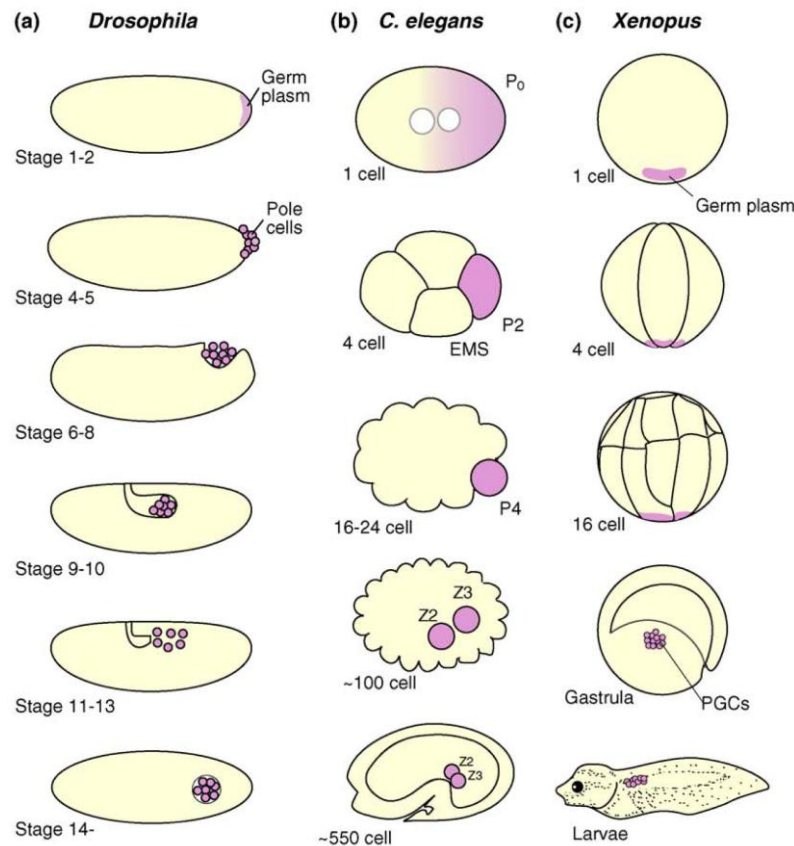


Figure 2: Early germ cell development in *Drosophila*, *C. elegans* and *Xenopus*. Schematic representation of different embryonic stages showing the localization of the germ plasm or the primordial germ cells (pink) in the model organisms *Drosophila* (a), *C. elegans* (b) *Xenopus* (c). (a) In *Drosophila* embryos, germ plasm aggregates during late oogenesis, localizes to the posterior pole where it is incorporated into the forming primordial germ cells. Subsequently, the primordial germ cells are carried to the interior of the embryo during gastrulation. They start migrating across the midgut epithelium, entering the body cavity to form embryonic gonads together with somatic gonadal precursors. (b) In *C. elegans*, the initially uniformly distributed germ plasm is redistributed towards the posterior pole upon fertilization and asymmetrically distributed during the first four cell cleavages. This results in the single germline founder blastomere P4, which gives rise to two primordial germ cells (Z2, Z3) at about 100-cell stage by symmetric division. Later on, they move inside the embryo to join somatic precursors of the gonad. (c) *Xenopus* germ plasm is located at the vegetal pole of the egg and segregates there unequally between the blastomeres during cleavage stage. Cells inheriting the germ plasm are specified to become primordial germ cells, remain in the endoderm during gastrulation and form a cluster of cells. Finally, they migrate through the endoderm in the tailbud stage and reach the genital ridges in the larvae. Figure modified from Nakamura et al. (2010).

The germ plasm localization of zebrafish will be outlined separately (Chapter 1.3).

Although the localization of the germ plasm in these organisms differs due to the implementation into the individual developmental formats, the general process of germ cell specification through inheritance of germ plasm is conserved among these animals. Furthermore, the resulting primordial germ cells share similar characteristics, for which germ plasm or germ granules are frequently accounted responsible.

1.2.3 Characteristics of primordial germ cells

Inheritance of germ plasm specifies the hosting cells to follow a germ cell fate. Some characteristic features are necessary to maintain this fate and are shared by all primordial germ cells throughout the animal kingdom.

One characteristic of primordial germ cells is the presence of unique cytoplasmic organelles referred to as germ granules. These germ granules are a common characteristic of metazoans, even in species that specify their germ cells by induction (Kloc et al., 2004; Toyooka et al., 2000). They were identified in close proximity to the nucleus in *Drosophila*, *C. elegans*, *Xenopus* and zebrafish (Ikenishi et al., 1996; Knaut et al., 2000; Mahowald, 1971; Strome and Wood, 1983). Germ granules have even been identified in close association with nuclear pores and are attributed to be involved in posttranscriptional control of gene expression (Knaut et al., 2000; Strome and Lehmann, 2007; Updike et al., 2011). Some components of the germ granules, such as Vasa and its homologs, are conserved. Others, such as Osk in *Drosophila* and Pgl-1 in *C. elegans*, are species specific. In zebrafish, these granules are present in the perinuclear region of primordial germ cells at 6 hours post fertilization (hpf). At that stage, the granules show a broad variation in size. Microtubules, the motor protein dynein, as well as Tdrd7 are involved in the change of granule morphology towards a more homogeneous population at 24 hpf (Strasser et al., 2008).

Another common property of early primordial germ cells is that they are transcriptionally silenced. Most likely, this is to repress the transcription of somatic determinants and thus to prevent the primordial germ cells from differentiating unintentionally into somatic cells. On the one hand transcriptional silencing is achieved by repression of the transcriptional machinery in the germline, e.g. by Pie-1 in *C. elegans*, by Pgc, Nanos and Pumilio in *Drosophila* or by Blimp1 in mouse (Seydoux and Braun, 2006). On the other hand there is also chromatin-based transcriptional repression, which is regulated by Nanos in *C. elegans* and Nanos and Pgc in *Drosophila* (Strome and Lehmann, 2007). Both processes temporally regulate the transcription of zygotic genes in the germline (Nakamura 2010). Hence, germ plasm components contribute to the retention of the full developmental potential of primordial germ cells.

An additional hallmark feature of primordial germ cells is translational repression. One mechanism to repress the translation of mRNA is to target it for degradation via decapping of the mRNA. This process seems to be relevant in *C. elegans* as well as *Drosophila*, since proteins involved in decapping, co-localize with germ granules (Seydoux and Braun, 2006). Moreover, mRNA is translationally silenced by inhibition of cap-dependent translation initiation. In this mechanism, regulatory proteins interact with RNA-binding proteins that specifically recognize structural elements in the targeted mRNAs. *Drosophila* *osk* mRNA translation is repressed cap-dependently by interaction with Bruno and Cup (Kugler and Lasko, 2009). In addition, other conserved proteins, such as Nanos, have been shown in various organisms to be involved in translational repression, which makes it a common mechanism in primordial germ cells (Lai and King, 2013).

The above mentioned characteristics of primordial germ cells ensure the proper development of the germline. To develop these characteristics, primordial germ cells depend on specific germ plasm components. Hence, the most important mechanism to ensure proper

development of the germline is the proper aggregation and localization of all germ plasm components.

1.3 Germline development in zebrafish

Among the model organisms, most functional data in germline development is available from invertebrates such as *Drosophila* and *C. elegans*. In the vertebrate model organism *Xenopus*, germ plasm research is focused on processes during oogenesis. In mouse, germline development is analyzed intensively in regard to effects on chromatin. However, among vertebrates that specify their germ cells through inheritance of germ plasm, most functional data on germline development is available in zebrafish. Furthermore, zebrafish offers advantages for early developmental studies. Embryos and oocytes are easily accessible and available in high numbers. Moreover, the transparent embryos enable tracing of fluorescently-tagged proteins *in vivo* and allow detection of endogenous proteins by immunostaining. As the genome is completely sequenced, genomic manipulations are possible and mutants can be identified by sequencing. Therefore, the vertebrate model organism zebrafish is very well suited for the analysis of germ cell development.

1.3.1 Germ plasm localization during oogenesis

At the beginning of zebrafish oogenesis, stage IA oocytes (7-20 μm) form interconnected nests (Figure 3) (Marlow and Mullins, 2008; Selman et al., 1993). The transparent stage IB oocytes are surrounded by a single layer of follicle cells and increase in size from 20 to 140 μm . At this stage, germ plasm components, such as *vasa*, *nanos* and *dazl* mRNA, aggregate to form the Balbiani body (Figure 3) (Kosaka et al., 2007). The axis formed by the germinal vesicle and the Balbiani body defines the animal-vegetal polarity in the oocyte and thereby, the first asymmetry in the oocyte is established. In addition, the oocyte goes into meiotic arrest at this stage (Selman et al., 1993).

The accumulation of cortical alveoli of variable size and form leads to loss of transparency in stage II oocytes (140-340 μm). Additionally, the acellular membrane surrounding the oocyte, called chorion, becomes more prominent and the Balbiani body starts to disassemble at the vegetal pole with germ plasm components localizing to the cortex (Figure 3) (Kosaka et al., 2007; Selman et al., 1993).

Stage III (340-690 μm) is the major growth stage as oocytes start taking up yolk proteins and crystalline yolk bodies accumulate within the oocyte. With the formation of the micropylar cell at the animal pole, the first morphological asymmetry becomes apparent (Selman et al., 1993). At this stage, the germ plasm components *vasa* and *nanos* mRNA spread along the cortex (Figure 3) (Kosaka et al., 2007). In stage IV oocytes (690-730 μm), yolk bodies become non-crystalline during oocyte maturation and yolk proteins are proteolytically cleaved, which results in increased transparency of the oocyte. Furthermore, the nuclear envelope breaks down, the first meiotic division occurs and the oocyte arrests in the second meiotic metaphase (Selman et al., 1993). The mature eggs (approx. 750 μm) are finally ovulated into the ovarian lumen in stage V and the micropylar cell forms the micropyle canal, by which sperm can cross the chorion. Thus, the egg is competent of fertilization (Figure 3) (Selman et al., 1993).

Upon fertilization, the egg is activated and the chorion elevates to prevent the embryo from mechanical damage. In 1-cell embryos, cytoplasm from the yolk compartment streams towards the animal pole and forms the blastodisc (Figure 3). Through this cytoplasmic streaming, germ plasm mRNAs become redistributed to the animal pole and enrich at the cytokinetic ring (Howley and Ho, 2000; Pelegri, 2003). Thus, the germ plasm shows a very specific, yet dynamic localization during zebrafish oogenesis.

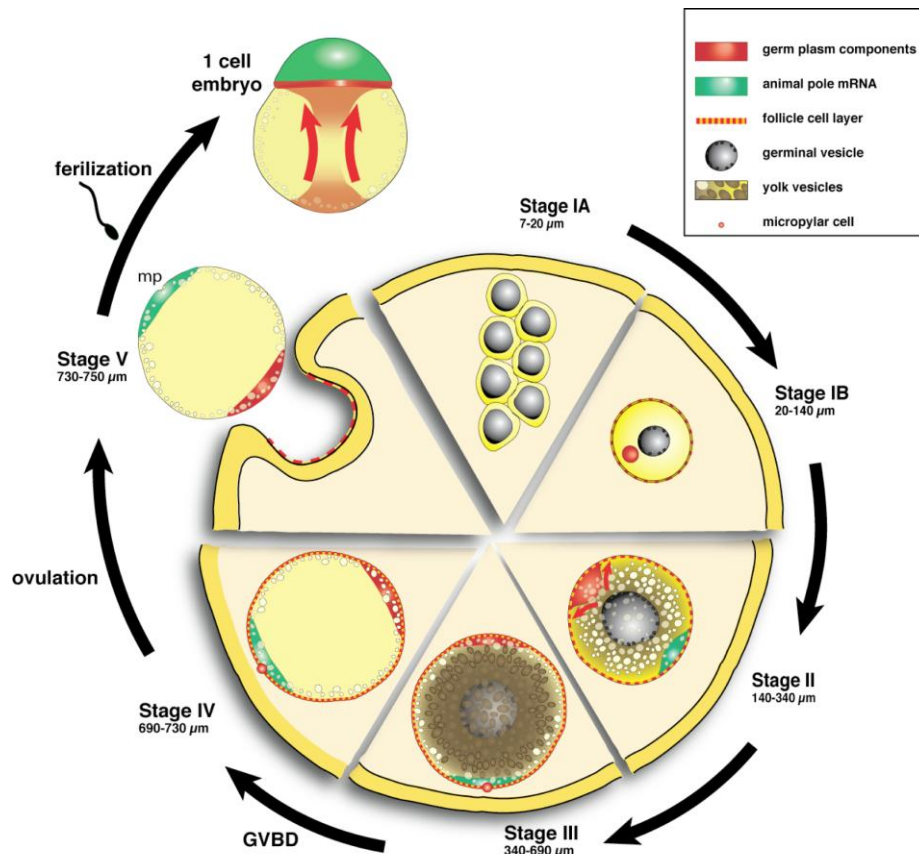


Figure 3: Schematic representation of germ plasm localization during zebrafish oogenesis. Different oocyte stages with the localized germ plasm (red) are depicted in a circular order. In each stage the vegetal pole is facing the center of the scheme. Note that transitions to the next stage are fluent and that in the zebrafish ovary, oocytes of different stages are intermingled. Schematic oocytes are not drawn to scale. Oocyte diameters are indicated. Figure modified from Bontems (2009).

1.3.2 Germ plasm localization during early embryogenesis

The localization of germ plasm was mainly described by detailed analysis of the germ plasm component *vasa* mRNA during zebrafish embryogenesis (Knaut et al., 2000; Yoon et al., 1997).

Germ plasm localization starts in the developing embryo after the fertilization of the egg. Upon fertilization, cytoplasm streams from the yolk to the animal pole and forms the blastodisc, which represents the first embryonic cell. Germ plasm components localize to the cytokinetic ring at the base of the forming blastodisc at this early stage (Figure 4A).

The subsequent cleavage period is characterized by DNA synthesis in all cells and little if any RNA transcription. The cell cycle is abbreviated and consists of rapid synchronous cell divisions that are driven by an internal oscillation interval of 15 min. The cell cleavages are

meroblastic with the diving embryo placed on top of the non-cleaving yolk cell (Kane and Kimmel, 1993). 45 minutes post fertilization, the cleavage period starts with the first cell division and germ plasm aggregates at both distal ends of the forming cleavage furrow (Figure 4B, C). The second cleavage furrow forms perpendicularly to the first and germ plasm localizes to the distal ends of the cleavage furrow for a second time, which results in four germ plasm aggregates at the 4-cell stage (1 hpf) (Figure 4D). At 8-cell stage and subsequent cleavages no additional stable aggregates form at the cleavage furrows (Figure 4E). However, the initial four aggregates remain stable and are asymmetrically inherited by only one daughter cell (Figure 4F). This keeps the number of germ plasm-containing cells constant to four cells that are distributed opposite of each other in 1k-cell stage (3 hpf) (Figure 4G). The asymmetric distribution of the germ plasm ensures proper development of primordial germ cells and at the same time liberates other blastomeres to pursue their somatic fate.

Asymmetric germ plasm distribution overlaps with blastula stage starting 2.25 hpf at 128-cell stage (Kimmel et al., 1995). At sphere stage (4 hpf), germ plasm spreads out in the cytoplasm and is symmetrically distributed to both daughter cells, now called primordial germ cells (Figure 4H). This leads to four independent clusters of primordial germ cells. The symmetric distribution of germ plasm coincides with the midblastula transition, which starts at the 512-cell stage, corresponding to cell cycle 10 (2.75 hpf), and ends at late cell cycle 13 (4 hpf) (Kane and Kimmel, 1993). In this phase, transcription of the zygotic genome starts, the embryo is cleared of maternal mRNAs by miRNA mediated decay and cells divide asynchronously (Giraldez et al., 2006; Kane et al., 1992). Additionally, three different lineages segregate: the yolk syncytial layer, the outer enveloping monolayered epithelial layer and the deep cells, forming both ectodermal as well as mesodermal germ layers (Kane et al., 1992). Subsequent to the formation of cell lineages, morphogenetic movements start during gastrulation (5-10 hpf) (Kimmel et al., 1995). In early gastrulation (6 hpf), primordial germ cell clusters start migrating dorsally towards the shield, which is the zebrafish Spemann organizer (Figure 4I, J). In addition, the intracellular germ plasm localization changes to the perinuclear region in primordial germ cells (Braat et al., 2000; Strasser et al., 2008).

In the following segmentation period (10-24 hpf), somites form, primary organs and the tail develop, and the embryo elongates (Kimmel et al., 1995). The primordial germ cells continue migrating towards the dorsal side of the embryo, forming two cell clusters left and right of the notochord at the level of the third somite (11 hpf) (Figure 4L). Until prim-5 stage (24 hpf), primordial germ cell clusters migrate towards the posterior and localize along the anterior part of the yolk extension before forming the future gonad together with somatic precursor cells, (Figure 4M). At this stage, 25-50 primordial germ cells populate the future gonad (Braat et al., 1999; Raz, 2003).

After 24 hpf, the embryo has formed all important organs and matures within the next two days into a larva, ready to hatch (Kimmel 1995). Post hatching, the larvae develops further to the juvenile stage (30 dpf) until the adult fish becomes fertile at 90 dpf. During this development, the primordial germ cells will differentiate into sperm or oocytes and thus specify the sex of the fish. The fertile fish then mate and give rise to the next generation, thus starting a new cycle of germ cell development.

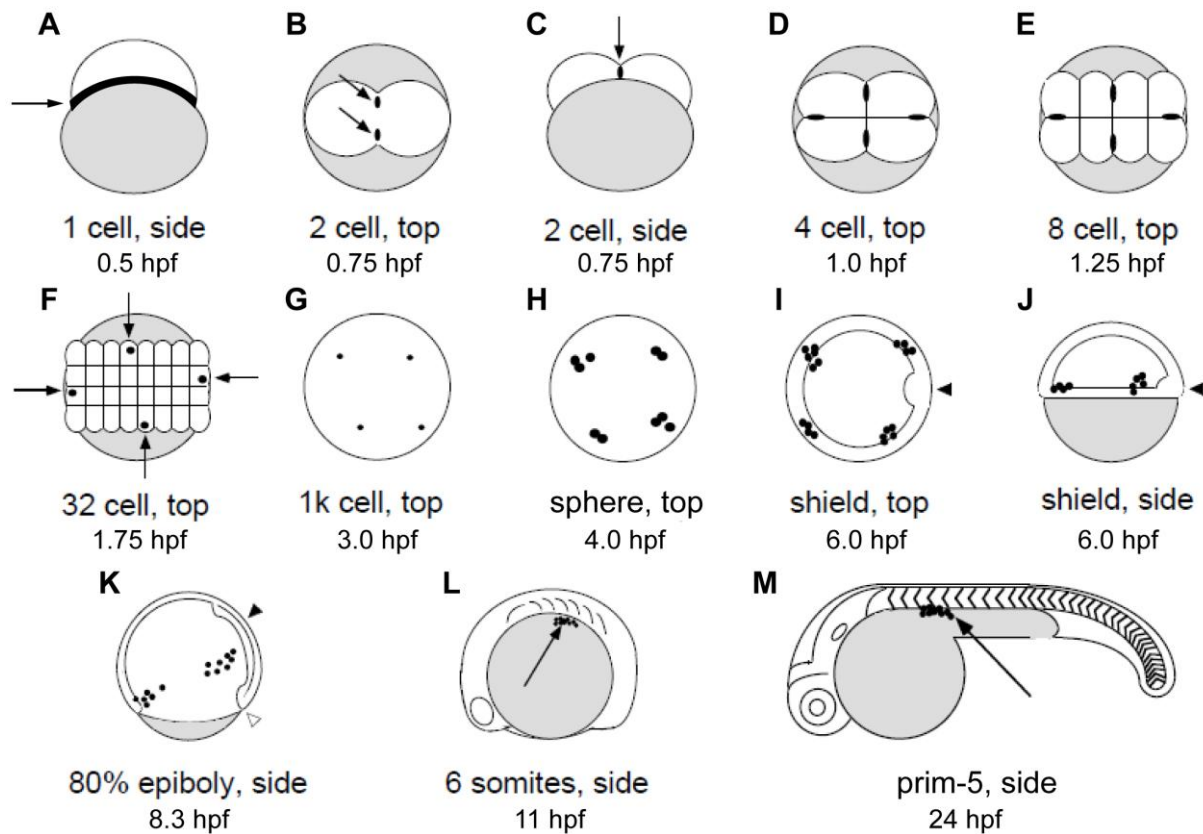


Figure 4: Schematic representation of germ plasm localization during zebrafish embryogenesis. Drawings represent different embryonic stages from 1-cell (A) until prim-5 stage (M) with the localized germ plasm (black) and indicated with black arrows. The yolk is shaded; orientation is indicated for each stage. The black arrowhead marks the Spemann organizer in shield stage. In the 80% epiboly embryo, the white arrowhead indicates the germ ring whereas the black arrowhead indicates the developing notochord. Embryos are not drawn to scale. Figure modified from Yoon et al. (1997).

1.4 Molecular composition of germ plasm

The localization of germ plasm in various organisms, including zebrafish, has been well described. However, the molecular composition of germ plasm and the molecular mechanism of germ cell specification have been barely characterized.

Germ plasm is a complex of numerous proteins, mRNAs and other types of small RNAs. For example, proteins as well as RNA molecules belonging to the piwi-interacting-RNA (piRNA) pathway, are present in the germ granules of gonads. piRNAs are thought to be involved in the silencing of transposable elements and therefore might promote genomic stability during gametogenesis (Cinalli et al., 2008). Loss of the germ plasm component Ziwi, involved in the piRNA pathway, leads to loss of germ cells (Houwing et al., 2007). Thus, the accurate composition of the germ plasm is crucial to its function.

Conserved maternally provided germ plasm components have been characterized and their localization was analyzed during early zebrafish embryogenesis. A selection of the most prominent ones will be described in the following.

1.4.1 RNA helicase Vasa is required for germ cell development

Vasa was first identified in *Drosophila* in a genetic screen for maternal-effect mutations that affect anterior-posterior polarity (Schupbach and Wieschaus, 1986). The embryos from

mutant mothers failed to localize germ plasm and therefore did not form germ cells (Lehmann and Nusslein-Volhard, 1991). *Vasa* encodes an RNA helicase of the DEAD box family (Hay et al., 1988). The protein is expressed throughout *Drosophila* life cycle specifically in the germline and is localized to the germ plasm at the posterior pole already in oocytes (Lasko and Ashburner, 1990). In contrast, the RNA is uniformly distributed in the cytoplasm of the oocyte and the early embryo (Hay et al., 1988). In *Drosophila*, *Vasa* protein co-localizes with the germ plasm organizer Oskar in oocytes as well as embryos and *in vitro* data suggest a direct interaction between Oskar and *Vasa* (Breitwieser et al., 1996). In *C. elegans*, the *Vasa* homologs *Glh-1* and *Glh-2* is likewise localized to the germline throughout their life cycle and associates with germ granules (Gruidl et al., 1996). Homologs of the highly conserved *vasa* gene have been identified in several invertebrates and vertebrates, such as mouse, chicken, human, frog and zebrafish. Loss of *Vasa* activity affects differentiation of germ cells and leads to loss of fertility in *Drosophila*, *C. elegans* and mouse, thus indicating a conserved *Vasa* function in germ cell development (Kuznicki et al., 2000; Styhler et al., 1998; Tanaka et al., 2000). Interestingly, the RNA helicase *Vasa* was recently identified to serve as a platform for the amplification of piRNA and hence plays a role in transposon silencing in germ cells (Xiol et al., 2014).

With the identification of *vasa* in zebrafish, the germline could be traced for the first time and the localization of the germ plasm could be analyzed (Knaut et al., 2000; Olsen et al., 1997; Weidinger et al., 1999; Yoon et al., 1997). In oogenesis, *vasa* mRNA localizes to the germ plasm in the Balbiani body, moves to the vegetal cortex in small granules and becomes localized to the cortical regions from late stage II onwards (Braat et al., 1999; Howley and Ho, 2000; Kosaka et al., 2007). With egg activation, maternally provided transcripts localize in granules to the cytokinetic ring at the base of the blastodisc in 1-cell stage zygotes and associate with the first and second cleavage furrow (Figure 4) (Braat et al., 1999; Yoon et al., 1997). A detailed analysis via electron microscopy revealed that *vasa* mRNA co-localizes with the germ plasm in the cleavage furrow at 4-cell stage and in the primordial germ cells at 1k-cell stage (Knaut et al., 2000). Additionally, localization to the third cleavage furrow was observed in embryos and *vasa* mRNA granules are detected at the cortical periphery (Wolke et al., 2002; Yoon et al., 1997). Nonetheless, these smaller aggregates and granules are not maintained and are most likely removed through degradation processes (Wolke et al., 2002). Interestingly, 180 nucleotides in a conserved region of the *vasa* 3' untranslated region (3'UTR) are sufficient for its proper localization in zebrafish embryos and also in *Xenopus* oocytes (Knaut et al., 2002). This indicates that a conserved machinery targets the mRNA to the germline by a signal in the *vasa* 3'UTR. From the four spots at the first two cleavage furrows, *vasa* mRNA is asymmetrically distributed to only one of the two daughter cells (Yoon et al., 1997). Thus, the number of *vasa* positive cells is kept constant to four cells until 1k-cell stage (Figure 4). At sphere stage, the *vasa* mRNA localization shifts to the cytoplasm and both daughter cells inherit *vasa* transcripts. By this, the population of *vasa* positive cells increases from 4 to 12 cells in 4k-cell stage reaching a total number of 25-50, which will eventually populate the gonad (Braat et al., 1999). Until early somitogenesis, *vasa* mRNA localizes to two cell clusters left and right of the notochord. At 24 hpf, these clusters are located along the anterior part of the yolk extension (Figure 4) (Weidinger et al., 1999; Yoon et al., 1997).

Less information is available about Vasa protein localization. The protein is detected in close proximity to the germinal vesicle in early oocytes, while this localization is lost after breakdown of the germinal vesicle between stage III and IV (Knaut et al., 2000). In the embryo, Vasa protein was detected in the perinuclear region of the primordial germ cells beginning at 6 hpf, although Vasa expression analysis indicated the presence of the protein throughout early embryogenesis (Braat et al., 2000; Knaut et al., 2000). Vasa protein is still present in the primordial germ cells and tightly associated with the nuclear envelope at 30 hpf (Knaut et al., 2000). The functional analysis of Vasa by morpholino knockdown did not show a phenotype (Braat et al., 2001). Hence, the role of Vasa in zebrafish germ cell formation is still unclear. Nevertheless, *vasa* mRNA marks germ plasm as well as primordial germ cells during early embryogenesis and Vasa protein serves as a useful marker of primordial germ cells.

1.4.2 RNA-binding protein Nanos is essential for primordial germ cell maintenance

Nanos encodes an RNA-binding protein containing a zinc finger domain, which is highly conserved among metazoans (Curtis et al., 1995; Mosquera et al., 1993). In *Drosophila*, Nanos protein has been shown to be involved in translational repression in early embryonic patterning (Gavis and Lehmann, 1994). In primordial germ cells lacking Nanos activity, germ cell genes are expressed prematurely, which leads to migration defects and loss of functional germ cells (Kobayashi et al., 1996). Furthermore, in *Drosophila*, *C. elegans* and mice *nanos* genes are directly or indirectly required for survival, migration, cell cycle arrest and chromatin remodeling of primordial germ cells (Nakamura and Seydoux, 2008). In zebrafish the *nanos* homolog *nanos3*, previously named *nanos1*, was shown to be essential for proper migration and survival of primordial germ cells by knockdown using morpholino antisense nucleotides (morpholinos) (Kopranner et al., 2001). This result could be confirmed in a *nanos3* mutant, in which primordial germ cells are specified, but are not maintained during further development (Draper et al., 2007). Analogous to observations in *Drosophila*, where *nanos* is essential for maintenance of germline stem cells in the adult animal, zebrafish *nanos3* is required for the maintenance of oocyte production and preservation of presumptive germline stem cells in adult females (Beer and Draper, 2013; Draper et al., 2007; Gilboa and Lehmann, 2004).

Maternally provided *nanos3* mRNA is localized similarly to *vasa* transcripts, thus confirming *nanos3* mRNA to be a component of the germ plasm (Kopranner et al., 2001; Kosaka et al., 2007). Similar to *vasa* mRNA, the signal for the specific localization of *nanos3* mRNA is present in its 3'UTR. The *nanos3* 3'UTR is sufficient to protect *gfp* mRNA from degradation in primordial germ cells, whereas it is degraded in the soma (Kopranner et al., 2001). This is consistent with the observation that localization of *nanos* mRNA is mediated by sequences within its own 3'UTR in *Drosophila* (Gavis and Lehmann, 1994). Hence, the 3'UTR of zebrafish *nanos* serves as a tool to target mRNA specifically to the primordial germ cells, although the localization mechanism is not understood on a molecular level.

1.4.3 RNA-binding protein Dazl is involved in translational regulation in primordial germ cells

DAZ (deleted in azoospermia) encodes an RNA-binding protein and has been first identified as a candidate gene for human Y-chromosome azoospermia (Reijo et al., 1995). The *DAZ* gene family consists of two additional members, namely *boule* and *dazl* (DAZ-like). All three originate from a common ancestor, but have distinct, yet overlapping functions in germ cell development (Xu et al., 2001). The *Drosophila* *DAZ* homolog, *boule*, is essential for spermatogenesis, as the loss of *boule* function results in block of meiotic divisions and thus leads to azoospermia and male sterility (Eberhart et al., 1996). Interestingly, the mouse homolog *dazl* is essential for germ cell development not only in the testis, but also in the ovary (Ruggiu et al., 1997). In *Xenopus*, *Xdazl* seems to play a role in spermatogenesis, since it rescues the meiotic phenotype in *boule* mutant flies (Houston et al., 1998). *Xdazl* mRNA localizes to the Balbiani body in the oocyte as well as to the germ plasm in the early embryo and is also present in testis (Houston et al., 1998). In zebrafish, *Dazl* binds to the 3'UTR of target mRNAs in primordial germ cells and activates the translation by inducing polyadenylation of the mRNA (Maegawa et al., 2002; Takeda et al., 2009). Recent studies describe *dazl* functions ranging from translational repression and transport of specific mRNAs to a role in differentiation of pluripotent stem cells towards functional gametes (Smorag et al., 2014). Although *Dazl* is involved in translational regulation within primordial germ cells, the mRNA is already localized earlier to the germ plasm. In zebrafish, *dazl* mRNA is localized to the Balbiani body and the vegetal cortex during early oogenesis and thus mimics the early localization of *vasa* and *nanos* mRNA. In contrast, *dazl* transcripts localize strictly to the vegetal cortex in stage II oocytes and do not spread along the cortex as described for *vasa* mRNA (Kosaka et al., 2007). This difference might be the reason for a delayed localization of *dazl* mRNA to the animal pole as the egg is activated, indicating a different separate localization pathway to the germ plasm (Theusch et al., 2006). In addition, during early embryogenesis *dazl* mRNA localizes to the germ plasm more distally in the cleavage furrows as described for *nanos* and *vasa* mRNA (Theusch et al., 2006). Interestingly, the processes of *dazl* mRNA localization, anchoring and assembly with the germ plasm, all depend on localization elements in its 3'UTR (Kosaka et al., 2007). Finally, *dazl* mRNA is localized to the primordial germ cells during sphere stage (Hashimoto et al., 2004). Hence, *dazl* does not seem to play a role in early germ plasm formation, although the transcripts are localized to the germ plasm already in oocytes.

In summary, many of the conserved maternally provided germ plasm components are RNA interacting proteins. They are involved in translational regulation, germ cell differentiation as well as maintenance of the germ cell fate. Although the activity is embodied in the protein, most localization analyses of these germ plasm components result from investigations of their mRNA localization. Since the localization of the corresponding proteins is mostly unknown, the temporal and spatial activity of these germ plasm components remains unclear.

1.5 Molecular mechanism of germ plasm localization in zebrafish

The critical point in germ cell specification by inheritance of germ plasm is the localization of germ plasm properly and exclusively to the primordial germ cells. If something went wrong during this process of localization, the germ plasm would become localized randomly, leading to an excess of germ cells. The challenge in this scenario would not be to have too few germ cells, but to have too few cells freed from the germline fate, which are able to differentiate into essential somatic fates. A second worst case scenario would be the total loss of germ plasm localization. In that case, all cells would follow a somatic fate and no primordial germ cells would be specified. This would result in a sterile organism, a dead end for a species' survival. The same would happen if the germ plasm disaggregated or got degraded after initial localization and specification of the primordial germ cells. The primordial germ cells would lose their undifferentiated state, start to express somatic determinants and differentiate into a somatic fate.

To prevent these scenarios, three things need to be ensured. First, the animal has to make sure that the germ plasm is assembled properly with all its components. Second, the germ plasm has to be localized appropriately to the prospective primordial germ cells. Third, it has to be ensured that the germ plasm is stably associated with the primordial germ cells. Hence, proper localization of germ plasm, acting as a cytoplasmic determinant is crucial for the embryo.

1.5.1 Germ plasm localization mechanisms in oocytes

Despite the importance of properly localized germ plasm in various stages of germline development, little is known about the mechanisms underlying its localization in zebrafish. The germ plasm components *brul* (*bruno-like*, homolog of *Drosophila bruno*) and *dazl* mRNA show a very similar localization pattern in zebrafish oocytes as well as in embryos (Hashimoto et al., 2004; Suzuki et al., 2000). The anchoring of *brul* mRNA to the vegetal cortex stage II and III oocytes depends on the subcortical actin network, but is independent of microtubules. Similar to *dazl*, *brul* mRNA is translocated to the animal pole through the process of ooplasmic streaming upon egg activation (Maegawa et al., 1999; Suzuki et al., 2000). Similar to other germ plasm mRNAs, localization in the oocyte is known, but the underlying mechanism has not been uncovered yet (Pelegri, 2003).

The only protein so far, described to localize to the germ plasm in oocytes, is the RNA-binding protein Rbpms2, a homolog of *Xenopus* Hermes. Rbpms2 protein localizes to the Balbiani body in zebrafish stage IB oocytes and to the vegetal cortex during stage II oocytes, though the localization mechanism of Rbpms2 has not been characterized (Kosaka et al., 2007).

1.5.2 Germ plasm localization mechanisms in embryos

The localization mechanism of germ plasm components during early cleavage stages is analyzed best for *vasa* transcripts in zebrafish. *Vasa* mRNA is localized at the distal ends of the cleavage furrows at 4-cell stage (Yoon et al., 1997). In *nebel* mutants, which are defective in cell adhesion and in the formation of the furrow microtubule array (FMA), *vasa* mRNA does not translocate to the distal ends (Pelegri et al., 1999). Treatment of embryos with the

microtubule-inhibiting drug nocodazole mimicked this *vasa* translocation phenotype. In addition, microscopic studies showed co-localization of *vasa* aggregates with tubulin at the cortex (Pelegri et al., 1999). These findings suggest an interaction between *vasa* mRNA containing aggregates and microtubules. On the contrary, germ plasm granules are adjacent or in the proximity of the actin cortex before aggregation of germ plasm at 1-cell stage. In the subsequent stages, few small granules are still detected along the actin cortex (Knaut et al., 2000). A role of actin in the initial germ plasm aggregation was also suggested by loss of accumulation to the cleavage planes upon actin inhibition by latrunculin B. Even though, this might be a secondary effect since furrow formation in general is inhibited (Knaut et al., 2000). To explain the changes in localization of germ plasm mRNA granules at 1-cell stage, Theusch and colleagues developed a model, in which the germ plasm RNA granules are bound to actin filaments in the first place (Figure 5) (Theusch et al., 2006). Due to the growth of astral microtubules, the actin filaments in complex with germ plasm granules become aligned at the cortex. In a second unknown process, the peripheral aggregates, adjacent to the forming furrow, are recruited to the furrow (Figure 5) (Theusch et al., 2006). As potential mediator between the tip of the astral microtubules and the actin microfilaments, *birc5b* was identified in zebrafish (Nair et al., 2013). Birc5b has been previously characterized as a component of the chromosomal passenger complex, involved in various processes during cell division (van der Waal et al., 2012). Furthermore, localization of germ plasm to the cleavage furrow depends on proper cell division. In embryos, mutant for the centriolar protein Sas-6, initiation of second cell division is defective, hence germ plasm does not localize any more (Yabe et al., 2007). Additionally, embryos mutant for Aurora B kinase, component of the chromosomal passenger complex, are defective in cytokinesis, thus cleavage furrows do not fully form and germ plasm granules cannot properly aggregate (Yabe et al., 2009).

In conclusion, the segregation of zebrafish germ plasm during the first cleavages depends on proper cleavage furrow formation and involves astral microtubule-dependent aggregation of actin-associated germ plasm granules to the forming furrow. Moreover, distal compaction of the germ plasm depends on proper formation of the furrow microtubular array (Figure 5) (Lindeman and Pelegri, 2010).

After the four germ plasm aggregates are established, they are asymmetrically segregated during cell cleavages (Figure 4). During this cleavage phase, germ plasm is localized close to one of the two spindle poles. This asymmetric germ plasm distribution results in just four primordial germ cells at the 1k-cell stage. At sphere stage, this mode changes and germ plasm is inherited by both daughter cells. This change in localization pattern is independent of DNA replication or transcription and the underlying mechanism has not yet been identified (Knaut et al., 2000).

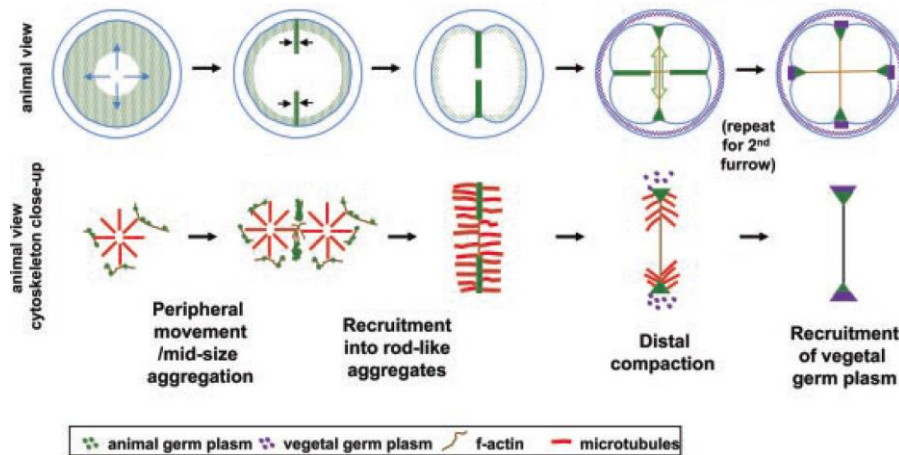


Figure 5: Germ plasm segregation during early zebrafish embryogenesis. Germ plasm components are initially bound in complexes to cortical filamentous actin (leftmost diagram). Astral microtubules move these complexes to the periphery of the blastomere, which leads to germ plasm aggregation and recruitment to the forming furrow (second and third diagram). Further aggregation and distal compaction of the germ plasm is associated with arrangements of the FMA (fourth diagram). This process is repeated for the formation of the second furrow and results in four stable germ plasm aggregates (rightmost diagram). Vegetal germ plasm components anchor to the distal ends after compaction of the germ plasm. Upper row shows 1-cell, 2-cell and 4-cell stage embryos in animal view. Bottom row shows corresponding close-ups on the cytoskeleton and the germ plasm aggregates. Figure modified from Lindeman and Pelegri (2010).

Among germ plasm proteins, Brul was the first protein that has been shown to localize to the germ plasm during early cleavage stages in zebrafish embryogenesis (Hashimoto et al., 2006). Similar to *vasa* mRNA, Brul localizes to the distal ends of the cleavage furrows during 4-cell stage. Surprisingly, this localization is not stable and completely disappears until 16-cell stage (Hashimoto et al., 2006). The molecular mechanism of Brul protein localization is not characterized. The germ plasm component Ziwi protein localizes to the cleavage furrows of 4-cell stage embryos as well as to the perinuclear region in primordial germ cells at 24 hpf (Houwing et al., 2007). Similarly, Vasa protein localizes to the perinuclear region in primordial germ cells from 6 hpf on (Braat et al., 2000). However, the mechanisms underlying the localization of both proteins have not been described so far.

The localization of mRNA germ plasm components in zebrafish is well described. In contrast, less is known about the localization of proteins in the germ plasm and their underlying localization mechanisms.

1.6 Bucky ball in zebrafish germ cell specification

To identify further maternal factors controlling early vertebrate development, a systematic maternal-effect mutant screen was carried out in zebrafish (Dosch et al., 2004). Among 15 mutants that showed a defect in processes prior to midblastula transition, one mutant showed radial segregation of cytoplasm instead of polar segregation to the animal pole (Figure 6). In addition, the fertilized mutant embryo does not show cellular cleavages and hence does not develop beyond 1-cell stage. Since the mutant embryo lacks polarity and resembles a Buckminsterfullerene, it was referred to as *bucky ball* (*buc*) (Dosch et al., 2004).

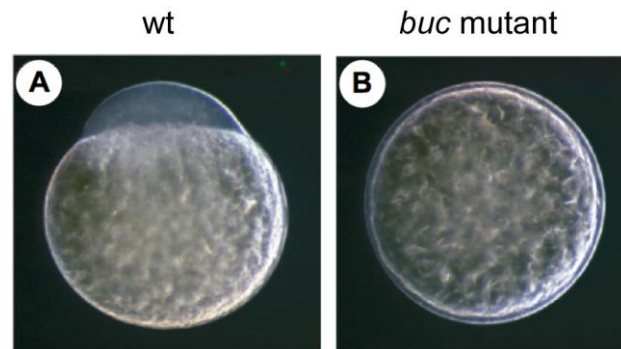


Figure 6: *buc* mutants show a defect in the embryonic animal-vegetal polarity. (A) Wild type embryo forming the blastodisc at the animal pole. (B) *buc* mutant embryo with a radial halo of cytoplasm surrounding the yolk. Embryos at 30 mpf are shown with animal pole to the top. Figure from Dosch et al. (2004).

1.6.1 Bucky ball is necessary and sufficient for germ plasm formation

The morphological phenotype of radially segregating cytoplasm in *buc* mutant embryos together with mislocalized mRNA polarity markers indicated a defect already in animal-vegetal polarity of the egg (Dosch et al., 2004). Indeed, the animal pole marker *pou2* mRNA as well as the vegetally localizing *brul* mRNA are no longer properly localized in *buc* mutant oocytes (Marlow and Mullins, 2008). Interestingly, the Balbiani body, which is the first morphological polarity marker of the oocyte, fails to form in *buc* mutant oocytes. In accordance with this, *dazl* mRNA, a germ plasm component localizing to the Balbiani body in early oocytes, is no longer properly localized (Bontems et al., 2009; Marlow and Mullins, 2008). In the same way, the germ plasm components *nanos* and *vasa* mRNA are no longer localized to the Balbiani body in *buc* mutant oocytes (Bontems et al., 2009). This indicated an important role of *buc* in the formation of the Balbiani body and the localization of germ plasm components.

The identification of the gene responsible for the *buc* mutant phenotype revealed a novel gene, which encodes for a protein with homologs among vertebrates. However, no known protein domains were detected in Buc protein, which would give insight into its biochemical function (Bontems et al., 2009). Nevertheless, 100 of 639 N-terminal amino acids, termed BUVE-motif, are conserved among Buc vertebrate homologs. The mutant alleles *buc*^{p106re} and *buc*^{p43bmb} (in the following referred to as *buc*^{p106} and *buc*^{p43}) both harbor nonsense mutations leading to predicted deletions of 38 (*buc*^{p106}) and 278 (*buc*^{p43}) amino acids at the Buc C-terminus (Bontems et al., 2009). *buc* transcripts are expressed during oogenesis and early embryogenesis until midblastula transition (4 hpf). In adult fish, *buc* mRNA is only detected in females (Bontems et al., 2009). These findings support a role of *buc* in germ plasm assembly and explain the lack of phenotype in *buc* mutant males. In addition, *buc* mRNA co-localizes with the germ plasm marker *dazl* mRNA to the Balbiani body in stage I oocytes and to the vegetal pole during early stage II (Bontems et al., 2009). Similarly, *Xvelo1* mRNA, the *Xenopus* homolog of *buc*, localizes to the germ plasm at the vegetal pole in *Xenopus* oocytes (Claussen and Pieler, 2004). However, *buc* mRNA localization changes to the animal pole in late stage III oocytes, where it co-localizes with the animal pole marker *foxH1* (Bontems et al., 2009). In *buc* mutant oocytes, proper localization of *buc* mRNA is lost and transcripts are detected at the animal pole in stage I oocytes.

In early zebrafish embryos, *buc* transcripts are not localized, although transcripts are detected by RT-qPCR. (Bontems et al., 2009). This indicates that *buc* mRNA is a component of the germ plasm only during early oogenesis. In contrast to *buc* mRNA, an overexpressed Buc-GFP fusion localizes to the germ plasm in early oocytes and early embryogenesis (Bontems, 2009).

In a functional approach Buc protein overexpression rescues *dazl* mRNA localization to the Balbiani body in *buc* mutant oocytes. More interestingly, *buc* overexpression induces the formation of ectopic primordial germ cells during embryogenesis (Bontems et al., 2009). Hence, Buc is the first vertebrate protein required for germ plasm localization in oocytes and sufficient for primordial germ cell formation in embryos.

1.6.2 A *buc-gfp* transgene rescues the mutant phenotype

To analyze the spatial and temporal expression of Buc protein *in vivo*, a transgenic line was generated in the *buc*^{p106} mutant background. An additional copy of the genomic *buc* locus, which contained an in frame insertion of *gfp* at the 3' end of the *buc* ORF, was integrated into the genome using the Tol2 transposon system (Bontems, 2009). Integration of the *buc-gfp* transgene rescues the mutant phenotype through the expression of the transgenic Buc-GFP fusion protein (Bontems, 2009). This indicates that the transgene replicates the activity of endogenous Buc. A first analysis indicated that transgenic Buc-GFP is localized to the germ plasm in oogenesis and embryogenesis (Bontems, 2009).

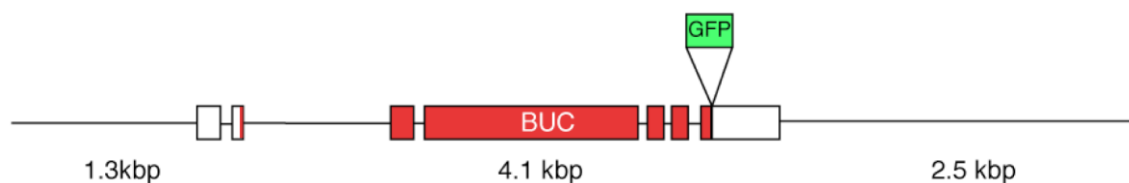


Figure 7: Construct used to make a transgenic *buc-gfp* zebrafish line. Schematic representation of the genomic *buc* locus with *gfp* (green) cloned to the 3' end of *buc* ORF (red) used to obtain transgenic fish. 1.3 kb upstream and 2.5 kb downstream of *buc* where included to imply potential regulatory elements. Boxes indicate the exon-intron structure of *buc*. Figure from Bontems (2009).

1.6.3 Oskar organizes germ plasm formation in *Drosophila*

Buc is the only known vertebrate protein that is involved in the regulation of germ plasm formation. Only one other protein is known that shares this particular function. Similar to *buc* in zebrafish, *oskar* (*osk*) is necessary and sufficient for germ plasm formation and thus essential for the specification of primordial germ cells in *Drosophila* (Ephrussi and Lehmann, 1992; Lehmann and Nusslein-Volhard, 1986). Homologs of *osk* are restricted to insects and have been identified in flies and mosquitoes (Dipterans), ants and wasps (Hymenoptera) as well as in crickets (Ahuja and Extavour, 2014; Ewen-Campen et al., 2012; Juhn and James, 2006; Lynch et al., 2011). *Osk* mutant embryos lack abdominal segmentation and do not form germ cells (Lehmann and Nusslein-Volhard, 1986). On the other hand, ectopic overexpression at the anterior pole leads to defects in anterior posterior polarity and to germ plasm assembly, resulting in the formation of ectopic germ cells (Ephrussi and Lehmann, 1992). These findings suggest that *osk* is a key regulator in germ plasm assembly as well as anterior-posterior polarity.

Osk mRNA is expressed early in oogenesis and localizes to the posterior pole during late *Drosophila* oogenesis (Ephrussi et al., 1991; Kim-Ha et al., 1991). Among other proteins, this localization depends on Staufen, microtubules, as well as the motor protein kinesin and is established through a biased random walk along a weakly polarized microtubular network (Brendza et al., 2000; Ephrussi et al., 1991; Kugler and Lasko, 2009; Zimyanin et al., 2008). In contrast to the posterior transport, anchoring of *osk* mRNA depends on the actin cytoskeleton and associated proteins (Babu et al., 2004). Furthermore, posterior endocytosis is involved in maintenance of *osk* mRNA localization (Tanaka and Nakamura, 2008). Even Osk protein itself seems to regulate *osk* mRNA localization in a positive feedback loop (Rongo et al., 1995). In addition, translation of *osk* is restricted to the posterior pole by translational repression of unlocalized transcripts via Cup and Bruno and by translational activation of localized mRNA via Aubergine or Orb (Castagnetti and Ephrussi, 2003; Chekulaeva et al., 2006; Kim-Ha et al., 1995; Nakamura et al., 2004; Wilson et al., 1996). These mechanisms ensure that *osk* translation is restricted to the posterior pole of the *Drosophila* embryo and by this strictly limit Osk activity to its site of action.

Moreover, Osk protein has to be anchored to the posterior pole after translation in late oocytes (Kim-Ha et al., 1995). *Osk* translation results in two isoforms (Short and Long Osk) through the alternative usage of start codons (Markussen et al., 1995). Long Osk is involved in anchoring of *osk* mRNA and Short Osk to the posterior pole while Short Osk directs the formation of germ plasm (Markussen et al., 1995; Vanzo and Ephrussi, 2002). Additionally, Short Osk has been shown to interact with Staufen and Vasa in a yeast two-hybrid assay as well as *in vitro*. Osk is upstream of Vasa and might mediate the localization of Vasa to the germ plasm at the posterior pole (Breitwieser et al., 1996). The biological significance of the Staufen-Osk interaction is unclear. Another downstream interactor of Osk protein is the germ plasm component Valois, which interacts with Osk *in vitro* and might thereby mediate Tudor localization to the germ plasm (Anne, 2010). Interestingly, the actin binding protein Lasp seems to be involved in accumulation of Osk protein to the posterior pole of embryos, since Lasp interacts genetically with Oskar. Besides that, both proteins co-localize in dependence on the Lasp SH3 domain at the posterior pole (Suyama et al., 2009).

In summary, Osk activity is restricted to the posterior pole of the embryo by proper mRNA localization, strict translational regulation of the transcripts and tight anchoring of the protein already during oogenesis.

1.6.4 Similarities and differences between Buc and Osk

Buc homologs have been identified only in vertebrate genomes, whereas *osk* is found exclusively in insects (Ahuja and Extavour, 2014; Bontems et al., 2009). Despite this evolutionary distance, Buc and Osk are both novel proteins that lack any recognizable functional domains. The main similarity of *buc* and *osk* is their functional analogy in germ plasm formation. Both mutants show a defect in polarity and germ cell formation caused by failure of proper germ plasm aggregation (Bontems et al., 2009; Ephrussi et al., 1991; Lehmann and Nusslein-Volhard, 1986; Marlow and Mullins, 2008). Ectopic overexpression induces in both cases the formation of supernumerary germ cells (Bontems et al., 2009; Ephrussi and Lehmann, 1992). Surprisingly, ectopic expression of *Drosophila osk* in zebrafish induces the formation of primordial germ cells similarly to *buc*. In contrast, a transgenic line

expressing *osk* from genomic DNA, flanked by *buc* 5' and 3'UTR, does not rescue the *buc* mutant phenotype (Bontems, 2009). On the molecular level, *buc* as well as *osk* mRNA localize with other germ cell specific molecules to the germ plasm during oogenesis. On the contrary, *osk* mRNA still localizes to the germ plasm in early embryos while *buc* mRNA localization to the germ plasm is lost during late oogenesis (Bontems et al., 2009; Kim-Ha et al., 1991). Osk protein is expressed at the posterior pole in late stage oocytes, is anchored there in the early embryo and finally localizes to the forming primordial germ cells (Kim-Ha et al., 1995; Markussen et al., 1995). The endogenous localization of Buc is not known, but overexpression of GFP-tagged Buc indicates localization of the protein to the germ plasm during oogenesis as well as early embryogenesis (Bontems, 2009). A lot of germ plasm components are conserved between *Drosophila* and zebrafish, but since no interaction partners of Buc are known, it is unclear if Buc and Osk act within a similar network.

1.7 Aims

Buc is the first vertebrate gene necessary and sufficient for the organization of germ plasm and therefore plays an important role in the process of germ cell specification (Bontems et al., 2009). Germ plasm has to be specifically localized in order to specify future germ cells, retain their ability to stay undifferentiated and to liberate further somatic cells to pursue their somatic fate. Thus, germ plasm localization is the critical step in germ cell development. As a consequence, the germ plasm organizer Buc has to be properly localized. Accordingly, the aim of this work is to characterize the molecular mechanism of Buc protein localization.

As nothing is known about its endogenous localization, the first objective is to study Buc protein localization in detail by making use of the transgenic *buc-gfp* line and by immunostaining endogenous Buc.

From previous studies it is known that the localization of Buc protein is independent of the localization of its mRNA. Hence, the second goal is to identify the Buc localization domain using two different approaches: a cross-species approach, to gain insight about Buc localization from the Buc functional analogue *Drosophila* Osk and a systematic structure-function analysis on Buc protein.

The third aim is to identify molecular interaction partners of Buc that might be involved in its localization and could give valuable insight into the molecular mechanism of Buc protein localization.

2 Materials and Methods

2.1 Zebrafish handling and maintenance

Zebrafish (*Danio rerio*) was used as a model organism. Fish were maintained and fed following the standard protocols (Westerfield, 2000). The AB*TLF zebrafish line was used as the wild type. For analysis of mutant *buc*, fish homozygous for the *buc*^{p106} or *buc*^{p43} mutant allele were used. The mutant zebrafish lines *buc*^{p106} and *buc*^{p43} were maintained by crossing a homozygous mutant male to a heterozygous mutant female. The progeny was genotyped by KASP genotyping (Chapter 2.1.3). The transgenic *buc-gfp* line, heterozygous for *buc-gfp* in the *buc*^{p106} mutant background (Bontems, 2009), was brought to homozygosity by crossing heterozygous fish. The progeny was genotyped by PCR based on short tandem repeats (Chapter 2.1.2). Oocyte and embryo stages were determined as previously described (Kimmel et al., 1995; Selman et al., 1993).

2.1.1 DNA extraction from zebrafish fins

For genotyping purposes, DNA was extracted from clipped fins by freezing them for 10 min at -80°C and subsequent lysis for 30 min at 55 °C in lysis buffer (0.2 mg/ml Proteinase K (Merck, Darmstadt), 100 mM Tris (pH 8.4), 500 mM KCl, 15 mM MgCl₂). Subsequently Proteinase K was inactivated for 10 min at 95 °C. Samples were stored at -20 °C.

2.1.2 Genotyping based on short tandem repeats

The transgenic *buc-gfp* line was genotyped for the mutant *buc*^{p106} allele and the *buc-gfp* transgene by conventional PCR (Chapter 2.6.6). To genotype for the mutant *buc*^{p106} allele, primers (Eurogentec, Cologne) were used that amplify short tandem repeats, which are located up and downstream of the gene, resulting in different band sizes for the wild type or the mutant allele (Table 1). To genotype for *buc-gfp*, primers (Eurogentec, Cologne) were used that amplify *gfp* and a part of the *buc* 3'UTR (Table 1).

Table 1: Primers used for genotyping of zebrafish.

Name	Sequence (5' to 3')	Genotyping usage
z13475fw	CTCTTCTCCCAGTGTGGAGC	<i>buc</i> ^{p106}
z13475rev	CCAGCCTGCAGATCTTTTTA	<i>buc</i> ^{p106}
z24206fw	ACACTCACTCTGAGCTGATGC	<i>buc</i> ^{p106}
z24206rev	GGAATAATGTGGCA GAGCGT	<i>buc</i> ^{p106}
GFPfw	ACATCTTCTTCAAGGACGACGG	transgenic <i>buc-gfp</i>
revpimer3utr	AGGTCAAGGTCTGGTACAGTG	transgenic <i>buc-gfp</i>

2.1.3 KASP genotyping

Buc^{p106} and *buc*^{p43} mutant embryos were genotyped for homozygosity by KASP genotyping (LGC, Teddington, UK). KASP genotyping is based on competitive allele-specific PCR and enables detection of single nucleotide polymorphisms by end-point fluorescent read out. Allele specific primers and genotyping reagents were purchased from (LGC, Teddington, UK). KASP-PCR was carried out as recommended by the manufacturer on a C1000 Touch Thermal Cycler with CFX96 Optics Module (Bio-Rad, Munich). The genotyping result was afterwards analyzed with the Bio-Rad CFX-Manager 3.1 software (Bio-Rad, Munich).

2.2 Manipulation of zebrafish embryos

2.2.1 Microinjection

Glass needles for injection (GB100F-8P; Science Products, Hofheim) were prepared in advance (Needle puller PN-30; Narishige, Tokyo, Japan). Before injection, the synthesized capped sense RNA (Chapter 2.6.10) was diluted into 0.1 M KCl and 0.05% phenol red (Sigma-Aldrich, Hannover). 1-cell stage zebrafish embryos were injected (PV 820; WPI, Sarasota, USA) with 1 nl capped sense RNA of the indicated molarity (Nüsslein-Volhard and Dahm, 2002).

2.2.2 Dechoriation

For imaging, embryos were mechanically dechorionated with forceps. High numbers of embryos were enzymatically dechorionated before deholking using pronase (30 mg/ml; Roche, Mannheim). Up to 200 embryos were incubated 3-5 min in pronase solution (approx. 3 mg/ml in 1x E3 medium (5 mM NaCl, 0.17 mM KCl, 0.33 mM CaCl₂, 0.33 mM MgSO₄, 0.00001 % methylene blue)) and afterwards washed three times with 1x E3 medium. After dechoriation a fire polished Pasteur pipette was used to transfer the embryos.

2.2.3 Deyolking

Up to 200 embryos were deholked to remove most of the yolk granules before lysis (Link et al., 2006). For deholking 1/2 Ginzburg Fish Ringer with Calcium was used (55 mM NaCl, 2.7 mM CaCl₂, 1.8 mM KCl, 1.25 mM NaHCO₃). After deholking the cell pellet was once washed with wash buffer (110 mM NaCl, 3.5 mM KCl, 2.7 mM CaCl₂, 10 mM Tris (pH 8.5)). The cell pellet was directly used for further experiments or frozen in liquid nitrogen and stored at -80°C.

2.2.4 Preparation of embryo lysates

To prepare embryo lysates for analysis by SDS-polyacrylamide gel electrophoresis (Chapter 2.7.2) deholked embryonic cell pellets were resuspended in 2x SDS loading buffer (100 mM Tris (pH 6.8), 20 % glycerol, 4 % SDS, 200 mM β-mercaptoethanol, 0.02 % bromophenol blue) and incubated at 96 °C for 5 min. After cooling of the sample on ice, it was loaded directly on a SDS-polyacrylamide gel or stored at -20°C.

2.3 *Drosophila* handling and manipulation

2.3.1 Breeding and crossing

Flies were kept and crossed at room temperature or 25 °C (Laupsien, 2013). Stocks were kept at 18 °C. To collect embryos the flies were kept in cages with apple juice agar plates at 25 °C.

2.3.2 Microinjections

To make transgenic flies, staged embryos were collected for 30 min, dechorionated using bleach and glued on a microscope cover slide. After 10-12 min of drying in a desiccator, embryos were covered with Voltalef 10 S oil (VWR, Hannover) and injected at the posterior end (FemtoJet Mikroinjector, Eppendorf, Hamburg) with approximately 0.1 nl of the respective plasmid DNA (approx. 200 ng/μl) with a glass injection needle (Chapter 2.2.1). After injection embryos were incubated at room temperature until hatching followed by incubation in food vials at 18 °C.

2.3.3 Germline transformation

To create transgenic fly lines expressing *buc-eGFP-bcd3'UTR*, *buc^{p43}-eGFP-bcd3'UTR*, *osk-eGFP-bcd3'UTR* or *osk⁰⁸⁴-eGFP-bcd3'UTR* the Φ31 integrase-based system was used (Bischof et al., 2007; Groth et al., 2004). In this system the gene encoding the integrase is already integrated in the genome of ΦX86Fb (Table 2) and an attP landing site is integrated on the third chromosome for chromosomal integration. After injection of the embryos with the corresponding pAttB plasmid (Table 3) as described oben, the resulting male flies were crossed with virgin yw-flies. Successful germline transformation gave red-eyed progeny due to the *white*⁺ included in the transformation vector. Single red-eyed males were crossed to TM3/TM6 virgin flies to balance the transgene. Stocks were kept at 18 °C.

Table 2: *Drosophila* lines used to make transgenic flies. Fly stocks were kindly provided by the group of Prof. Dr. Jörg Großhans (Department of Developmental Biochemistry, Georg August University Göttingen).

Name	Genotype
yw	y w
TM3/TM6B	w ; TM3, Sb Ser / TM6B, Tb Hu
CyO ; TM3	w ; Sp / CyO, hb-lacZ{ry+} ; Dr / TM3, Sb hb-lacZ{ry+}
ΦX86Fb	y w M(eGFP.vas-int.Dm)ZH-2A ; M(RFP.attP)ZH-86Fb
mat-Gal4 67	w; tub-Gal4-VP16{w+}[67] ; TM3, Sb Ser / TM6B, Tb Hu

To express the transgene, integrated into the genome by the Φ31-based integration system, the Gal4/UAS system (Brand and Perrimon, 1993) was used. Transgenic flies were crossed with mat-Gal4 67 flies, a driver line expressing Gal4 under the control of the maternal tubulin promoter. In the resulting progeny the expression of the transgene starts during oogenesis. To obtain flies that contain two copies of the driver construct as well as the transgene, the CyO ; TM3 balancer line was used (Table 2).

2.3.4 Cuticle preparation

To analyze for a phenotype in anterior-posterior patterning, Transgenic and wild type (yw) *Drosophila* embryos were collected on apple-juice agar plates and incubated 24 h at 25°C to fully develop. Embryos were then dechorionated with bleach and subsequently transferred to a microscope slide. For mounting a drop of Hoyer's medium mixed 1:1 with lactic acid was added and incubated over night at 65 °C (Wieschaus and Nüsslein-Volhard, 1986). Embryonic cuticles were analyzed using a microscope with dark field optics.

2.4 Chemicals

Chemicals were bought from Carl Roth (Karlsruhe), Sigma-Aldrich (Hannover), Applichem (Darmstadt), Invitrogen (Darmstadt), Biochrom (Berlin), Roche (Mannheim), Calbiochem (Darmstadt) or Biomol (Hamburg), if not indicated otherwise.

2.5 Plasmid vectors and constructs

2.5.1 Plasmid Vectors

The multipurpose expression vector pCS2+ contains a strong promoter/enhancer region (simian CMV IE94), a polylinker and a SV40 viral polyadenylation signal (Rupp et al., 1994). The SP6 viral promoter at the 5'UTR allows *in vitro* transcription of sense RNA for microinjection. The T7 viral promoter at the 3'UTR allows *in vitro* transcription of antisense RNA for in situ hybridization. The vector backbone originates from the pBluescript II KS+ vector, including an ampicillin resistance gene.

pDONR221 (Life Technologies, Carlsbad, USA) is a Gateway-adapted vector that can be used to generate attL-flanked entry clones after recombination of the attP recombination sites with an attB PCR product. For selection in *E. coli*, it contains a kanamycin resistance gene.

pCSDest2 is a Gateway-adapted expression vector, based on the pCS-backbone (Villefranc et al., 2007). It can be used to generate C-terminal fusions in a multisite Gateway LR recombination reaction. For selection in *E. coli*, it contains an ampicillin resistance gene. p3EeGFP and p3EmCherry are Gateway-adapted entry vectors that can be used to generate a C-terminal eGFP/mCherry-tag in a multisite Gateway LR recombination reaction. (Villefranc et al., 2007). For selection in *E. coli*, it contains a kanamycin resistance gene.

pAttB_UASp2B3 is based on the pUASTattB vector, designed to generate transgenic flies by the Φ 31 integrase-based system (Bischof et al., 2007). pAttB_UASp2B3 contains the 3'UTRbcd subsequent to a multiple cloning site (gifted by Dr. Ulrike Loehr, MPI-BPC, Goettingen). For selection in *E. coli*, it contains an ampicillin resistance gene

2.5.2 Cloned vector and expression constructs

Vector constructs were cloned to be used in generation of transgenic flies (Table 3) by conventional restriction enzyme cloning (Chapter 2.6.1). Expression constructs to be used for analysis of *buc* deletion constructs and to express Buc interaction candidates (Table 4) were mostly cloned by Gateway cloning (Chapter 2.6.1).

Table 3: Cloned vector constructs used to generate transgenic flies.

Name	Vector	Insert	Cloning strategy
pCS2 ⁺ buc-eGFP	pCS2 ⁺	<i>buc-egfp</i>	(Bontems et al., 2009)
pCS2 ⁺ buc ^{p43} -eGFP	pCS2 ⁺	<i>buc^{p43}-egfp</i>	<i>buc^{p43}</i> sequence was amplified from pCS2 ⁺ buc-eGFP, using the primers Clalbuc_for, Buc-p43-XbaI-rev. The PCR product was cut with ClaI, XbaI and ligated into pCS2 ⁺ buc-eGFP.
pCS2 ⁺ osk-eGFP	pCS2 ⁺	<i>osk-egfp</i>	<i>osk-egfp</i> sequence was amplified from pCS2 ⁺ osk-eGFP (without Stop-Codon), Osk_BamHI_fw, GFP-STOP-SpeI-rev. The PCR product was cut with BamHI, SpeI and ligated into pCS2 ⁺ .
pCS2 ⁺ osk ⁰⁸⁴ -eGFP	pCS2 ⁺	<i>osk⁰⁸⁴-egfp</i>	<i>osk⁰⁸⁴</i> sequence was amplified from pCS2 ⁺ osk-eGFP, using the primers Osk_BamHI_fw, Osk-084-XbaI-rev. The PCR product was cut with BamHI, XbaI and ligated into pCS2 ⁺ osk-eGFP.
pAttB buc-eGFP	pAttB_UASp2B3	<i>buc5'UTR-buc-eGFP-bcd3'UTR</i>	(Natascha Zhang, unpublished)
pAttB buc ^{p43} -eGFP	pAttB_UASp2B3	<i>buc5'UTR-buc^{p43}-eGFP-bcd3'UTR</i>	<i>buc^{p43}-egfp</i> sequence was amplified from pCS2 ⁺ buc ^{p43} -eGFP, using the primers Buc-Bcl1-fw, GFP_KpnI_rev. The PCR product was digested with Bcl1, KpnI and ligated into pAttB_UASp2B3.
pAttB osk-eGFP	pAttB_UASp2B3	<i>osk-eGFP-bcd3'UTR</i>	<i>osk-egfp</i> sequence was amplified from pCS2 ⁺ osk-eGFP, using the primers Osk_BamHI_fw, GFP_KpnI_rev. The PCR product was digested with BamHI, KpnI and ligated into pAttB_UASp2B3.
pAttB osk ⁰⁸⁴ -eGFP	pAttB_UASp2B3	<i>osk⁰⁸⁴-eGFP-bcd3'UTR</i>	<i>osk⁰⁸⁴-egfp</i> sequence was amplified from pCS2 ⁺ osk ⁰⁸⁴ -eGFP, using the primers Osk_BamHI_fw, GFP_KpnI_rev. The PCR product was digested with BamHI, KpnI and ligated into pAttB_UASp2B3.

Table 4: Cloned expression plasmids used for *in vitro* transcription of Buc deletion constructs or Buc interaction candidates.

Name	Vector	Insert	Cloning strategy
Buc deletions			
pENTR221 buc1-158	pDONR221	<i>buc1-158</i>	<i>buc1-158</i> sequence was amplified from pCS2+ buc-eGFP, using the primers buc_attB1_1-474bp_fw, buc_attB2_1-474bp_rv. The PCR product was recombined into pDONR221.
pEXPPCSDest2 buc1-158-eGFP	pCSDest2	<i>buc1-158-egfp</i>	pENTR221 buc1-158 was recombined with pCSDest2 and p3EeGFP.
pENTR221 buc159-361	pDONR221	<i>buc159-361</i>	<i>buc159-361</i> sequence was amplified from pCS2+ buc-eGFP, using the primers buc_attB1_475-1083bp_fw, buc_attB2_475-1083bp_rv. The PCR product was recombined into pDONR221.
pEXPPCSDest2 buc159-361-eGFP	pCSDest2	<i>buc159-361-egfp</i>	pENTR221 buc159-361 was recombined with pCSDest2 and p3EeGFP.
pENTR221 buc11-88	pDONR221	<i>buc11-88</i>	<i>buc11-88</i> sequence was amplified from pCS2+ buc-eGFP, using the primers buc_attB1_20-264bp_fw, buc_attB2_20-264bp_rv. The PCR product was recombined into pDONR221.
pEXPPCSDest2 buc11-88-eGFP	pCSDest2	<i>buc11-88-egfp</i>	pENTR221 buc11-88 was recombined with pCSDest2 and p3EeGFP.
pEXPPCSDest2 buc11-88-mCherry	pCSDest2	<i>buc11-88-mcherry</i>	pENTR221 buc11-88 was recombined with pCSDest2 and p3EmCherry.
pENTR221 buc89-158	pDONR221	<i>buc89-158</i>	<i>buc89-158</i> sequence was amplified from pCS2+ buc-eGFP, using the primers buc_attB1_265-474bp_fw, buc_attB2_1-474bp_rv. The PCR product was recombined into pDONR221.
pEXPPCSDest2 buc89-158-eGFP	pCSDest2	<i>buc89-158-egfp</i>	pENTR221 buc89-158 was recombined with pCSDest2 and p3EeGFP.
pENTR221 buc11-47	pDONR221	<i>buc11-47</i>	<i>buc11-47</i> sequence was amplified from pCS2+ buc-eGFP, using the primers buc_attB1_20-264bp_fw, buc_attB2_31-141bp_rv. The PCR product was recombined into pDONR221.
pEXPPCSDest2 buc11-47-eGFP	pCSDest2	<i>buc11-47-egfp</i>	pENTR221 buc11-47 was recombined with pCSDest2 and p3EeGFP.
pENTR221 buc48-88	pDONR221	<i>buc48-88</i>	<i>buc48-88</i> sequence was amplified from pCS2+ buc-eGFP, using the primers buc_attB1_142-264bp_fw, buc_attB2_20-264bp_rv. The PCR product was recombined into pDONR221.

Name	Vector	Insert	Cloning strategy
pEXPPCSDest2 buc48-88-eGFP	pCSDest2	<i>buc48-88-egfp</i>	pENTR221 buc48-88 was recombined with pCSDest2 and p3EeGFP.
pCS2 ⁺ bucΔ11-88-eGFP	pCS2 ⁺	<i>bucΔ11-88-egfp</i>	<i>bucΔ11-88-egfp</i> sequence was amplified using a 3-step PCR from pCS2 ⁺ buc-eGFP, using the primers buc_265bp_fw, buc_1bp_wo-loc_fw, Buc_1bp_ClaI_fw, eGFP_end_XbaI_rv. The PCR product was cut with ClaI, XbaI and ligated into pCS2 ⁺ .
Interaction candidates			
pENTR221-loc792544	pDONR221	<i>loc792544</i>	<i>loc792544</i> sequence was amplified from cDNA, using the primers Loc792544_attB1_1-3207bp_fw, Loc792544_attB2_1-3207bp_rv. The PCR product was recombined into pDONR221.
pEXPPCSDest2-loc792544-eGFP	pCSDest2	<i>loc792544-eGFP</i>	pENTR221-loc792544 was recombined with pCSDest2 and p3EeGFP.
pENTR221-pard3	pDONR221	<i>pard3</i>	<i>pard3</i> sequence was amplified from cDNA, using the primers pard3_attB1_1-3360bp_fw, pard3_attB2_1-3360bp_rv. The PCR product was recombined into pDONR221.
pEXPPCSDest2-pard3-eGFP	pCSDest2	<i>pard3-eGFP</i>	pENTR221-pard3 was recombined with pCSDest2 and p3EeGFP.
pENTR221-sept2	pDONR221	<i>sept2</i>	<i>sept2</i> sequence was amplified from cDNA, using the primers sept2_attB1_1-1107bp_fw, sept2_attB2_1-1107bp_rv. The PCR product was recombined into pDONR221.
pEXPPCSDest2-sept2-eGFP	pCSDest2	<i>sept2-eGFP</i>	pENTR221-sept2 was recombined with pCSDest2 and p3EeGFP.
pENTR221-magoh	pDONR221	<i>magoh</i>	<i>magoh</i> sequence was amplified from cDNA, using the primers magoh_attB1_1-441bp_fw, magoh_attB2_1-441bp_rv. The PCR product was recombined into pDONR221.
pEXPPCSDest2-magoh-eGFP	pCSDest2	<i>magoh-eGFP</i>	pENTR221-magoh was recombined with pCSDest2 and p3EeGFP.
pENTR221-exosc9	pDONR221	<i>exosc9</i>	<i>exosc9</i> sequence was amplified from cDNA, using the primers rrp45_attB1_1-1179bp_fw, rrp45_attB2_1-1179bp_rv. The PCR product was recombined into pDONR221.
pEXPPCSDest2-exosc9-eGFP	pCSDest2	<i>exosc9-eGFP</i>	pENTR221-exosc9 was recombined with pCSDest2 and p3EeGFP.
pENTR221-prkacaa	pDONR221	<i>prkacaa</i>	<i>prkacaa</i> sequence was amplified from cDNA, using the primers prkaca_attB1_1-1056bp_fw, prkaca_attB2_1-1056bp_rv. The PCR product was recombined into pDONR221.
pEXPPCSDest2-prkacaa-eGFP	pCSDest2	<i>prkacaa -eGFP</i>	pENTR221-prkacaa was recombined with pCSDest2 and p3EeGFP.

Name	Vector	Insert	Cloning strategy
pENTR221-ywphae1	pDONR221	<i>ywphae1</i>	<i>ywphae1</i> sequence was amplified from cDNA, using the primers <i>ywphae_attB1_1-756bp_fw</i> , <i>ywphae_attB2_1-756bp_rv</i> . The PCR product was recombined into pDONR221.
pEXPpCSDest2-ywphae1-eGFP	pCSDest2	<i>ywphae1-eGFP</i>	pENTR221-ywphae1 was recombined with pCSDest2 and p3EeGFP.

2.6 Molecular biology methods

2.6.1 PCR

DNA fragments were amplified in a standard PCR reaction (Mullis et al., 1986) (Table 5). 100 ng DNA was used as template in a 50 μ l reaction containing 1x Phusion High Fidelity buffer (New England BioLabs, Ipswich, USA), 0.4 μ M of each primer (Table 6) (Eurogentec, Cologne), 0.2 mM of each dNTP (Thermo Scientific, Wilmington, USA) and 1 U of Phusion polymerase (5 U/ μ l, New England BioLabs, Ipswich, USA). TPersonal or TProfessional TRIO thermocycler (Biometra, Goettingen) were used to run the PCR.

Table 5: Standard PCR program for DNA amplification with Phusion polymerase.

Step	Temperature [$^{\circ}$ C]	Time	Number of cycles
Initial denaturation	98	30 s] 30-39
Denaturation	98	10 s	
Primer annealing	Depending on Primer T_m	15 s	
Elongation	72	30 s/kb	
Final elongation	72	10 min	

Table 6: Primers used for conventional restriction enzyme cloning and gateway cloning.

Name	Sequence (5' to 3' direction)	Cloning purpose
Conventional restriction enzyme cloning		
ClalBuc_for	GGGATCGATAATGTGGATCTCTGGAAACAG	pCS2 ⁺ plasmids
Buc-p43-XbaI-rev	GCTCTAGAGCTGTAGGAATAAGCACTGC	pCS2 ⁺ plasmids
Osk_BamHI_fw	GGGGGATTCATGACCATCATCGAGAGCAC	pCS2 ⁺ / pAttB plasmids
GFP-STOP-SpeI-rev	CCCACTAGTTTACTTGTACAGCTCGTCCATGCC	pCS2 ⁺ plasmids
Osk-084-XbaI-rev	GCTCTAGATGGTATGTTCTCCAGGGACGG	pCS2 ⁺ plasmids
GFP_KpnI_rev	GGGGGTACCTTACTTGTACAGCTCGTCCAT	pAttB plasmids

Name	Sequence (5' to 3' direction)	Cloning purpose
Buc-Bcl1-fw	GGGTGATCAATGTGGATCTCTGGAAACA GA	pAttB plasmids
buc_265bp_fw	ATTAACCCCCACTACCCCTCAGT	Buc deletions
buc_1bp_wo-loc_fw	ATGGAAGGAATAAATAACAATTCACAACC AATTAACCCCCACTACCCCTCAGTTGCAT CC	Buc deletions
Buc_1bp_ClaI_fw	GGGATCGATATGGAAGGAATAAATAACAA TTCAC	Buc deletions
eGFP_end_XbaI_rv	GGGTCTAGATTACTTGTACAGCTCGTCCA TGC	Buc deletions
Gateway Cloning		
buc_attB1_1-474bp_fw	GGGGACAAGTTTGTACAAAAAAGCAGGC TCTATGGAAGGAATAAATAACAATTCA	Buc deletions
buc_attB2_1-474bp_rv	GGGGACCACTTTGTACAAGAAAGCTGGG TTAGGGGTAGAAGAGACTACATTGTT	Buc deletions
buc_attB1_475- 1083bp_fw	GGGGACAAGTTTGTACAAAAAAGCAGGC TCTATGGATGTGGTGCAGGGAGAGAA	Buc deletions
buc_attB2_475- 1083bp_rv	GGGGACCACTTTGTACAAGAAAGCTGGG TTGCTGTAGGAATAAGCACTGCC	Buc deletions
buc_attB1_20-264bp_fw	GGGGACAAGTTTGTACAAAAAAGCAGGC TTAATGGGAGTTGGGCAACCTCA	Buc deletions
buc_attB2_20-264bp_rv	GGGGACCACTTTGTACAAGAAAGCTGGG TATCTTCTGTAATCAATTGGCT	Buc deletions
buc_attB1_265-474bp_fw	GGGGACAAGTTTGTACAAAAAAGCAGGC TTAATGATTAACCCCCACTACCCCTC	Buc deletions
buc_attB2_31-141bp_rv	GGGGACCACTTTGTACAAGAAAGCTGGG TAGCCATATGGATTCATGGGCC	Buc deletions
buc_attB1_142-264bp_fw	GGGGACAAGTTTGTACAAAAAAGCAGGC TTAATGCATTACGGTTTTTCCCGGGCC	Buc deletions
Loc792544_attB1_1- 3207bp_fw	GGGGACAAGTTTGTACAAAAAAGCAGGC TTAATGGAGTGTGCTGTGAAAAGTGTG	Interaction candidates
Loc792544_attB2_1- 3207bp_rv	GGGGACCACTTTGTACAAGAAAGCTGGG TACCGTGTCTCATCCTCATCATCT	Interaction candidates
pard3_attB1_1- 3360bp_fw	GGGGACAAGTTTGTACAAAAAAGCAGGC TTAATGAAAGTGACGGTGTGTTTTG	Interaction candidates
pard3_attB2_1- 3360bp_rv	GGGGACCACTTTGTACAAGAAAGCTGGG TAGTACCTGTCTGAAGTGGAGGGG	Interaction candidates
sept2_attB1_1- 1107bp_fw	GGGGACAAGTTTGTACAAAAAAGCAGGC TTAATGTCTCAAGCTGATAAACTGAAGC	Interaction candidates
sept2_attB2_1-1107bp_rv	GGGGACCACTTTGTACAAGAAAGCTGGG TACGCATCTTCATCTCCCTGCTTC	Interaction candidates
magoh_attB1_1- 441bp_fw	GGGGACAAGTTTGTACAAAAAAGCAGGC TTAATGTCCACGAGTGACTTTTATTTGA	Interaction candidates

Name	Sequence (5' to 3' direction)	Cloning purpose
magoh_attB2_1-441bp_rv	GGGGACCACTTTGTACAAGAAAGCTGGG TAGATGGGCTTGATTTTGAAGTGG	Interaction candidates
rrp45_attB1_1-1179bp_fw	GGGGACAAGTTTGTACAAAAAAGCAGGC TTAATGAGGGATACTCCGCTGTCAA	Interaction candidates
rrp45_attB2_1-1179bp_rv	GGGGACCACTTTGTACAAGAAAGCTGGG TATTTCTGCTTAGAAGTCTTCTTGGAT	Interaction candidates
prkaca_attB1_1-1056bp_fw	GGGGACAAGTTTGTACAAAAAAGCAGGC TTAATGGGCAACGCGCCCACCGCCA	Interaction candidates
prkaca_attB2_1-1056bp_rv	GGGGACCACTTTGTACAAGAAAGCTGGG TAGAATTCAGCAAACCTCTTCCACAT	Interaction candidates
ywhae_attB1_1-756bp_fw	GGGGACAAGTTTGTACAAAAAAGCAGGC TTAATGGGTGACCGGGAGGATTTGG	Interaction candidates
ywhae_attB2_1-756bp_rv	GGGGACCACTTTGTACAAGAAAGCTGGG TATTGGTTTTTCATCCTCCACATCT	Interaction candidates

2.6.1.1 Colony-PCR

A standard colony-PCR (Table 7) was used to verify for correct ligation clones after chemical transformation. Little of the bacteria colony was used as template in a 10 µl reaction containing 0.4 µM of each primer (Table 6, Table 9), 0.2 mM of each dNTP (Thermo Scientific, Wilmington, USA), 1 U of Taq polymerase (40 U/ml, homemade) in 1x PCR buffer (100 mM Tris (pH 8.4), 500 mM KCl, 15 mM MgCl₂, 0.01% gelatin, 1 mg/ml BSA). A TPersonal thermocycler (Biometra, Goettingen) was used to run a colony-PCR.

Table 7: Colony PCR program.

Step	Temperature [° C]	Time	Number of cycles
Initial denaturation	98	10 min] 25
Denaturation	98	10 s	
Primer annealing	Depending on Primer T _m	15 s	
Elongation	72	1 min/kb	
Final elongation	72	10 min	

2.6.2 Agarose gel electrophoresis

DNA or RNA was separated in an agarose gel, to which a horizontal electrical field was applied (Sharp et al., 1973). Depending on the size of the expected DNA or RNA fragments 0.5-2 % agarose gels were prepared in 1x TBE buffer (90 mM Tris (pH 8.0), 90 mM boric acid, 2 mM EDTA). 0.5 µg/ml ethidium bromide was added to the gel to visualize nucleic acids. Before loading, DNA samples were mixed with 10x loading dye (50 % glycerol, 0.4 % bromophenol blue), RNA samples were mixed with gel loading buffer II (Life Technologies, Carlsbad, USA). Gels were run in 1x TBE buffer at 80-100V. The 1 kb Plus DNA ladder (Life Technologies, Carlsbad, USA) was used to determine the size of DNA/RNA fragments. Gels were documented with the ChemiDoc gel documentation system (Bio-Rad, Munich). If

necessary, DNA fragments were cut out of the gel for purification using the UV-transilluminator (Herolab, Wiesloch) (Chapter 2.6.2.).

2.6.3 Purification of DNA

DNA was purified from agarose gels with the Invisorb Spin DNA Extraction Kit according to the manufacturer's instructions (Stratec Molecular, Berlin).

2.6.4 Restriction enzyme cloning

Restriction enzyme cloning was mostly used to attach an *egfp*-tag to the indicated genes and clone them into a pCS2⁺ expression vector (Table 3). Subsequently, the pCS2⁺ plasmids were used as templates to clone *egfp*-tagged genes into the pAttB_UASp2B3 vector (Table 3). The resulting constructs were used for generating transgenic flies (Chapter 2.3.3). Inserts were amplified by PCR and subsequently digested with the indicated restriction enzymes (Table 3). The digested insert was purified on an agarose gel and afterwards ligated into the indicated digested vector (Table 3).

2.6.4.1 Restriction enzyme digestion

DNA was digested with restriction endonucleases according to the manufacturer's instructions (Fermentas Life Sciences, St. Leon-Rot).

2.6.4.2 Ligation of DNA

DNA was ligated with T4 DNA ligase according to the manufacturer's instructions (Fermentas Life Sciences, St. Leon-Rot). A molar ratio of vector DNA and insert DNA of 1:5 was applied with a 50 ng of vector DNA. 5 U of T4 DNA ligase (Fermentas Life Sciences, St. Leon-Rot) were used in a 20 µl reaction. The ligation reaction was incubated overnight at 16 °C and 10 µl of the ligation reaction were subsequently transformed into bacteria (Chapter 2.6.6).

2.6.5 Gateway cloning

The Gateway cloning technology (Life Technologies, Carlsbad, USA) is based on a site-specific recombination reaction, with which DNA-fragments can be transferred between plasmids without the use of restriction enzymes. Gateway cloning was used to clone the *buc* fragments *egfp*- or *mcherry*-tagged and to clone the *Buc* interaction candidates *egfp*-tagged. Inserts were amplified by PCR with primers containing an "attB" recombination site (Table 6). The PCR product, containing "attB" recombination sites, was purified and directly used for a Gateway BP recombination reaction into the donor vector pDONR221, which contains "attP" recombination sites. In the successfully cloned entry clone, the recombination sites were recombined to "attL" recombination sites. In a so-called multisite Gateway LR recombination reaction, the entry clone itself was recombined with the destination vector (containing "attR" recombination sites) and another entry clone, containing the tag of choice (containing an "attR" and an "attL" recombination site). The resulting expression vector,

containing the gene of interested cloned to the selected tag, was subsequently used for *in vitro* transcription (Chapter 2.6.10). Constructs were recombined as described by the manufacturer (Life Technologies, Carlsbad, USA) with the exception that 50 % of the recommended enzyme amount was used.

2.6.6 Chemical transformation

100 µl of competent XL1-Blue (*ecA1 endA1 gyrA96 thi-1 hsdR17 supE44 relA1 lac* [F' *proAB lacIqZΔM15 Tn10* (Tetr)]; Stratagene, Waldbronn) or DH5α (F- Φ80*lacZΔM15 Δ(lacZYA-argF)* U169 *recA1 endA1 hsdR17* (rK-, mK+) *phoA supE44 λ- thi-1 gyrA96 relA1*; Life Technologies, Carlsbad, USA) were thawed on ice. Once thawed, 100-500 ng of plasmid DNA or 5 µl of ligation mix were added. The mixture was incubated for 60 min on ice followed by a heat shock for 90 s at 42 °C and incubation for 2 min on ice. After addition of 900 µl LB medium (1 % Bacto-Trypton, 1 % NaCl, 0.5 % yeast extract, pH 7.5), the cells were shaken for 60 min at 37 °C and 220 rpm. Afterwards the bacteria were seeded on 1.5 % LB-agar plates supplemented with the appropriate antibiotics for the selection of transformed bacteria (0.1 mg/ml ampicillin, 0.05 mg/ml kanamycin; Biomol, Hamburg) and incubated at 37 °C overnight.

2.6.7 Plasmid DNA preparation

Plasmid DNA from bacteria culture was isolated with the NucleoBond Xtra Midi Kit (Macherey and Nagel, Dueren) according to the manufacturer's instructions. The DNA was quantified with the NanoDrop 2000c spectrophotometer (Thermo Scientific, Wilmington, USA).

2.6.8 DNA sequencing analysis

To validate the sequence of a cloned construct, the DNA was sequenced by the Dye-termination method (modified from Sanger et al. (1977)) using the Big Dye Terminator Kit (Applied Biosystems, Darmstadt) according to the manufacturer's instructions. 200-400 ng DNA were added to the sequencing PCR mix (1.5 µl Seq-mix, 1.5 µl Seq-buffer, 1 µM sequencing primer (Table 9) (Eurogentec, Cologne), ad 10 µl dH₂O). After the PCR (Table 8) the DNA fragments were precipitated in ethanol (100% ethanol, 60 mM sodium acetate (pH 5.4)) for 5 min at room temperature. The sample was centrifuged for 15 min at maximum speed and the pellet washed in 70 % ethanol. After air-drying, the pellet was dissolved in 15 µl HiDi buffer (Applied Biosystems, Darmstadt). The samples were sequenced with the ABI 3100 Automated Capillary DNA Sequencer (Applied Biosystems, Darmstadt).

Table 8: Sequencing PCR program.

Step	Temperature [° C]	Time	Number of cycles
Initial denaturation	96	5 min	25
Denaturation	96	30 s	
Primer annealing	Depending on Primer Tm	20 s	
Elongation	60	4min	

Table 9: Primers used for sequencing.

Name	Sequence (5' to 3')
SP6	ATTTAGGTGACACTATAGAA
T7 (Pcs2+)	GTAATACGACTCACTATAG
T3	TATTAACCCTCACTAAAGGG
eGFP-end_fw	ACATGGTCCTGCTGGAGTTC
GFP_begin_rv	CTTCATGTGGTCGGGGTAGC
GFPfor	CACAAGTTCAGCGTGTCCGG
GFPrev	CAAAGACCCCAACGAGAAGC
mCherry-end_fw	CGGCGCCTACAACGTCAACA
mCherry-begin_rv	TTGGTCACCTTCAGCTTGGC
4rev	CTTTTGAATTCTCTTATCTGCT
4fw	ACTTTGGCCGTCCCTATATG
3rev	CGGGAAAACCGTAATGGC
Name	Sequence (5' to 3')
new_fifw	GCACAGTAATAAAAACAAAGACA
HP2	CAGGGTAGATTGGATGAATGT
Hp4	CAATCTCTCGTTCAAGACTGAG
oskexon3rev	GATCGTCAGTCCGGATACAC
oskexon2fw	CGAAAACCTGACGGGCAATCC
prd3_seq1_fw	CACTGCGCACCAATATGCCT
prd3_seq2_fw	GGAGATCTGCGCAACGTTCG
prd3_seq3_fw	TCTCTCTGCTAAGGGCGACG
prd3_seq4_fw	GCACAAATAACCGCAAAATG
loc792544_seq1_fw	CGATCACTTTCAGACACTAAA
loc792544_seq2_fw	CCAAGACGTCGAAGTAAATC
loc792544_seq3_fw	ACAGCAGGGTCAGAAGAAGA

2.6.9 cDNA synthesis

2.6.9.1 RNA extraction from oocytes

Total RNA extracted from oocytes was used as template for cDNA synthesis. Half an ovary was lysed in 500 μ l peqGOLD TriFast (PEQLAB Biotechnologie, Erlangen) and vortexed for 1 min until the ovary completely dissolved. 80 μ l of chilled chloroform was added, the sample was vortexed for 30 s and subsequently centrifuged for 10 min at 4 °C. The upper phase was mixed with 200 μ l of chloroform, vortexed for 30 s and centrifuged for 5 min at 4 °C. Nucleic acids were precipitated in 200 μ l isopropanol for 30 min at -20 °C and subsequently pelleted by centrifugation for 30 min at 4 °C. The pellet was washed with 400 μ l of 80 % ethanol. After air-drying, the pellet was resuspended in 12.5 μ l RNase free water. DNA was digested and RNA purified with the RNAqueous-Micro Kit (Life Technologies, Carlsbad, USA) according to the manufacturer's instructions. RNA concentration was determined with the NanoDrop 2000c spectrophotometer (Thermo Scientific, Wilmington, USA). Extracted RNA was stored at -20 °C.

2.6.9.2 Reverse transcription

Complementary DNA (cDNA) was synthesized from 100 ng extracted RNA in a 10 μ l reaction containing 1x Go Taq Flexi buffer (Promega, Fitchburg, USA), 5 mM MgCl₂, 5 mM dNTPs (Thermo Scientific, Wilmington, USA), 2.5 μ M random hexamer primers (Life Technologies, Carlsbad, USA), 8 U Ribolock RNase inhibitor (40 U/ μ l; Thermo Scientific, Wilmington, USA) and 8 U MuLV reverse transcriptase (20 U/ μ l; Roche, Mannheim). The random primers were annealed for 10 min at 20 °C, cDNA was synthesized for 60 min at 42 °C and the reaction was terminated for 5 min at 95 °C. cDNA was stored at -20 °C and used as template in cloning PCRs.

2.6.10 *In vitro* transcription

Capped sense RNA for microinjection into zebrafish was synthesized *in vitro* embryos using the SP6 mMessage mMachine kit as described by the manufacturer (Life Technologies, Carlsbad, USA). 0.5-1 μ g of linearized DNA was used as template in a 3 h reaction at 37 °C. The RNA was afterwards purified with Illustra Probe Quant G-50 columns as described by the manufacturer (GE Healthcare, Little Chalfont, UK). RNA quantity was determined with the NanoDrop 2000c spectrophotometer (Thermo Scientific, Wilmington, USA) and RNA quality was verified by agarose gel electrophoresis (Chapter 2.6.2).

2.7 Biochemical methods

2.7.1 Generation of Buc antibody

The Buc antibody was raised in guinea pig against recombinant full length Buc (BioGenes, Berlin). The serum was column purified and tested for the specific binding to recombinant Buc. The antibody specificity was verified in western blots of embryonic *buc-gfp* lysates immunostained for Buc and GFP.

2.7.2 SDS-polyacrylamide gel electrophoresis

Proteins were separated under denaturing conditions corresponding to their molecular weight by SDS-polyacrylamide gel electrophoresis (SDS-PAGE) (Laemmli, 1970). Protein samples were mixed with 2x SDS loading buffer (100 mM Tris (pH 6.8), 20 % glycerol, 4 % SDS, 200 mM β -mercaptoethanol, 0.02 % bromophenol blue), incubated for 5 min at 96 °C and loaded on a 8-10 % gel, depending on the size of the expected band (Sambrook and Russel, 2001). The Page Ruler prestained protein ladder (Thermo Scientific, Wilmington, USA) was separately loaded to determine the molecular weight of the proteins. SDS-polyacrylamide gels were run vertically in 1x Laemmli buffer (25 mM Tris, 250 mM glycine, 0.01 % SDS) at a constant voltage of 70 V. After the dye front reached the resolving gel, the voltage was raised to 120 V. Subsequent to the run, the gel was Coomassie stained or further used for western blotting.

2.7.3 Coomassie staining

Proteins in a SDS-polyacrylamide gels were visualized by Coomassie staining. Gels were rinsed with dH₂O and incubated in Coomassie staining solution (50 % methanol, 10 % glacial acetic acid, 0.1 % Coomassie Brilliant Blue) for 1 h at room temperature. Subsequently, gels were rinsed three times with dH₂O and incubated in destaining solution (40 % methanol, 10 % glacial acetic acid) over night at room temperature.

2.7.4 Western blotting

To detect specific proteins in a protein lysate, proteins were transferred to a nitrocellulose membrane after SDS-PAGE by semi-dry blotting (Sambrook and Russel, 2001; Towbin et al., 1979). The proteins were transferred for 70min at 25 V soaked in protein blotting buffer (39 mM glycine, 48 mM Tris, 0.037 % SDS, 20 % methanol). After protein transfer, the membrane was incubated in 5 % milk powder in TBST (10 mM Tris (pH 8.0), 150 mM NaCl, 0.05 % Tween20) for 1 h at room temperature to prevent unspecific binding of the primary antibody. Subsequently, the membrane was incubated overnight at 4 °C in TBST + 5 % milk containing the diluted antibody (Table 10). After washing the membrane 3 x 5 min in TBST, the membrane was incubated light-protected for 1 h at room temperature in TBST containing the diluted fluorescently coupled secondary antibody (Table 10). Next, the membrane was washed 3 x 5 min in TBST and the fluorescent signal was detected by the Li-Cor Odyssey CLx Infrared Imaging system (Li-Cor, Lincoln, USA) and analyzed with the Image Studio Software (Li-Cor, Lincoln, USA).

Table 10: Antibodies used for western blotting.

Antibody	Dilution
guinea pig- α -Buc (BioGenes, Berlin)	1:5000
mouse- α -Actin (MerckMillipore, Darmstadt)	1:1000
goat- α -guinea pig 800CW (IRDye, Li-Cor)	1:20000
goat- α -mouse 680CW(IRDye, Li-Cor)	1:20000

2.7.5 Co-Immunoprecipitation

Co-immunoprecipitation (Co-IP) was used to investigate Buc protein-protein interactions. For each sample 500 deyolked high stage embryos (Chapter 2.2.3) were homogenized on ice in lysis buffer (10 mM Tris (pH 7.5), 150 mM NaCl, 0.5 mM EDTA, 0.5 % NP-40, 1x complete protease inhibitor cocktail (Roche, Mannheim)). The supernatant was subsequently used for the Co-IP using a GFP-binding protein coupled to magnetic beads (GFP-Trap_M; ChromoTek, Planegg-Martinsried). Co-IP was performed according to the manufacturer's instructions. Subsequent to the Co-IP, the magnetic beads with the bound proteins were either incubated with 2x SDS loading buffer for 5 min at 96 °C and analyzed via SDS-PAGE and western blotting or handed over for analysis by mass spectrometry (Core Facility of Proteome Analysis, UMG, Goettingen).

2.7.6 Fixation of zebrafish oocytes

Zebrafish oocytes were fixated for subsequent immunostaining. To collect the oocytes, a female fish was sacrificed, the ovaries were dissected and transferred into OR2 buffer (5 mM HEPES (pH 7.5), 82.5 mM NaCl, 2 mM KCl, 1 mM MgCl₂). Ovaries were dissociated for 3 min at room temperature in Proteinase K solution (0.1 M Tris (pH 7.5), 10 mM EDTA, 50 µg/ml Proteinase K (Merck, Darmstadt)). Afterwards, the oocytes were washed twice with MEMFA (0.1 M MOPS (pH7.4), 1 mM MgSO₄, 2 mM EGTA, 3.7 % formaldehyde) and subsequently fixated for 1 h at room temperature in MEMFA. Afterwards, the ovaries were washed three times with PBT (137 mM NaCl, 10 mM Na₂HPO₄, 2.7 mM KCl, 1.76 mM KH₂PO₄ (pH 7.4), 0.1 % Triton X-100, 0.2 % BSA). Ovaries were stored in PBT at 4 °C for up to 5 days or directly used for immunostaining.

2.7.7 Fixation of zebrafish embryos

Zebrafish embryos were fixated for subsequent immunostaining. Embryos were collected at the stage of choice, dechorionated by pronase treatment (Chapter 2.2.2) and fixated for 6 h at room temperature and subsequently overnight at 4 °C in 4 % paraformaldehyde in PBS (137 mM NaCl, 10 mM Na₂HPO₄, 2.7 mM KCl, 1.76 mM KH₂PO₄ (pH 7.4)). Subsequently, the embryos were washed three times with PBS and dehydrated in a methanol dilution series. The embryos were stored in 100 % methanol at -20 °C until further usage. Before the embryos were immunostained, they had to be gradually rehydrated in PBT

2.7.8 Immunostaining of zebrafish embryos and oocytes

After the distinct fixation protocols for oocytes and embryos, they were immunostained to visualize endogenous protein with the same protocol. For reasons of legibility only oocytes will be named in the following. Oocytes were blocked for 2 h at room temperature in PBT blocking solution (PBT (Chapter 2.7.6), 2 % BSA, 2 % horse serum) to prevent unspecific binding of the primary antibody. Afterwards the oocytes were incubated overnight at 4 °C in PBT blocking solution containing the diluted primary antibody (Table 11). After washing 3 x 15 min with PBT, the oocytes were incubated overnight at 4 °C in PBT blocking solution containing the diluted secondary antibody (Table 11). Subsequent to washing for 3 x 15 min

with PBT, oocytes were counterstained for 1 h at room temperature with PBT blocking solution containing 0.8 $\mu\text{g/ml}$ DAPI. After washing 3 x 15 min with PBT, the oocytes were dehydrated in a methanol dilution series and stored in 100 % methanol at -20°C . For imaging, the oocytes were transferred to a imaging dish (Fluorodish 35 mm; WPI, Sarasota, USA), the methanol was removed and the yolk was cleared by addition Murray's clearing medium (2/3 benzyl benzoate, 1/3 benzyl alcohol). Embryos were manually deyolked prior to clearance of the remaining yolk. Oocytes and embryos were imaged using a LSM780 confocal microscope (Carl Zeiss Microscopy, Jena) and images were analyzed using the ZEN 2011 software (Carl Zeiss Microscopy, Jena).

Table 11: Antibodies used for immunostaining.

Antibody	Dilution
guinea pig- α -Buc (Biogenes, Berlin)	1:5000
rabbit- α -Vasa (gifted by Prof. Dr. Knaut; (Knaut et al., 2000))	1:500
rabbit- α -Exosc9 (Aviva Systems Biology San Diego, USA)	1:200
rabbit- α -p-NMII (Cell Signaling Technology, Danvers, USA)	1:50
GFP-booster Atto 488 (ChromoTek, Planegg-Martinsried)	1:500
goat- α -guinea pig Alexa Fluor 488 (Life Technologies, Carlsbad, USA)	1:500
goat- α -rabbit Alexa Fluor 594 (Life Technologies, Carlsbad, USA)	1:500

2.8 Cell biology methods

2.8.1 Live-Cell Imaging

Living embryos of the transgenic *buc-gfp* line were imaged to analyze the localization of Buc-GFP. For imaging with the stereo microscope SteREO Lumar.V12 (Carl Zeiss Microscopy, Jena), embryos were manually dechorionated and mounted in 1.5 % agarose coated dishes filled with 1x E3 medium (Chapter 2.2.2). Images were analyzed using the software Axio Vision Rel. 4.8 (Carl Zeiss Microscopy, Jena). For imaging with the LSM780 confocal microscope (Carl Zeiss Microscopy, Jena) embryos were mechanically dechorionated, placed in a Fluorodish (WPI, Sarasota, USA) with a handmade grid, covered with 1x E3 and imaged from below. Images were analyzed using the ZEN 2011 software (Carl Zeiss Microscopy, Jena).

2.9 Bioinformatics methods

2.9.1 Pairwise sequence alignment

Protein sequences were pairwise aligned by the Needleman-Wunsch algorithm with the EMBL-EBI alignment software EMBOSS Needle (McWilliam et al., 2013). Standard settings

were applied. Zebrafish Bucky ball (H0WFA5), Vasa (O42107), *Drosophila* Oskar (short isoform C, P25158-2; long isoform A, P25158) and *Drosophila* Vasa (P09052) sequences have been used for the alignments.

2.9.2 Multiple sequence alignments

Multiple sequence alignments of Buc and Osk homologs have been accomplished in collaboration with Dr. Thomas Lingner (Department of Bioinformatics, Georg August University Göttingen) with the T-Coffee software of the EMBL-EBI (McWilliam et al., 2013). Following Buc vertebrate homologs (gi number is given) were used: 292610748, 47225100, 148230857, 301615136, 118086206, 513169733, 73976581, 327275069, 642119256, 410909482, 432930267.

2.9.3 Hidden Markov models analysis

Hidden Markov models analysis was performed in collaboration with Dr. Thomas Lingner by HMMER (<http://hmmer.janelia.org/>) (Finn et al., 2011). Using this method, remote homologs can be detected more accurately in comparison to BLAST.

2.9.4 Protein sequence analysis

The amino acid composition of protein sequences was calculated with ProtParam (<http://web.expasy.org/protparam/>) (Gasteiger et al., 2003). Putative SH3 domain interaction sites were identified by SH3-Hunter (<http://cbm.bio.uniroma2.it/SH3-Hunter/>) (Ferraro et al., 2007). To avoid false positives, a precision level of 70 % or more was set as a threshold.

2.9.5 Analysis mass spectrometry data

Overlaps in protein interactions between each Co-IP sample were analyzed using a Venn diagram generator (<http://jura.wi.mit.edu/bioc/tools/venn3way/index.php>).

The Kyoto Encyclopedia of Genes and Genomes (KEGG, <http://www.genome.jp/kegg/>) has been used to classify the BucLoc-eGFP interaction candidates in collaboration with Dr. Thomas Lingner.

2.10 Statistical methods

For statistical analysis of experiments the indicated statistical tests have been carried out with the Prism software (GraphPad Software, La Jolla, USA).

3 Results

3.1 Buc is a permanent germ plasm component

Vertebrates including birds, frogs and zebrafish specify their primordial germ cells by inheritance of cytoplasmic determinants compacted in the structure of the germ plasm. Thus, proper localization of the germ plasm is a critical process during the early development of the embryo. Buc regulates the formation of primordial germ cells in the embryo and germ plasm aggregation in the oocyte (Bontems et al., 2009). Therefore, the localization of Buc as a germ plasm regulator is essential for proper germ cell specification. However, so far nothing was known about the endogenous localization of Buc protein.

3.1.1 Buc is continuously localized to the germ plasm during oogenesis

The loss of the Balbiani body structure in the *buc* mutant indicates a role of endogenous Buc already early in oogenesis (Bontems et al., 2009). Nonetheless, it was not known whether Buc localizes to the germ plasm in the Balbiani body. To investigate the so far unknown localization of endogenous Buc, a new polyclonal antibody was obtained, raised against recombinant full length Buc (BioGenes, Berlin).

3.1.1.1 Buc is a permanent germ plasm component in oocytes

To examine the localization of Buc during zebrafish oogenesis, oocytes of different stages were immunostained for Buc and analyzed by confocal fluorescence microscopy.

Buc was localized to the Balbiani body, positioned between the nucleus and the vegetal cortex, already in early oocytes (stage IA) (Figure 8A) (see Figure 3 for oocyte stages). In parallel with the growing oocyte the Balbiani body increased in size and converged to the cortex at early stage IB (Figure 8B). This localization has been reported previously for *buc* mRNA and other RNA germ plasm components (Bontems, 2009; Howley and Ho, 2000; Kosaka et al., 2007). At late stage IB, the Balbiani body localized to the vegetal cortex and started to disassemble into Buc positive aggregates, spreading along the vegetal cortex (Figure 8C, D). Buc was spread almost along the entire cortex from vegetal to animal pole at early stage II, while some Buc aggregates were present in the cytoplasm (Figure 8E). These aggregates disappeared during progression through stage II, while the cortical Buc aggregates were stable (Figure 8F). At stage III, Buc was no longer detected (Figure 8G). The localization pattern of Buc in early oogenesis is consistent with the localization of the germ plasm marker *vasa* mRNA (Braat et al., 1999; Howley and Ho, 2000).

The germ plasm regulator Buc localizes as expected to the Balbiani body and in addition continues to be localized to the germ plasm throughout oogenesis. So far, the localization dynamics of germ plasm in oogenesis have been described in detail only by germ plasm mRNAs (Braat et al., 1999; Howley and Ho, 2000). Thus, Buc is the first protein that marks to the germ plasm throughout early zebrafish oogenesis.

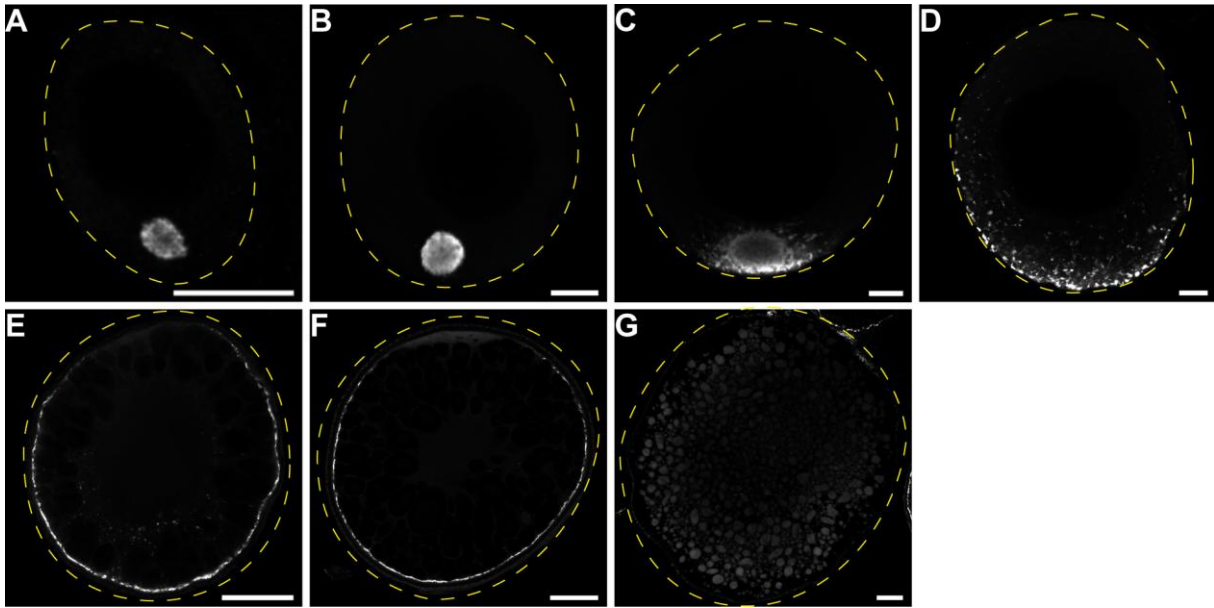


Figure 8: Endogenous Buc localizes to the Balbiani body and spreads along the vegetal cortex during oogenesis. Wild type oocytes stages IA (A), early IB (B), late IB (C,D), early II (E), late II (F) and III (G) immunostained for Buc and imaged by confocal fluorescence microscopy. Oocytes are shown in lateral view, animal pole to the top and outlined by a yellow dashed line. Scale bars represent 10 μm (A-D) and 50 μm (E-F).

3.1.1.2 Localization of Buc is lost in *buc* mutant oocytes

In the early oocyte, Buc function is already required for assembly of the Balbiani body and proper localization of germ plasm components (Bontems et al., 2009; Marlow and Mullins, 2008). The *buc* mutant alleles *buc^{p106}* and *buc^{p43}* contain nonsense mutations that result in premature stop codons (Bontems et al., 2009). Hence, before analyzing Buc protein in mutant oocytes, the specificity of the newly generated polyclonal Buc antibody had to be investigated. To analyze if the Buc antibody detects Buc^{p43}, embryos were lysed after overexpression of *buc^{p43}-egfp*, and analyzed by western blotting with α -Buc and α -Actin. The Buc antibody detected a band slightly below 70 kDa, which matches the expected size of 67.5 kDa for Bucp43-eGFP (Figure 9A). This shows that the newly generated Buc antibody is able to detect the Buc^{p43} mutant protein.

To examine if Buc mutant protein is expressed and properly localized in the *buc^{p106}* and *buc^{p43}* mutants, wild type, *buc^{p106}* and *buc^{p43}* mutant oocytes were immunostained for Buc, co-stained with Vasa and analyzed by confocal fluorescence microscopy. In wild type stage IB oocytes, Buc localized to the Balbiani body as expected and Vasa localized around the germinal vesicle as described previously (Figure 9B) (Knaut et al., 2000). However, in *buc^{p106}* as well as *buc^{p43}* mutant oocytes no localization of Buc was detected. On the contrary, Vasa was still localized to the perinuclear region (Figure 9B).

This result shows that Buc localization is absent in mutant oocytes and indicates that this loss might lead to the defect in Balbiani body formation as described previously for *buc* mutant oocytes (Bontems et al., 2009; Marlow and Mullins, 2008). Moreover, the immunostainings suggest the loss of Buc protein expression in the mutant oocytes.

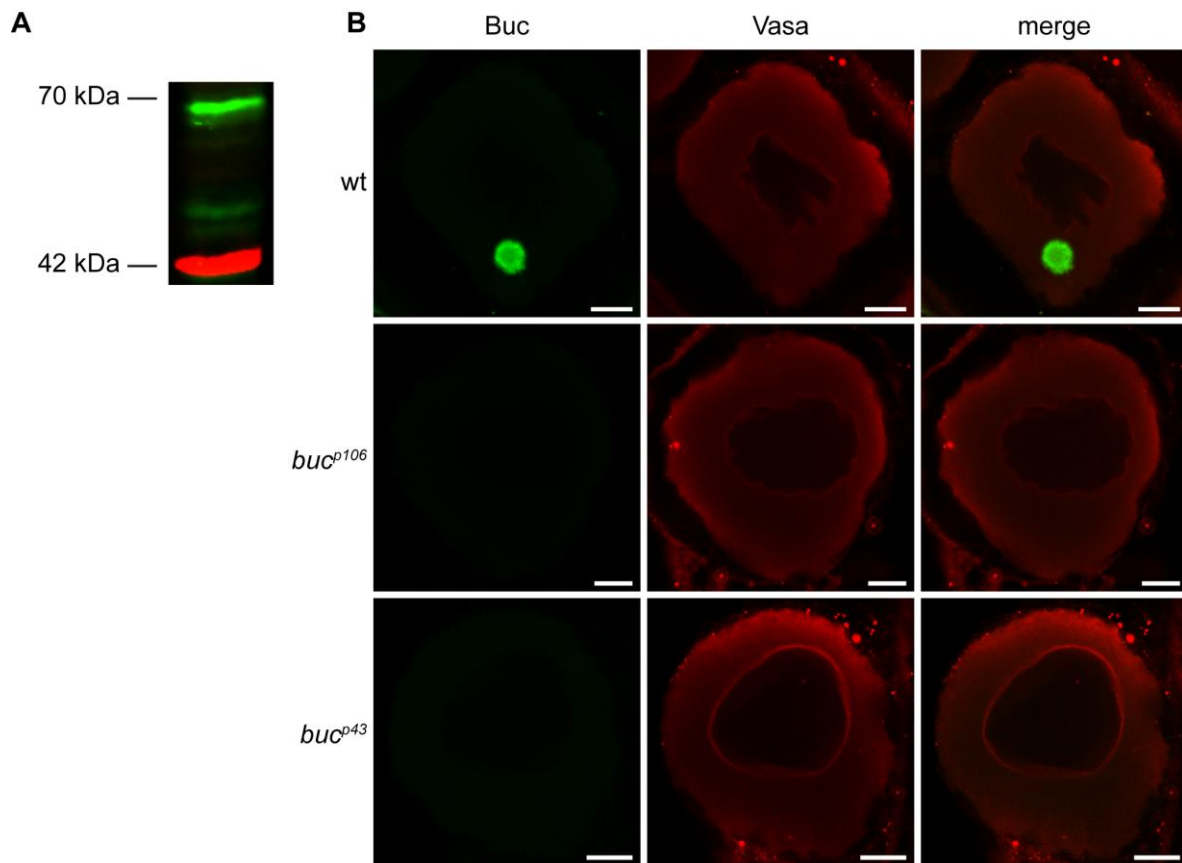


Figure 9: Buc does not localize to the Balbiani body in *buc* mutant oocytes. (A) Western blot of Buc^{p43}-eGFP detected with α -Buc (green) by Li-Cor infrared detection. Actin (red) served as a loading control. An equivalent amount to ten wild type embryos (2.5 hpf), overexpressed with Buc^{p43}-eGFP, was loaded. (B) Wild type, mutant *buc*^{p106} and mutant *buc*^{p43} oocytes (early IB stage) immunostained for Buc (green) and Vasa (red) and imaged by confocal fluorescence microscopy. Vasa served as an immunostaining control. Oocytes are shown in lateral view, animal pole to the top. Scale bars represent 10 μ m.

3.1.1.3 Transgenic Buc-GFP reflects endogenous Buc in oocytes

The localization dynamics of zebrafish Buc are of special interest as Buc regulates the germ plasm aggregation in the oocyte and formation of primordial germ cells in the embryo (Bontems et al., 2009). To study the dynamic localization of Buc, a transgenic zebrafish *buc-gfp* line expressing one copy of *buc-gfp* in the *buc*^{p106} homozygous mutant background was generated (Bontems, 2009). In this study, this line was crossed further to obtain a stable line with two copies of *buc-gfp*. This transgenic *buc-gfp* line rescued the mutant phenotype, demonstrating that the transgene mirrors the activity of endogenous Buc.

To analyze if transgenic Buc-GFP localizes to the germ plasm similar to endogenous Buc, wild type and *buc-gfp* transgenic oocytes were immunostained for endogenous Buc or GFP and examined by confocal fluorescence microscopy. In wild type stage IB oocytes, transgenic Buc-GFP was localized to the Balbiani body near the vegetal pole of the oocyte (Figure 10C). During late stage IB, Buc-GFP was relocated to the vegetal pole and started spreading along the cortex (Figure 10D). This localization of transgenic Buc-GFP is identical to endogenous Buc (Figure 10A, B). To rule out differences in the localization of Buc-GFP and endogenous Buc due to the use of different antibodies, transgenic *buc-gfp* stage IB oocytes were additionally immunostained for endogenous Buc. Both antibodies marked the Balbiani body (Figure 10C, C'). Most likely due to different penetration abilities, the GFP antibody gave a

more uniform signal in comparison to the Buc antibody, which gave a stronger signal at the Balbiani body periphery.

In conclusion, transgenic Buc-GFP localizes to the germ plasm in oocytes and thus reflects the localization of endogenous Buc. Therefore, the transgenic *buc-gfp* line can be used to analyze the localization of Buc *in vivo*.

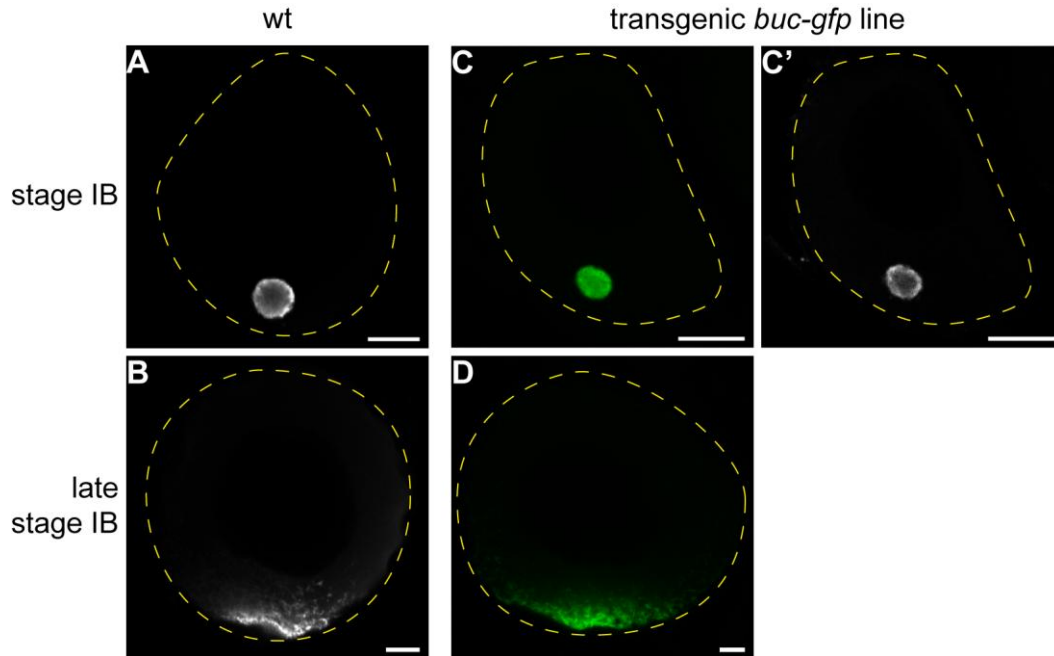


Figure 10: Transgenic Buc-GFP reflects the localization of endogenous Buc in oocytes. Wild type (A, B) and transgenic *buc-gfp* (C, C', D) stage IB and late stage IB oocytes immunostained for Buc (white; A, B, C') or GFP (green; C, D) and imaged by confocal fluorescence microscopy. Note that Buc as well GFP antibodies mark the Balbiani body in the transgenic *buc-gfp* line. Oocytes are shown in lateral view, animal pole to the top and outlined by a yellow dashed line. Scale bars represent 10 μm .

In summary, these results show that throughout oogenesis, endogenous Buc is localized to the germ plasm and this localization is reflected by transgenic Buc-GFP. Hence, Buc protein localization correlates with the expected localization deduced from the functional observations in the *buc* mutant.

3.1.2 Buc is localized to the germ plasm during early embryogenesis

So far, the localization of germ plasm during early embryogenesis (0-4 hpf) has been examined in detail only by analyzing localization of mRNA germ plasm components, such as *vasa* mRNA (Braat et al., 1999; Yoon et al., 1997). However, very little is known about the localization of protein germ plasm components during cleavage and blastula stages.

3.1.2.1 Transgenic Buc-GFP marks germ plasm *in vivo*

The localization of zebrafish Buc during early embryogenesis is of special interest as Buc is able to induce the formation of primordial germ cells in the embryo (Bontems et al., 2009). As *buc* mRNA was not localized and only expressed during the first four hours of early embryogenesis, it was unclear how Buc protein is localized or if it is expressed at all.

The transgenic *buc-gfp* line was used to investigate the localization of Buc in different stages

of living embryos by stereo or confocal fluorescence microscopy. In 1-cell stage embryos, Buc-GFP was localized in small granules at the cytokinetic ring by the vegetal part of the embryo, leaving the animal pole free of granules (Figure 11). During cytokinesis, these granules were recruited to the distal ends of the first and second cleavage furrows, thus forming four aggregates at the 4-cell stage (Figure 11). At this stage, a considerable amount of small granules was still present at the cortex of the embryo. The four aggregates were stable during early cleavage stages resulting in a 256-cell stage embryo with four aggregates in the cortical region of the embryo (Figure 11). Until this stage, Buc-GFP granules and other smaller aggregates had disappeared, suggesting their degradation or fusion with the four main aggregates.

Buc-GFP localization in living *buc-gfp* embryos mimics the localization pattern of previously described germ plasm components such as *vasa* mRNA (Yoon et al., 1997). Hence, the newly generated transgenic *buc-gfp* line is the first transgenic line that marks the germ plasm *in vivo* throughout cleavage and blastula stages.

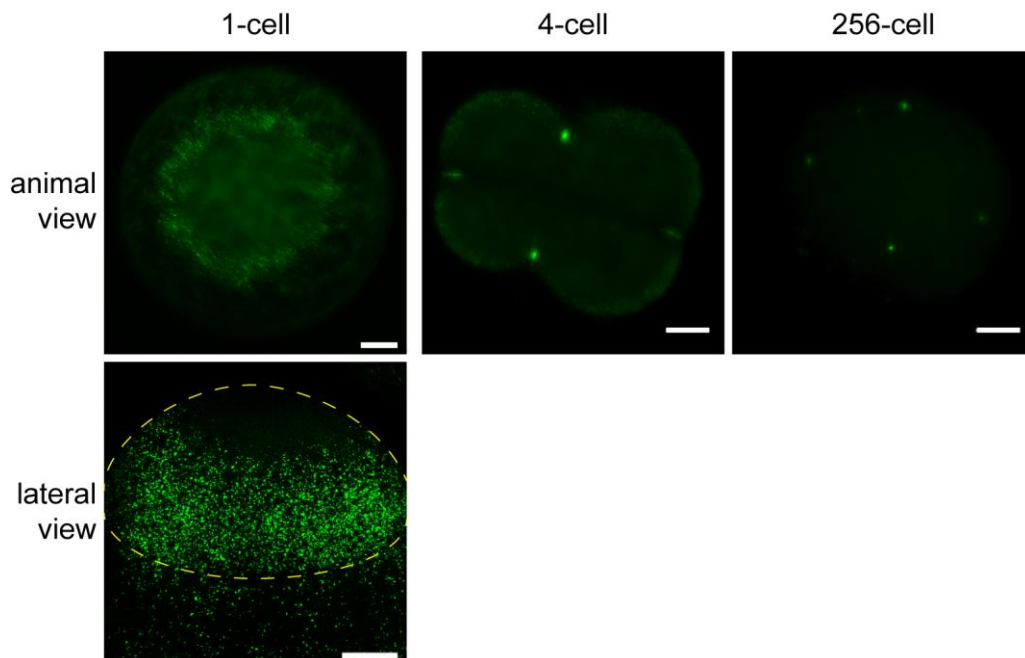


Figure 11: Buc-GFP localizes to the germ plasm during early embryogenesis. Transgenic *buc-gfp* embryos at indicated stages imaged by fluorescence microscopy. Embryos are depicted in animal view. A Confocal z-stack projection of a 1-cell stage embryo is additionally depicted in a lateral view, animal pole to the top. The Blastomere is outlined by a yellow dashed line. The image of the 256-cell stage embryo is likewise a z-stack projection. Scale bars represent 100 μm .

3.1.2.2 Buc-GFP is maintained only in the first and second cleavage furrow

It has been described previously that, in addition to the four aggregates at the cleavage furrows, small granules of *vasa* mRNA are localized to the distal cortex of all four cells in 4-cell stage embryos (Wolke et al., 2002). However, due to the lack of *in vivo* reporters, the role of these granules at the cortex is not known.

To study the dynamics of these additional granules in detail, living transgenic *buc-gfp* embryos were imaged in high resolution time-lapse movies (digital Appendix, Chapter 7.4). Similar to *vasa* transcripts, Buc-GFP protein localized in these granules at the cortex in early

cleavage stages (Figure 12). At the onset of 8-cell stage, small Buc-GFP granules seemed to fuse with the closely adjacent aggregates in the first and second cleavage furrow. Additionally, granules accumulated at the distal ends of the forming third cleavage furrows (Figure 12). However, the aggregations in the third cleavage furrows were unstable and disassembled at the beginning of the 16-cell stage. The disassembled granules as well as the smaller granules in the cortical region were strongly reduced in number during further development of the embryo (Figure 12). In contrast to the small granules, the four aggregates originating from the first two cleavage furrows were stabilized in a rod-like structure.

Hence, smaller cortical Buc-GFP granules are only temporary stable whereas the first four aggregates at the distal ends of the first and second cleavage furrow are stable. This observation suggests that proper localization of germ plasm is crucial for its stabilization and the inheritance of the germ cell fate. This four cells with inherited Buc-GFP labeled germ plasm are in line with the identification of four founding primordial germ cells at late blastula stage (Wolke et al., 2002; Yoon et al., 1997).

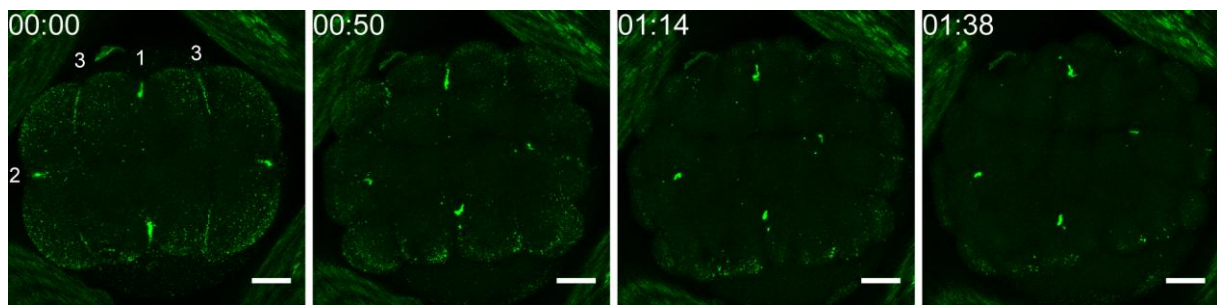


Figure 12: Buc-GFP is stable only in four condensed rod-like aggregates during early embryogenesis. Still pictures of a time lapse movie showing a transgenic *buc-gfp* embryo starting at onset of 8-cell stage and ending at onset of 128-cell stage imaged by confocal fluorescence microscopy. Note that the signal at the cortex disappears over time. Embryo is shown in animal view. Numbers at eight-cell stage indicate first, second and third cleavage furrows. Images are z-stack projections. Scale bars represent 100 μ m.

3.1.2.3 Transgenic Buc-GFP reflects endogenous Buc during early embryogenesis

The transgenic *buc-egfp* line marks the germ plasm *in vivo*. However, the GFP-tag might alter the localization and thus Buc-GFP does not reflect endogenous Buc.

To investigate, whether Buc-GFP localization resembles the so far unknown localization of endogenous Buc during early zebrafish embryogenesis, wild type embryos were analyzed by Buc immunostaining and subsequent confocal fluorescence microscopy. For comparison, living transgenic *buc-gfp* embryos were examined by stereo fluorescence microscopy at comparable stages. Endogenous Buc was localized in two aggregates at the distal ends of the first cleavage furrow in 2-cell stage embryos (Figure 13A). In addition, smaller granules were localized at the cortex of the embryo, similar to Buc-GFP in living transgenic embryos (Figure 13B). Identical localization of endogenous Buc and transgenic Buc-GFP persisted throughout early embryogenesis, leading to four aggregates and some smaller clusters at early blastula stages (2.5-3 hpf, Figure 13A, B).

These results show that endogenous Buc is localized to the germ plasm till blastula stage as previously described for the germ plasm component *vasa* mRNA (Yoon et al., 1997). The

endogenous Buc localization during early embryogenesis is reflected by transgenic Buc-GFP in living embryos.

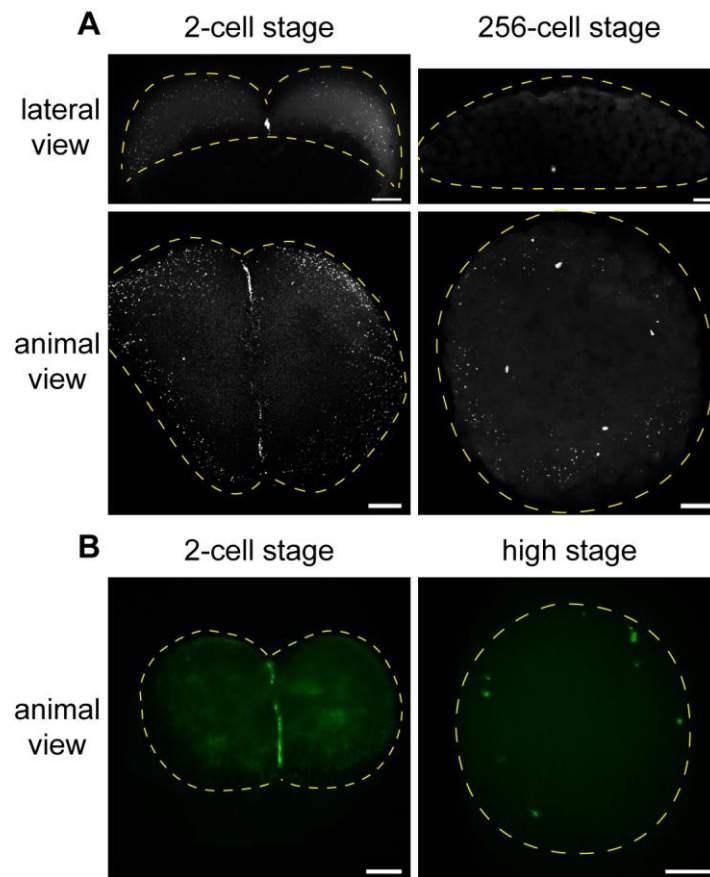


Figure 13: Endogenous Buc and transgenic Buc-GFP are localized to the germ plasm in early embryos. (A) Wild type embryos immunostained for Buc at 2-cell respectively 256-cell stage imaged by confocal fluorescence microscopy. Embryos are shown animal and in lateral view, animal pole to the top (images in animal view are z-stack projections). (B) Living transgenic *buc-gfp* embryos at 2-cell and high stage imaged by stereo fluorescence microscopy. Embryos are shown in animal view. Embryos are outlined by a yellow dashed line. Scale bars represent 50 μm (A) and 100 μm (B).

In summary, these results show that throughout cleavage and blastula stages endogenous Buc is localized to the germ plasm and this localization is reflected by Buc-GFP in living embryos of the transgenic *buc-gfp* line. Therefore, the transgenic line can be used as an *in vivo* marker line, representing the endogenous Buc localization throughout oogenesis and early zebrafish development.

3.1.3 Buc is a germ plasm component in primordial germ cells

Buc shows the same localization as the germ plasm marker *vasa* mRNA in oogenesis and early embryogenesis. The continuous presence of Buc in germ plasm suggest that Buc is also present in primordial germ cells and thus should co-localize with the germ cell marker Vasa (Braat et al., 2000; Knaut et al., 2000).

To investigate for co-localization of both proteins, wild type embryos were stained for Vasa and Buc and analyzed by confocal fluorescence microscopy. Vasa consistently marked the primordial germ cells along the lateral border of the trunk mesoderm at 10-somite stage as

described previously (Figure 14A) (Knaut et al., 2000). Buc co-localized with Vasa in all primordial germ cells (Figure 14A). Detailed analysis of subcellular localization revealed co-localization of Buc and Vasa in granules surrounding the nucleus (Figure 14B). This specific pattern has been described previously for germ plasm granules (Knaut et al., 2000). Buc and Vasa still co-localized in the primordial germ cells in the future gonad region at 48 hpf (Figure 14C). Furthermore, the subcellular clustered localization was preserved in the perinuclear region (Figure 14D).

These results reveal that Buc protein is stable far beyond cleavage and blastula stage although the mRNA is degraded at 4 hpf. Moreover, this shows that Buc is a component of the germ plasm in primordial germ cells and suggests that its activity might be required until 48 hpf.

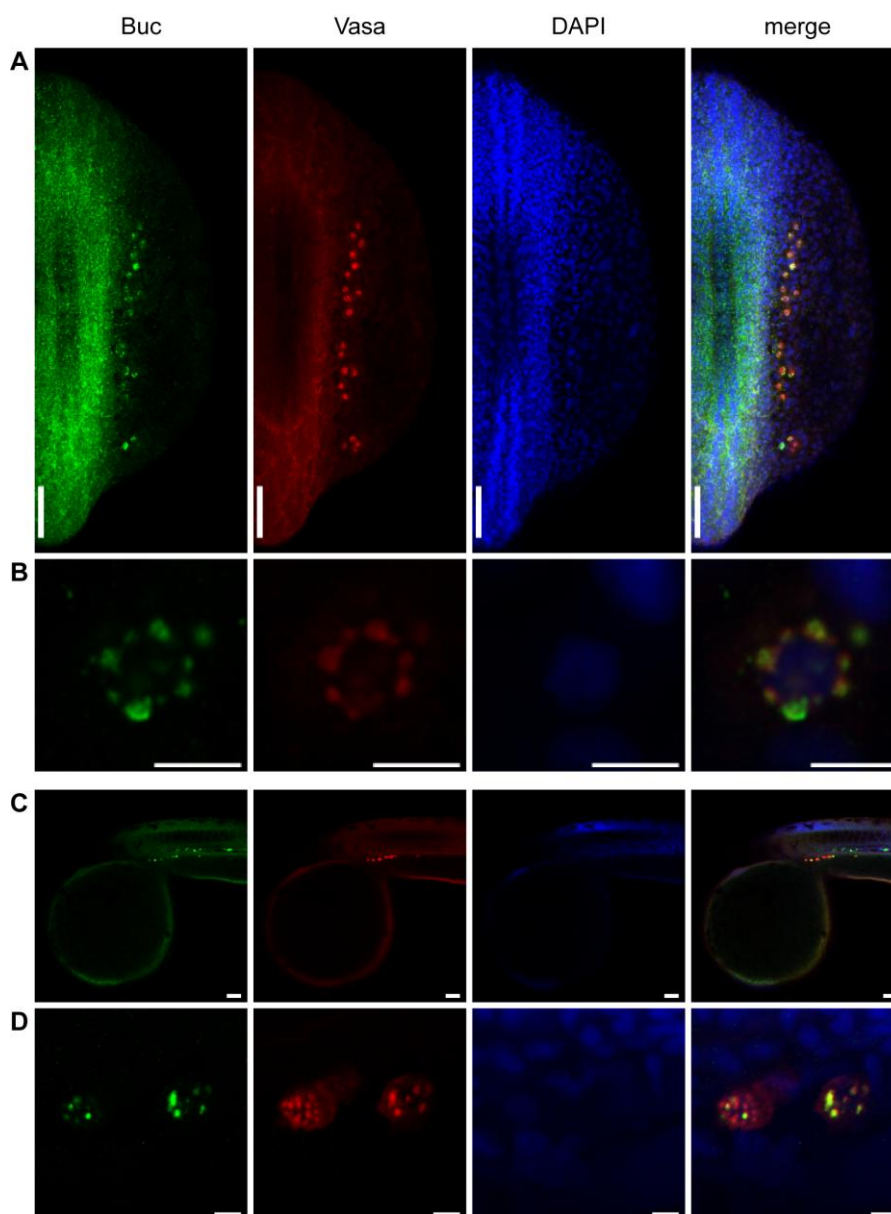


Figure 14: Endogenous Buc is localized to the perinuclear region of primordial germ cells during early embryogenesis. Wild type embryos at 10 somite stage (A, B) and at 48 hpf (C, D) immunostained for Buc (green), Vasa (red), stained for DNA (DAPI, blue) and imaged by confocal fluorescence microscopy. (A) Right hemisphere of a 10-somite stage embryo is shown in dorsal view, anterior to the top (z-stack projections). (B) Magnified view of a single primordial germ cell at 10 somite stage. (C) Embryo at 48 hpf showing the gonad region in lateral view, anterior to the left. (D) Magnified view of primordial germ cells in (C). Scale bars represent 50 μm (A, C) and 5 μm (B, D).

Overall, the analysis of Buc localization revealed that Buc localizes continuously to the germ plasm throughout zebrafish oogenesis and embryogenesis. Buc is the first germ plasm protein showing such a permanent association. Thus, Buc has the potential to develop into a standard protein marker for zebrafish germ plasm similar to *vasa* on the mRNA level. With the generated transgenic *buc-gfp* line, it is even possible to observe the germ plasm dynamics *in vivo* in living zebrafish embryos and oocytes.

3.2 BucLoc is essential for Buc localization

The consistent Buc localization to the germ plasm raises the question of how this specific localization is achieved. As *buc* mRNA is not localized in the embryo and rapidly degraded at 4 hpf, the protein must contain a signal that directs its localization (Bontems et al., 2009). Such a signal would be crucial for the proper spatial distribution of Buc and thus might be essential for germ cell specification during early embryogenesis.

3.2.1 Cross-species approach indicates distinct localization mechanisms of Buc and Osk

Buc is necessary for germ plasm formation in oocytes and sufficient to induce the formation of ectopic germ cells in embryos (Bontems et al., 2009). These unique features are shared with one other protein, Osk in *Drosophila*. In contrast to the recently identified Buc, Osk is a well characterized germ plasm organizer. In addition, *Drosophila* Osk seems to be able to induce germ cells in zebrafish embryos after overexpression (Bontems, 2009). Therefore, it seemed promising and time-saving to find out whether these functionally very similar proteins share an evolutionary conserved mechanism for their protein localization. Therefore, zebrafish Buc and *Drosophila* Osk were analyzed in parallel in a cross-species approach to examine for similarities in their localization mechanisms. Similarities were analyzed in respect to their sequence, to their localization as well as in respect to a potentially shared function.

3.2.1.1 Buc and Osk are divergent in sequence and do not share conserved domains

As *Drosophila* Osk and zebrafish Buc share a functional analogy, both proteins might share a protein localization motif.

To address this question, sequences of Osk and Buc were pairwise aligned and sequence similarity was calculated. The sequence similarity between Buc and Short Osk, the Osk isoform involved in germ plasm formation, was 11.5 % (Figure 15A). In contrast, conserved Vasa proteins of zebrafish and *Drosophila* showed 59.4 % sequence similarity (Figure 15A). Surprisingly, the two functionally unrelated proteins Buc and *Drosophila* Vasa shared higher sequence similarity than Buc and Osk (18.5 %) (Figure 15A). Thus, sequence similarity of Buc and Osk is not conserved. However, a small conserved domain might be sufficient as localization signal. Hence, Buc sequence was analyzed in collaboration with Dr. Thomas Lingner for conserved regions by multiple sequence alignments of Buc related vertebrate proteins. This analysis revealed two N-terminal conserved domains (aa 24-84 and 114-128), located in the so-called BUVE-motif (aa 23-136) (Bontems et al., 2009). Additionally, a conserved central domain (aa 372-394) was identified (Figure 15B).

Nevertheless, none of these newly identified conserved domains showed a homology to known protein domains or to any domain present in Osk protein.

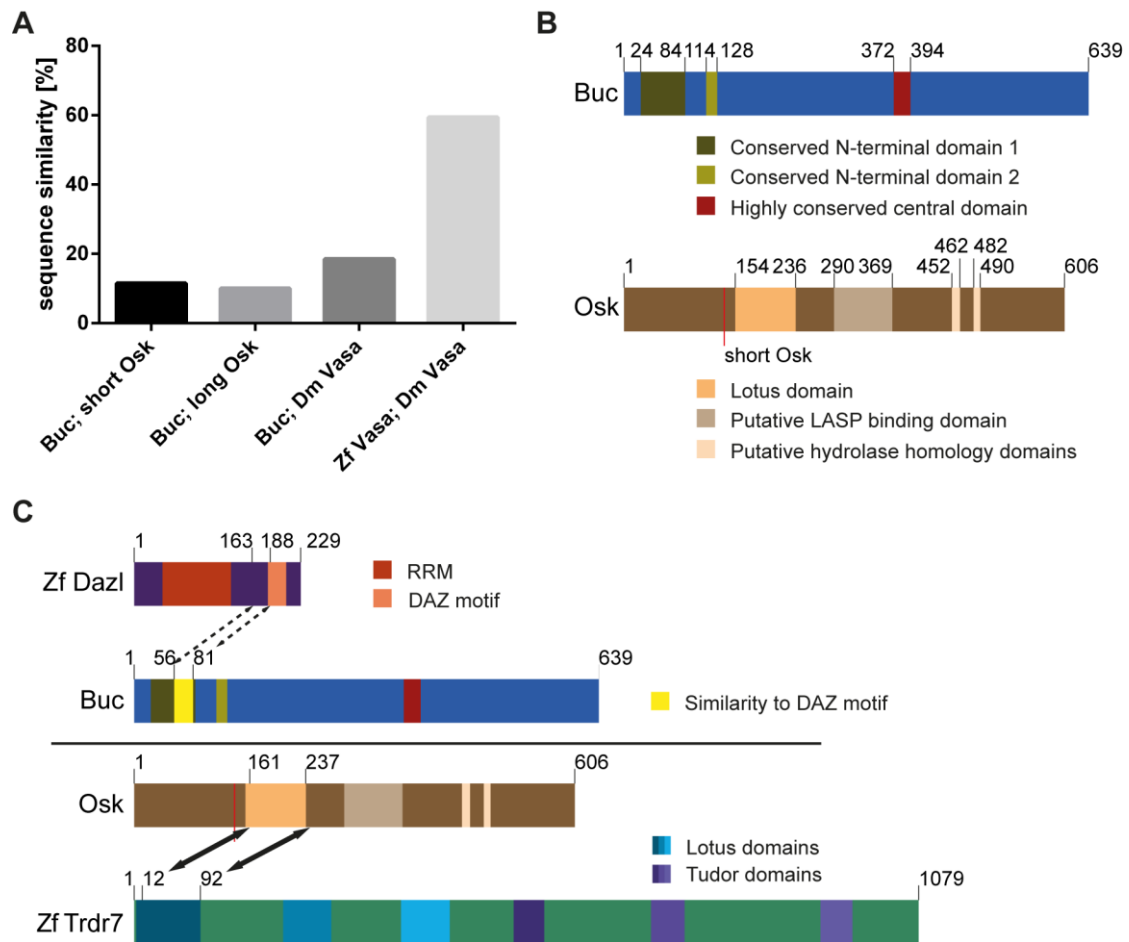


Figure 15: Zebrafish Buc and *Drosophila* Osk are divergent in sequence and show sequence homologies to other proteins. (A) Graph shows sequence similarity of zebrafish Buc with the isoforms of *Drosophila* Osk based on pairwise sequence alignments. Alignment of the conserved proteins zebrafish Vasa and *Drosophila* Vasa served as positive control. Alignment of zebrafish Buc and *Drosophila* Vasa served as negative control. (B) Schematic representation of Buc protein sequence and its newly identified conserved domains, identified by multiple sequence alignments of Buc homologs in other vertebrates. For comparison, Osk protein is shown with known conserved and putative domains (Callebaut and Mornon, 2010; Lynch et al., 2011; Suyama et al., 2009). (C) Schematic representation of Buc and Osk protein sequence with conserved regions and significant remote sequence similarity with indicated proteins, based on HMMER analysis. For Buc, no sequence similarity to any *Drosophila* protein could be identified (Appendix, Table 15). Multiple sequence alignments and HMMER analysis were done in collaboration with Dr. Thomas Lingner.

However, it cannot be excluded that conserved domains of Buc and Osk diverged during evolution and thus cannot be identified by sequence alignments.

To detect potential distantly related domains in Buc and Osk, hidden Markov models (HMMs) of Buc and Osk were used to search within the respective other protein database. Although the Buc HMM did not find any similarities in the *Drosophila* database, a distant similarity to a fraction of the DAZ motif in zebrafish Dazl was detected in the conserved N-terminal domain of Buc (Figure 15; Appendix Table 15). The Osk HMM detected highest similarity to zebrafish Tdrd7. In this case, the sequence similarity was detected in the known Lotus domain present in *Drosophila* Osk as well as in zebrafish Tdrd7 (Callebaut and Mornon, 2010).

Taken together, these results show that zebrafish Buc and *Drosophila* Osk neither share similarity in total sequence nor in conserved domains.

3.2.1.2 Buc does not mimic Osk localization in *Drosophila* embryos

Similar to Buc, overexpression of Osk induces the formation of ectopic germ cells in zebrafish embryos (Bontems, 2009). Although Buc and Osk do not share sequence similarity, this functional analogy suggests a structural similarity, which might lead to a similar localization pattern. However, structural data is neither available for Osk nor for Buc.

To compare the localization pattern of Buc and Osk, transgenic flies were generated expressing Buc-eGFP or Osk-eGFP ectopically at the anterior pole of the embryo by fusion of the constructs to the *bicoid* 3'UTR (Figure 16A). eGFP-tagged non-functional mutants of Buc (Buc^{p43}, lacking 278 of 639 amino acids) and Osk (Osk⁰⁸⁴, lacking 354 of 468 amino acids) served as negative controls. The localization of the different constructs was analyzed in the respective transgenic line of living *Drosophila* embryos by confocal microscopy. Osk-eGFP localized in condensed aggregates to the most distal part of the anterior pole (Figure 16B). In contrast, Buc-eGFP showed widespread protein distribution along the cortex of the anterior pole (Figure 16B). Nevertheless, Buc-eGFP was detected in small granules similar to what was observed in zebrafish embryos of the transgenic *buc-gfp* line. This granule formation was also present in *buc^{p43}-egfp* transgenic embryos (Figure 16B). In general, *buc^{p43}-egfp* transgenic embryos showed a localization pattern similar to that of *buc-egfp* transgenic embryos, while Osk⁰⁸⁴-eGFP was equally distributed at the anterior pole.

Thus, Osk-eGFP and Buc-eGFP showed different protein localization in *Drosophila* embryos. This indicates that a localization signal recognized in *Drosophila* Osk is not present in zebrafish Buc.

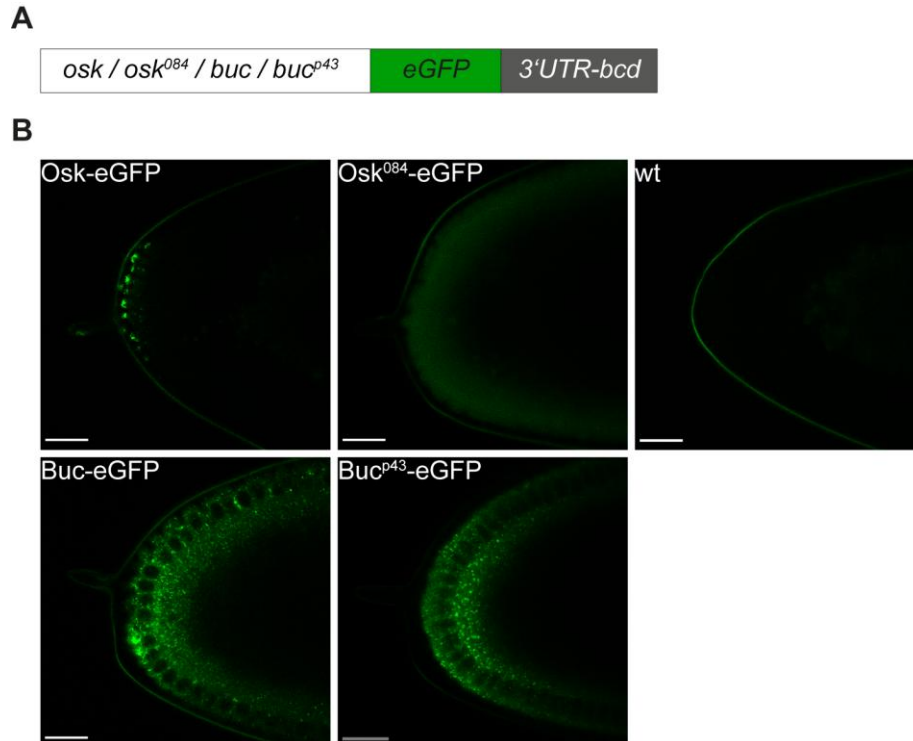


Figure 16: Buc-eGFP shows a different localization pattern in *Drosophila* compared to Osk-eGFP. (A) Constructs used to make transgenic flies. All genes were tagged with eGFP to visualize the protein and the 3'UTR of *bicoid* to locate the RNA to the anterior pole. (B) Anterior pole of living *Drosophila* stage 5 embryos expressing indicated transgenic constructs, imaged by confocal fluorescence microscopy. Note that Osk-eGFP localizes in a condensed manner to the cortex of the anterior pole. Scale bars represent 20 μm .

3.2.1.3 Ectopic Buc expression does not result in a phenotype in *Drosophila* embryos

Ectopic overexpression of Osk at the anterior pole in *Drosophila* embryos leads to defects in anterior-posterior patterning, bicaudal phenotypes and even formation of ectopic germ cells (Ephrussi and Lehmann, 1992).

To examine whether the observed difference in localization of Buc and Osk in *Drosophila* embryos is functionally relevant, embryonic cuticles of the transgenic lines were analyzed for defects in anterior-posterior patterning. 93.7 % of *osk-egfp* transgenic embryo cuticles showed patterning defects, including loss of the head skeleton or a bicaudal phenotype with a filzkörper at the posterior and anterior pole (Figure 17). In contrast, only 3.4 % of the *buc-egfp* transgenic embryos showed patterning defects (Figure 17B). The *osk⁰⁸⁴-egfp* and *buc^{p43}-egfp* transgenic embryos did not show any defects in anterior-posterior patterning (Figure 17B).

This result shows that ectopic Osk-eGFP disrupts anterior-posterior patterning whereas Buc-eGFP does not show a phenotype in the *Drosophila* embryo. Therefore, the observed difference in ectopic localization of Buc and Osk in *Drosophila* embryos might result in the distinct phenotype.

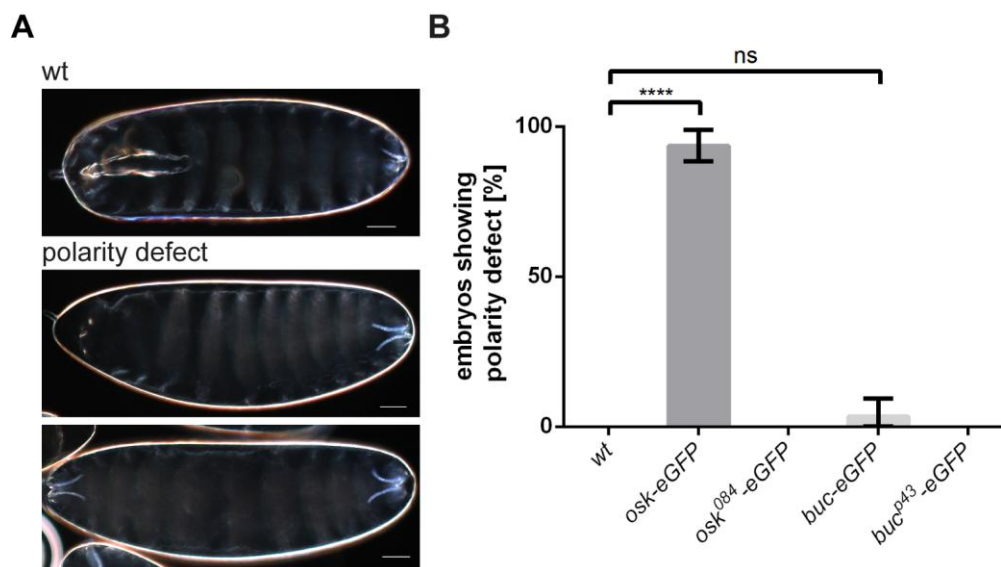


Figure 17: *osk-egfp* transgenic embryos show defects in anterior-posterior patterning. (A) *Drosophila* embryonic cuticles showing wild-type and patterning defects including loss of head skeleton and bicaudal phenotype. Anterior pole is to the left. Scale bars represent 5 μ m. (C) Quantification of cuticle analysis of the indicated transgenic strains. Error bars represent the standard deviation (**** $p < 0.0001$, unpaired t-test, $N=2-3$, $n=65-222$).

3.2.1.4 Osk does not localize in zebrafish

The expression of Osk-eGFP and Buc-eGFP in *Drosophila* points towards an importance of proper protein localization during early embryonic development and germ cell formation. To investigate whether the functional similarity of Osk and Buc in zebrafish is based on a similar localization pattern (Bontems, 2009), a localization assay for both proteins was carried out in zebrafish embryos.

RNA encoding Buc-eGFP and Osk-eGFP was injected into 1-cell stage embryos and protein localization was analyzed 3 hpf by stereo fluorescence microscopy (Figure 18A). RNAs

encoding the two non-functional mutants Buc^{P43} -eGFP and Osk^{O84} -eGFP were injected likewise. Both, Osk -eGFP and Osk^{O84} -eGFP were distributed homogeneously in the embryo (Figure 17B). In contrast, Buc -eGFP and Buc^{P43} -eGFP were localized in four aggregates and 2-3 smaller clusters, similarly to Buc -GFP in the transgenic zebrafish line (Figure 11). This indicates that Buc and Buc^{P43} contain a localization signal, directing the protein to the germ plasm in zebrafish, while Osk does not seem to contain such a signal.

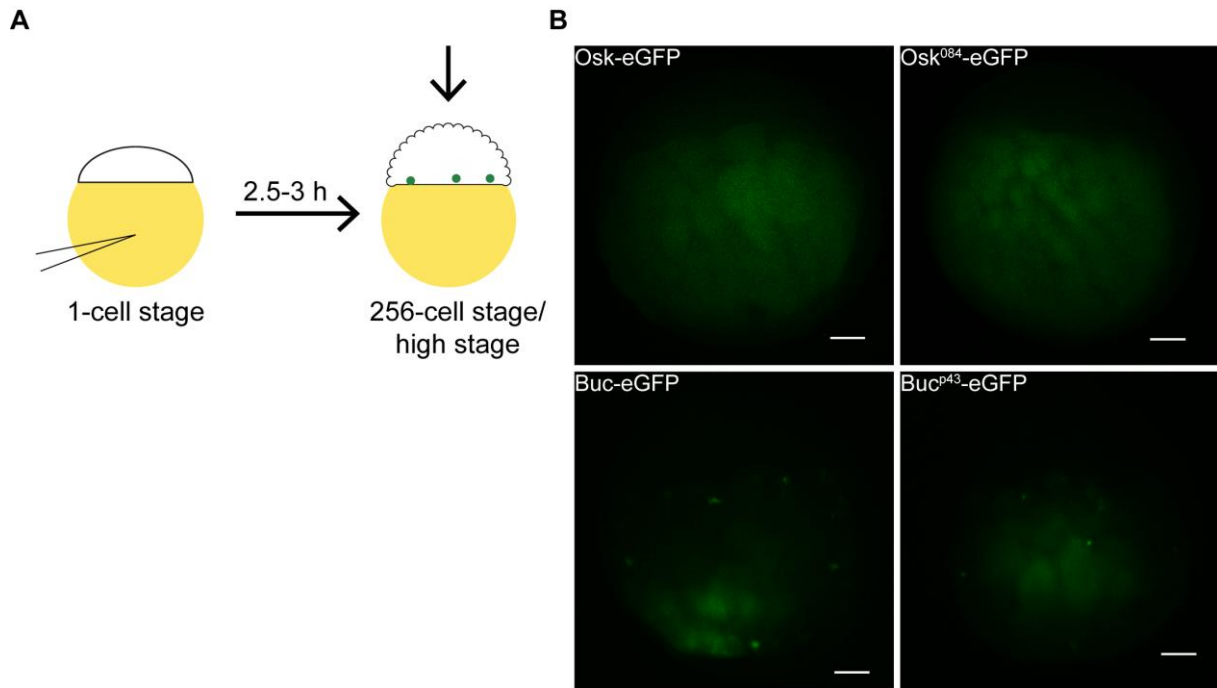


Figure 18: Osk-eGFP does not resemble the localization pattern of Buc-eGFP in zebrafish. (A) In the localization assay 200 pg of the respective RNA was injected in 1-cell stage zebrafish embryos with and imaged 2.5-3 hpf at 256-cell stage/high stage. (B) 256-cell stage embryos expressing the indicated constructs imaged by stereo fluorescence microscopy. Note the spotted protein localization of Buc -eGFP and Buc^{P43} -eGFP. Embryos are shown in animal view. Scale bars represent 200 μm .

In summary, this cross-species approach led to two major findings. First, Osk protein contains a localization signal that is able to specifically localize it at ectopic sites in *Drosophila*, which is not conserved in Buc . Second, zebrafish Buc contains a localization signal in the N-terminal half, which is not conserved in Osk . Thus, Buc and Osk neither share similarity their sequences nor in their localization mechanisms.

3.2.2 Proline-rich localization domain BucLoc is essential for Buc localization

The cross-species approach did not reveal a similarity in the localization mechanisms of Buc and Osk . However, the localization assay revealed that Buc^{P43} is able to localize in zebrafish embryos, indicating that a potential localization signal is still present (Figure 18). Consequently, another approach was pursued to identify the localization domain in Buc . In an extensive structure-function analysis, Buc deletion fragments were analyzed systematically for their localization in zebrafish embryos.

3.2.2.1 BucLoc is necessary and sufficient for Buc localization to the germ plasm

The *buc*^{p43} mutant allele is predicted to encode a protein with a C-terminal truncation of 278 amino acids (Bontems, 2009). Nevertheless, Buc^{p43} contains the two N-terminal conserved domains that were identified in the multiple sequence alignments, but lacks the central conserved domain (Figure 15, Figure 19). This suggested that the N-terminus of Buc protein might contain a potential localization signal.

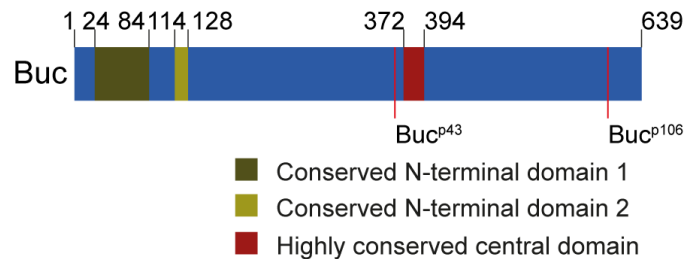


Figure 19: Buc^{p43} sequence contains conserved N-terminal domains. (A) Schematic representation of Buc protein sequence and its conserved domains (see also Figure 15). Predicted sizes of the mutant proteins Buc^{p43} and Buc^{p106} are indicated. Note that the central conserved domain is no longer present in Buc^{p43}.

To identify the potential localization domain in Buc, systematic deletion fragments of *buc* were cloned and fused to *egfp*. RNA encoding these fragments was injected into 1-cell stage zebrafish embryos to analyze the protein localization at 2.5-3 hpf with stereo fluorescence microscopy (Figure 20A). Buc^{p43}-eGFP localized in protein aggregates at the cortex of the embryo close to the yolk compartment as shown for Buc-eGFP (Figure 20B). The N-terminal half of Buc^{p43} retained this localization pattern in contrast to the C-terminal half that showed only diffuse protein expression (Figure 20C). By continuously splitting the localizing fragment in half, the domain sufficient for proper localization of the fusion protein could be narrowed down to the N-terminal amino acids 11-88 in Buc (Figure 20C, D). A deletion construct of full length Buc, lacking amino acids 11-88, did not localize any more.

Therefore, Buc11-88 encodes a domain that is necessary and sufficient for localizing Buc protein during early zebrafish embryogenesis. Hence, the presence of other essential localization domains in Buc is unlikely. In accordance with its function, the Buc11-88 localization domain was given the name BucLoc.

Furthermore, these data indicate that the localization signal is not lost in Buc^{p43} and Buc^{p106} mutant protein and therefore the loss of localization in *buc* mutant oocytes is most likely due to loss of protein expression (Figure 9B). Therefore, *buc*^{p43} and *buc*^{p106} are most likely protein null-alleles.

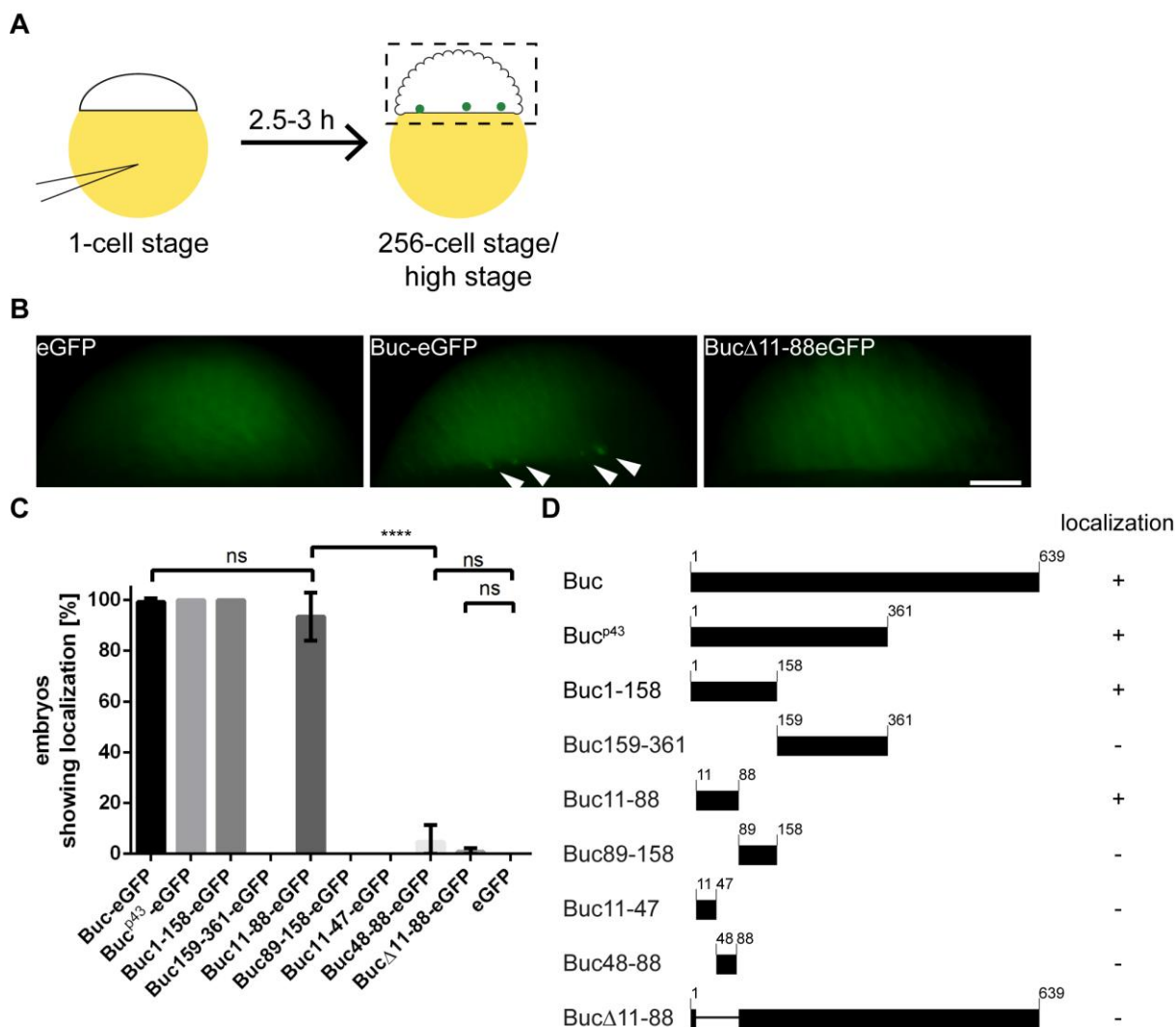


Figure 20: Buc11-88 is necessary and sufficient for Buc localization in embryos. (A) Zebrafish embryos were injected at 1-cell stage with 100-350 amol RNA encoding the indicated construct and imaged 2.5-3 hpf at 256-cell stage/high stage by stereo fluorescence microscopy. (B) Blastomeres of high stage embryos expressing the indicated constructs imaged by stereo fluorescence microscopy. Note the protein localization of Buc-eGFP in aggregates (arrowheads). Blastomeres on top of the yolk sac are shown in a lateral view, animal pole to the top. Scale bar represents 100 μ m. (C) Quantification of localization analysis. Error bars represent standard deviation (**** $p < 0.0001$, unpaired t-test, $N = 3-7$, $n = 94-231$). (D) Schematic representation of Buc protein deletions and summary of their localization potential.

In the localization assay, overexpression of BucLoc-eGFP led to formation of aggregates, but it was unclear whether these BucLoc-eGFP aggregates indeed localize to the germ plasm. To examine if BucLoc aggregates directly localize to the germ plasm, RNA encoding mCherry-tagged BucLoc was injected into 1-cell stage transgenic *buc-gfp* embryos. Subsequently, co-localization between the localization domain BucLoc-mCherry and the germ plasm marker Buc-GFP was analyzed at 3.5 hpf. In addition, the localization was analyzed by confocal fluorescence microscopy to obtain a higher resolution. The aggregates formed by BucLoc-mCherry co-localized with Buc-GFP aggregates (Figure 21A). A higher resolution, revealed a compact, elongated structure of the aggregates that seemed to contain smaller inclusions (Figure 21B).

This experiment showed that the localization domain BucLoc is responsible for localization of Buc to the germ plasm in early zebrafish embryogenesis. Thus, BucLoc provides a targeting signal to localize any protein to the germ plasm and by this to the germline.

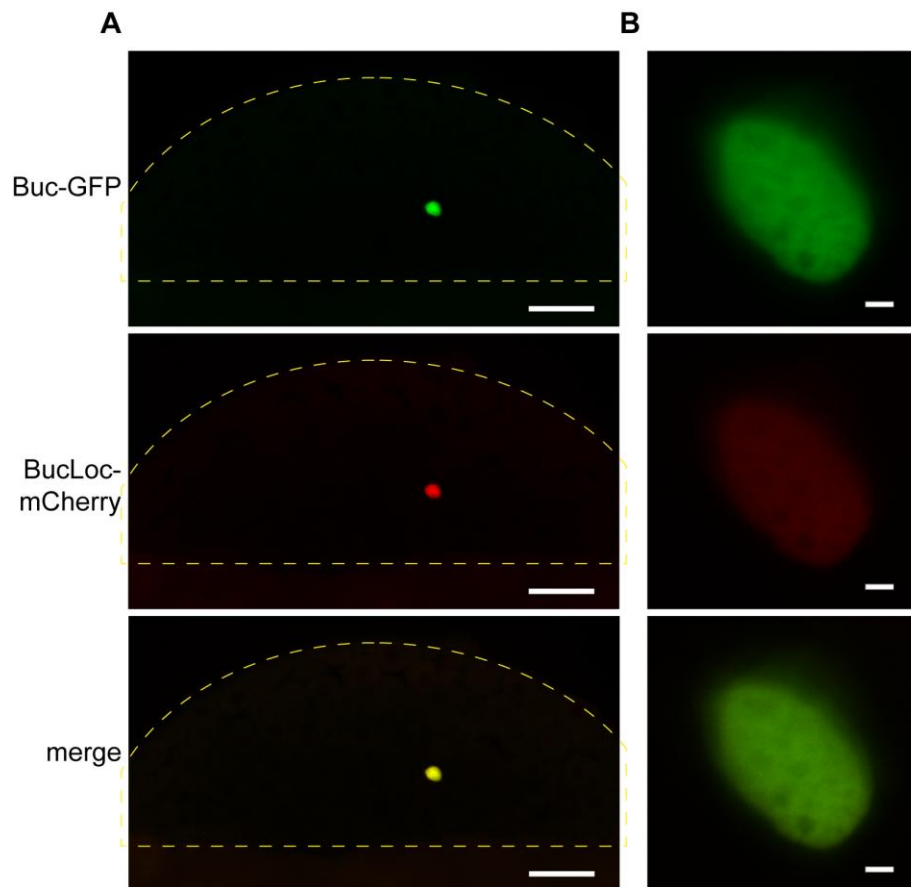


Figure 21: BucLoc-mCherry co-localizes with transgenic Buc-GFP to the germ plasm. (A) Living sphere stage transgenic *buc-gfp* (green) embryos injected at 1-cell stage with 750 amol RNA encoding BucLoc-mCherry (red) and imaged by confocal fluorescence microscopy. Blastomeres on top of the yolk sac are outlined by a yellow dashed line. Embryo is shown in a lateral view, animal pole to the top. (B) High magnification of the condensed localized aggregate shown in A. Scale bars represent 50 μm (A) and 2 μm (B).

3.2.2.2 BucLoc is rich in proline and aromatic amino acids

Interestingly, the Buc localization domain BucLoc harbors one of the conserved N-terminal domains (amino acids 24-84) identified in the previous multiple sequence analysis of Buc vertebrate homologs (Figure 15, Figure 19).

Analysis of BucLoc by BLAST search did not reveal any known interaction motifs. Therefore, the amino acid composition of BucLoc was analyzed with the ProtParam web tool (Gasteiger et al., 2003). Surprisingly, proline was the most frequent amino acid accounting for more than 20% of the amino acids within the BucLoc localization domain (Figure 22A). Furthermore, aromatic amino acids were contributing more than 29 % to BucLoc. Thus, half of the amino acids present in BucLoc were either aromatic or proline. On the contrary, charged amino acids were present in small numbers (7 %) with lysine as well as glutamic acid being not present at all (Figure 22A). To research if full length Buc shared these characteristics with BucLoc, the amino acid composition of full length Buc was compared with the amino acid composition of BucLoc. In BucLoc phenylalanine levels were about

280 % higher compared to full length Buc, while other aromatic amino acids showed an enrichment of 105-192 % (Figure 22B). The proline content of BucLoc was 167% higher as in full length Buc. Additionally, the hydrophobic amino acid methionine content was enriched by 227 % in BucLoc. On the other side, polar and charged amino acids were significantly less in BucLoc compared to full length Buc (Figure 22B). This shows that BucLoc is specifically enriched for proline and aromatic amino acids.

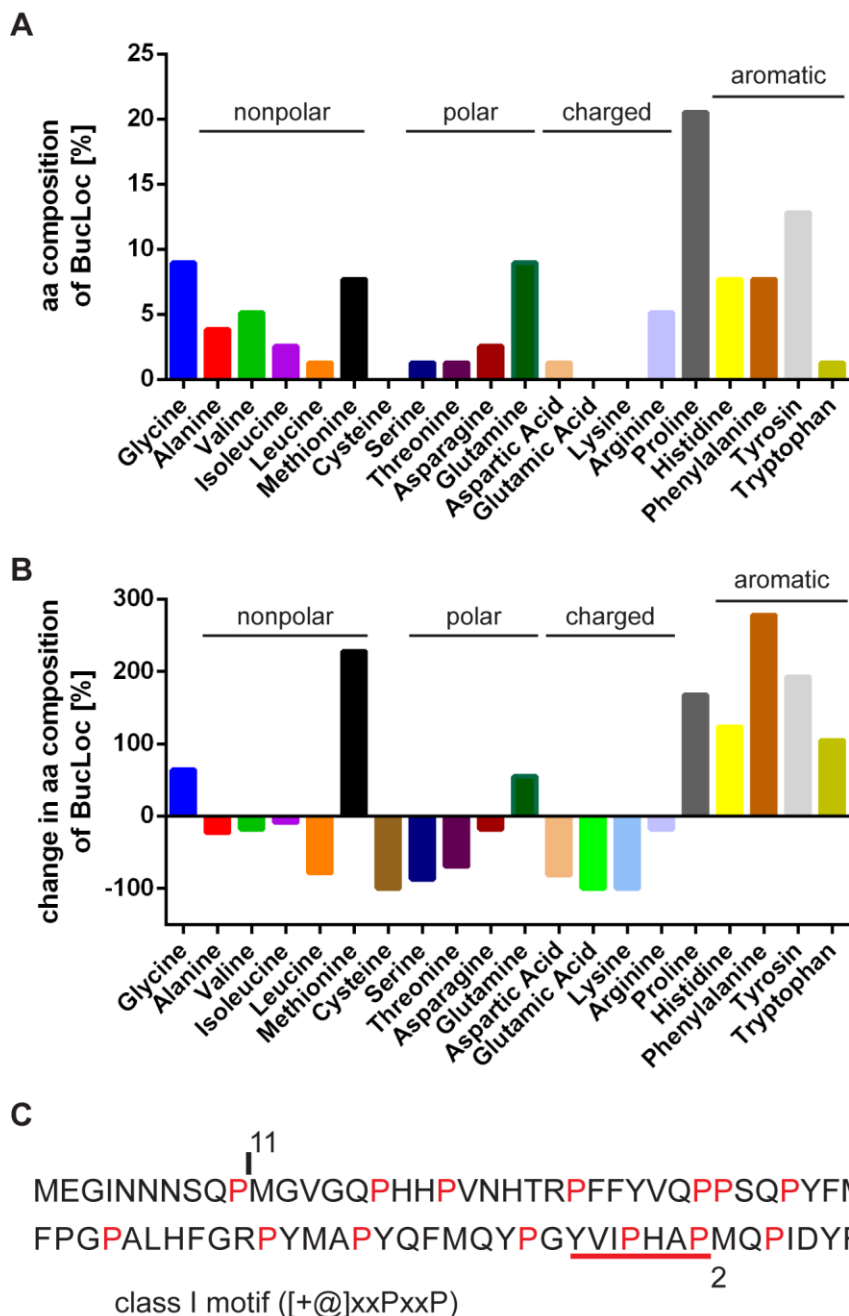


Figure 22: BucLoc is highly enriched in proline and aromatic amino acids and SH3 binding sites are predicted. (A) Graph shows the amino acid composition of BucLoc. (B) Graph shows change in amino acid composition of BucLoc in comparison with Buc. Amino acids are clustered due to their general chemical characteristics and structure. (C) Identification of SH3-domain interaction sites within the first 100 amino acids of Buc predicted by SH3-Hunter. [+] stands for positively charged amino acids (His, Arg or Lys), [@] corresponds to aromatic amino acids (Phe, Tyr, Trp), x stands for any amino acid, P stands for proline. All prolines in the sequence are highlighted in red.

The next question was whether the surprisingly high enrichment in proline and aromatic amino acids in BucLoc was important for its localization mechanism. Specific protein binding motifs, such as Src homology 3 (SH3) binding sites, are known to exist within proline-rich regions (Kay et al., 2000).

To examine if Buc contains SH3 binding sites, the protein sequence was screened for SH3 binding motifs using the web server SH3-Hunter (Ferraro et al., 2007). Two class I SH3 binding motifs were predicted at the N-terminus of Buc. The first one was predicted outside of BucLoc within the amino acids 88-94. The second motif was predicted within the amino acids 74-80 at the C-terminal end of BucLoc (Figure 22C). Other motifs present in proline-rich regions, such as WW ligand core motifs, were not identified in BucLoc.

This analysis revealed the proline-rich sequence of BucLoc to contain a predicted SH3 binding site. Thus, BucLoc might be localized through interaction with SH3 domain containing proteins.

In summary, the proline-rich localization domain BucLoc is necessary and sufficient to localize Buc to the germ plasm during early zebrafish embryogenesis. Hence, BucLoc is the first protein localization domain identified in a metazoan, which is able to target proteins specifically to the germ plasm.

3.3 BucLoc interacts with non-muscle myosin II

3.3.1 Identification of the BucLoc interactome

The isolation of the Buc localization domain provides a powerful tool for the identification of the Buc localization mechanism. This tool can be used to specifically address the question, with which proteins BucLoc is interacting to properly localize Buc to the germ plasm during zebrafish embryogenesis. Identification of the molecular network involved in Buc localization will give insight into the mechanism underlying the localization process.

3.3.1.1 Identification of 213 interaction candidates of BucLoc

To identify the protein network involved in localization of Buc, BucLoc interactors were purified directly out of the embryo at the stage, in which Buc is localized to the prospective primordial germ cells.

Embryos were injected at 1-cell stage with RNA encoding BucLoc-eGFP, lysed at high stage and immunoprecipitated by the GFP-tag. Embryos injected with RNA encoding eGFP were used as a negative control, whereas embryos of the transgenic *buc-gfp* line were used to control for overexpression artifacts and served as a positive control. Co-immunoprecipitated proteins of the three samples were analyzed by mass spectrometry (Figure 23A). Using this approach, 3464 proteins were identified in the mass spectrometry analysis (Figure 23B) (digital Appendix, Chapter 7.4). 1817 of them interacted with Buc-GFP as well as BucLoc-eGFP (Figure 23B). To identify significant interaction candidates, a set of criteria was applied. First, all proteins, below a background threshold of five in BucLoc-eGFP, were considered as not significant and were sorted out (Figure 23B, I). Furthermore, only proteins with counts in BucLoc-eGFP that were at least twice as high as in the negative control eGFP were considered as significant (Figure 23B, II). To reduce overexpression artefacts, another

criterion was that enrichment in the positive control and in the sample had to be within a magnitude of ± 4 -fold (Figure 23B, III). Applying these selection criteria, the number of potential BucLoc interaction proteins could be restricted to 213 interaction candidates (Figure 23B; Appendix, Table 17).

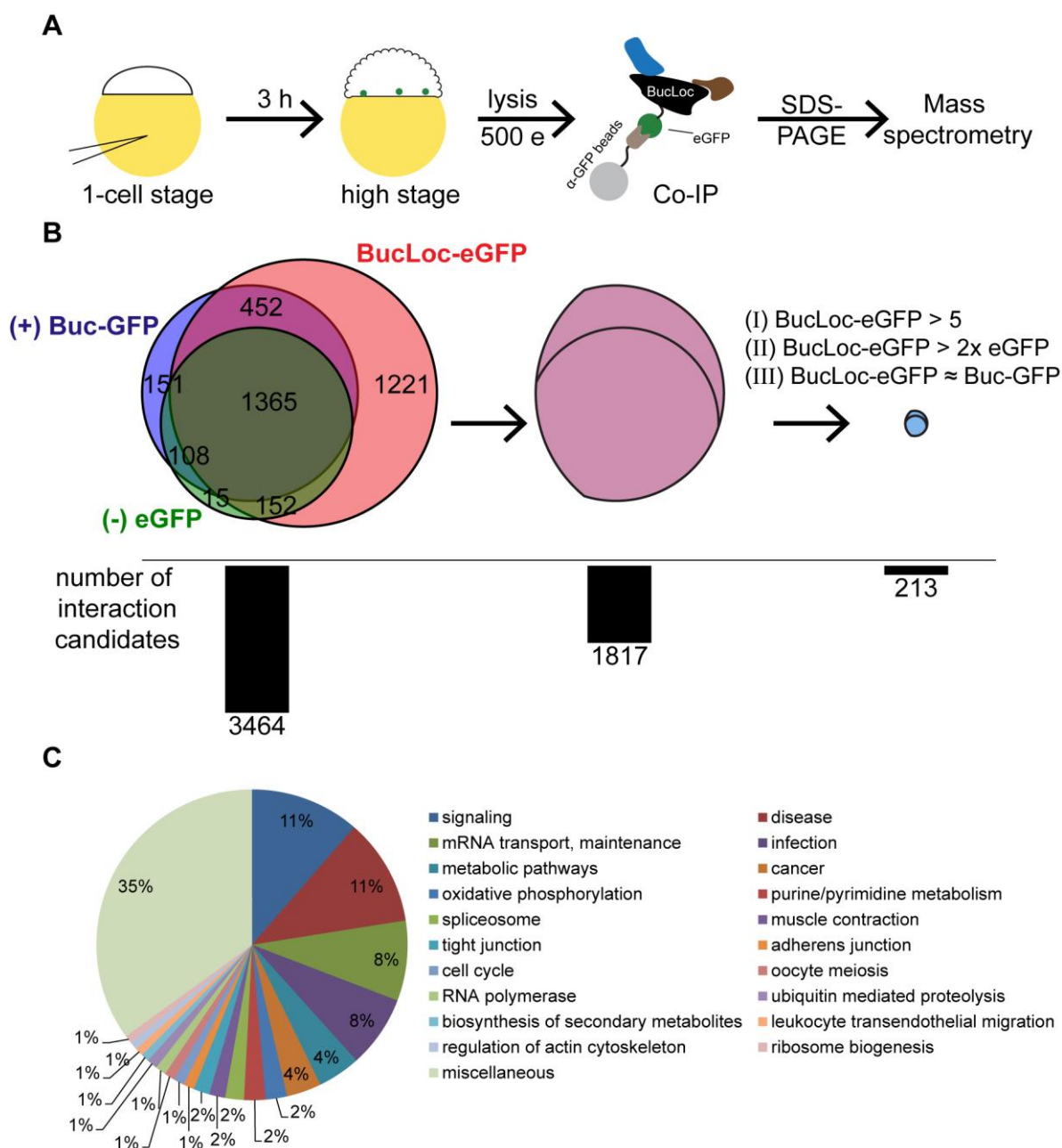


Figure 23: 213 specific interaction partners of BucLoc are involved in diverse molecular pathways. (A) Wild type embryos were injected with RNA encoding for BucLoc-eGFP and lysed at high stage. Embryos of the transgenic *buc-gfp* line were used as positive control, *egfp* RNA injected embryos were used as negative control. Subsequent to lysis an IP against the GFP-tag was carried out. Interacting proteins were identified by mass spectrometry (Core Facility of Proteome Analysis, UMG, Goettingen). (B) Venn diagram showing the overlap of a total of 3464 protein hits split among the three samples BucLoc-eGFP, Buc-GFP (+) and eGFP (-). Overlap of BucLoc-eGFP with Buc-GFP was further reduced to 213 interaction candidates by applying the criteria described in the text (Appendix, Table 17). (C) Graph showing annotation of BucLoc interaction candidates to different molecular pathways. 132 of 213 candidates could be annotated by KEGG analysis (in collaboration with Dr. Thomas Lingner). Multiple annotations were possible.

In the following, the 213 interaction candidates were analyzed with the Kyoto Encyclopedia of Genes and Genomes (KEGG) in collaboration with Dr. Thomas Lingner to determine if a majority of interaction candidates is involved in a specific molecular pathway. About 62 % of the proteins could be annotated to different molecular pathways, including signaling (11 %), splicing (2 %), adherens and tight junctions (2 %), mRNA transport, surveillance and degradation (8 %) (Figure 23C). Using KEGG annotation, no striking enrichment in one of the molecular pathways was detected. Cytoskeletal elements, expected to be involved in Buc localization, were present, but not strongly enriched due to KEGG annotation (Figure 23C). Nevertheless, the Co-IP with BucLoc identified 213 interaction candidates involved in various molecular pathways that might play a role in the localization of Buc during early embryogenesis.

3.3.1.2 Selection of BucLoc interaction candidates for further analysis

As no molecular pathway was strikingly overrepresented among the 213 BucLoc interaction candidates, the list of candidates was manually analyzed and single candidates were selected for further analysis. Since nothing is known about the molecular function and the localization mechanism of Buc protein, nine proteins that are involved in different processes or components of different complexes were chosen for a first analysis (Table 12).

Interestingly, three of four core proteins of the exon junction complex, involved in post-transcriptional regulation of mRNA, were identified. One of these proteins was Magoh (Mago nashi homolog), whose *Drosophila* homolog is involved in the establishment of oocyte polarity and assembly of the germ plasm (Table 12) (Micklethwait et al., 1997; Newmark and Boswell, 1994). Furthermore, five of ten proteins of the exosome complex, involved in RNA degradation, were identified among the 213 candidates, with the exosome complex exonuclease RRP45 (*exosc9*) having the highest counts (Table 12).

14-3-3 epsilon (*ywhae1*) was chosen as an adapter protein involved in a broad spectrum of signaling pathways. Additionally, 14-3-3 epsilon is involved in germ cell migration in *Drosophila* (Table 12) (Tsigkari et al., 2012). cAMP-dependent protein kinase catalytic subunit alpha (*prkacaa*) was selected as a kinase involved in regulation of protein activity through phosphorylation (Table 12).

Septin-2 (*sept2*) is a filament-forming cytoskeletal GTPase involved in a broad spectrum of cellular processes, e.g. chromosome congression in oocytes (Table 12) (Zhu et al., 2010). Septins form hetero-oligomeric complexes, further assemble into filamentous or ring-like structures and often serve as scaffold for protein recruitment. (Mostowy and Cossart, 2012). In addition, myosin light chain 12, genome duplicate 2 (*myl12.2*), a component of the non-muscle myosin II complex, which directly binds to the actin cytoskeleton, was chosen to be analyzed further (Table 12). As an antibody was available, the localization of this candidate was directly targeted by immunostaining (Chapter 3.3.3).

Pard3 (*pard3*) is an adapter protein involved in the establishment and maintenance of cell polarization processes and asymmetrical cell division (Table 12) (Ahringer, 2003). Moreover, the tight junction protein ZO-2 isoform 1 (*tjp2a*) was included in the list for further analysis as it contains a SH3-domain and is associated with the cytoskeleton (Table 12) (Gonzalez-Mariscal et al., 2000). Unfortunately, the localization of Tjp2a could not be investigated as cloning of *tjp2a* was not successful.

Since the molecular function of Buc is unknown, so far uncharacterized proteins might be involved in Buc localization. Therefore, the uncharacterized protein LOC792544 (*si:dkey-67c22.2*) was included in the analysis (Table 12).

Thus, eight out of 213 BucLoc interacting proteins were manually selected to be analyzed further for their role in Buc localization to the germ plasm.

Table 12: BucLoc interaction candidates selected for further analysis. Candidates were chosen to cover a broad spectrum of processes, protein sizes and enrichments. Fold enrichment for BucLoc-eGFP as well as Buc-eGFP in comparison to eGFP is given for each candidate. Detailed information is presented in the appendix (Table 17).

Name	Gene	Human homolog	Process / Structure	Fold enrichment	
				BucLoc-eGFP	Buc-eGFP
Uncharacterized protein LOC792544	<i>si:dkey-67c22.2</i>	-	unknown	12.8	5.3
Pard3 protein	<i>pard3</i>	<i>PARD3</i>	polarity	18.3	35.6
Septin-2	<i>sept2</i>	<i>SEPT2</i>	cytoskeleton	17.6	13.3
Protein mago nashi homolog	<i>magoh</i>	<i>MAGOH</i>	exon junction complex	2.6	4.2
Exosome complex exonuclease RRP45	<i>exosc9</i>	<i>EXOSC9</i>	exosome	8.4	20.2
cAMP-dependent protein kinase catalytic subunit alpha	<i>prkaca</i>	<i>PRKACA</i>	protein regulation	14.9	8.8
14-3-3 protein epsilon	<i>ywhae1</i>	<i>YWHAE</i>	signaling	10.4	2.7
Tight junction protein ZO-2 isoform 1	<i>tjp2a</i>	<i>TJP2</i>	cell junctions	29.2	13.5
Myosin, light chain 12, genome duplicate 2	<i>myl12.2</i>	<i>MYL12A</i>	cytoskeleton	23.1	2.5

3.3.1.3 Exosomal protein Exosc9 co-localizes with BucLoc

The most important criterion for an interaction of two proteins is co-localization of both proteins *in vivo*. In order to study the co-localization of BucLoc with the interaction candidates, their genes were cloned from cDNA and fused with *egfp* using Gateway cloning. To verify co-localization, RNA encoding the eGFP-tagged interaction candidates was co-injected with RNA encoding BucLoc-mCherry into 1-cell stage wild type embryos. Co-localization was analyzed at 2.5-3 hpf by confocal fluorescence microscopy (Figure 24A). Magoh did not co-localize with BucLoc and showed a homogeneous nuclear localization, consistent with the localization previously reported for Mago in *Drosophila* (Figure 24B) (Micklem et al., 1997). The cytoskeletal protein Sept2 localized as previously reported to filamentous structures in the cytoplasm of the cells (Figure 24C) (Mostowy and Cossart, 2012). These filaments, did not co-localize with BucLoc (Figure 24C). Pard3, involved in establishment and maintenance of cell polarity, localized along the cell-cell contact region to the plasma membrane and thus did not co-localize with BucLoc (Figure 24D) (Ahringer, 2003). Co-localization with BucLoc was also not observed with Ywhae1 and Prkaca (Figure

24E, G). Both proteins, involved in signal transduction, showed homogeneous cytoplasmic localization. A similar cytoplasmic localization pattern, without a co-localization with BucLoc, was observed for the uncharacterized protein Loc792544 (Figure 24F). However, upon overexpression of Exosc9-eGFP, co-localization with BucLoc-mCherry was detected in aggregates (Figure 24H, I-I''). These results show that Exosc9 and BucLoc fulfill the important interaction criterion of co-localization *in vivo*.

A

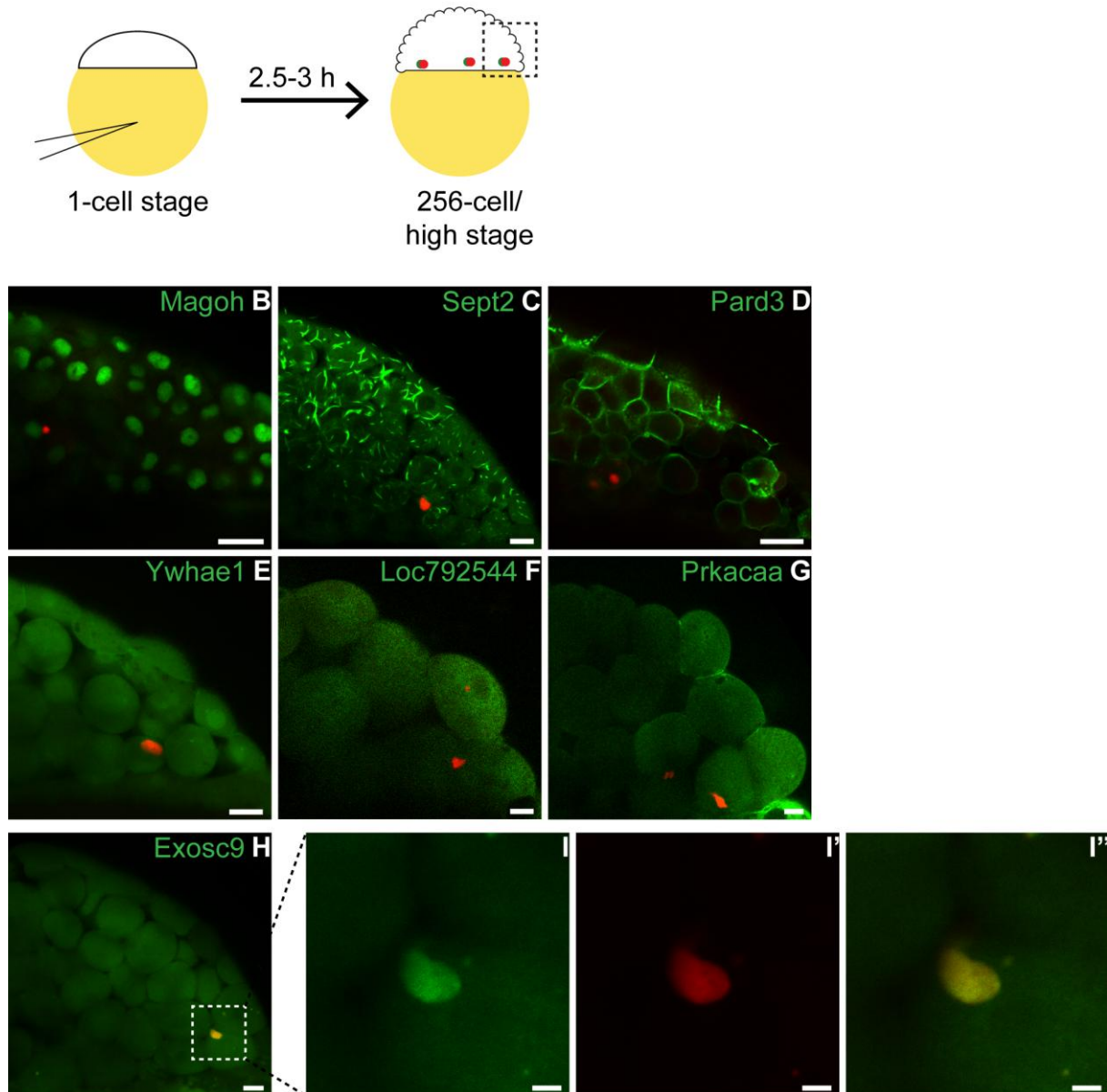


Figure 24: Exosc9-eGFP co-localizes with BucLoc-mCherry. (A) 1-cell stage wild type embryos were co-injected with RNA encoding the eGFP-tagged interaction candidate (120-230 pg) and BucLoc-mCherry (120 pg) and imaged at 2.5-3 hpf. (B-H) Living (B-E, H) or fixed (F, G) wild type embryos at high (B-E, H) or 256-cell stage (F, G) expressing the localization reporter BucLoc-mCherry (red) together with a eGFP-tagged interaction candidate imaged by confocal fluorescence microscopy (green, B, Magoh; C, Sept2; D, Pard3; E, Ywhae1; F, Loc792544; G, Prkacaa; H, Exosc9). Sections through cortical blastomeres are shown in lateral view, animal pole to the top. (I, I', I'') Magnified view of localization aggregate in H, showing co-localization of Exosc9-eGFP (green, I) and BucLoc-mCherry (red, I') (merge, I''). Scale bars represent 20 μm (B-H) and 5 μm (I-I'').

In summary, the analysis of the BucLoc interactome led to 213 potential interaction candidates. Out of seven tested proteins, Exosc9 shows co-localization with BucLoc *in vivo*. Hence, Exosc9 might be involved in a functional interaction with Buc leading to its localization to the germ plasm.

3.3.2 Endogenous Exosc9 co-localizes with Buc in oocytes

The annotation of five out of ten exosomal proteins by KEGG analysis indicates that the whole exosome complex might be involved in the interaction with Buc. The exosome has not been described as a component of the germ plasm so far. Going back to the full list of 3464 interaction candidates, in total nine of ten proteins of the cytoplasmic exosome complex were identified (Appendix, Table 17, Table 16). All of them were enriched 3.0-11.3 fold in BucLoc-eGFP and 7.8-32.6 fold in Buc-GFP (Table 13). This indicates that the complete cytoplasmic exosome complex is in the same compound with Buc and thus is a component of the germ plasm in early embryogenesis.

Table 13: Exosomal proteins identified by mass spectrometry analysis. Fold enrichment for Buc11 88-eGFP as well as Buc-eGFP in comparison to eGFP is given for each candidate. Detailed information is presented in the appendix (Table 17, Table 16).

	Name	Gene	Human homolog	Fold enrichment in	
				BucLoc-eGFP	Buc-eGFP
peripheral	3'-5' exoribonuclease CSL4 homolog	<i>exosc1</i>	<i>EXOSC1</i>	4.4	21.2
	exosome complex exonuclease RRP4	<i>exosc2</i>	<i>EXOSC2</i>	3.0	7.8
	exosome complex exonuclease RRP40	<i>exosc3</i>	<i>EXOSC3</i>	4.5	10.2
core	exosome complex exonuclease RRP41	<i>exosc4</i>	<i>EXOSC4</i>	4.5	12.4
	exosome component 5	<i>exosc5</i>	<i>EXOSC5</i>	3.7	14.1
	exosome complex component MTR3	<i>exosc6</i>	<i>EXOSC6</i>	8.4	14.8
	-	<i>exosc7</i>	<i>EXOSC7</i>	-	-
	MGC174638 protein	<i>exosc8</i>	<i>EXOSC8</i>	8.0	7.8
	exosome complex exonuclease RRP45	<i>exosc9</i>	<i>EXOSC9</i>	8.4	20.2
Exo-nuclease	- (only nuclear)	<i>exosc10</i>	<i>EXOSC10</i>	-	-
	DIS3-like exonuclease 1	<i>dis3l</i>	<i>DIS3L1</i>	11.3	32.6

To study if endogenous Buc and Exosc9 co-localize, wild type 256-cell stage embryos were immunostained for Buc and Exosc9 and analyzed by confocal fluorescence microscopy. Surprisingly, Buc and Exosc9 did not co-localize at the 256-cell stage (Figure 25A). Exosc9 was localized in small granules to the cytoplasm of all cells. Buc was localized to the germ plasm aggregates in the presumptive primordial germ cells and to a few small Buc granules in the cortical region as described before (Figure 25A, Figure 13). To examine if Buc and Exosc9 co-localize earlier, oocytes were analyzed as described above. In early stage IA oocytes, endogenous Buc and Exosc9 co-localized to the Balbiani body (Figure 25B). Additionally, a strong Exosc9 signal was detected within the germinal vesicle. The

localization of Exosc9 to the germinal vesicle was no longer detected at stage IB, although Buc and Exosc9 still co-localized to the Balbiani body (Figure 25).

Together with the mass spectrometry data of the BucLoc interaction partners, this indicates that endogenous Buc and Exosc9 interact via the localization domain BucLoc within the germ plasm. However, this interaction might be transient in the embryo. Furthermore, these results suggest the cytoplasmic exosomal complex as a newly identified component of the germ plasm in zebrafish oocytes.

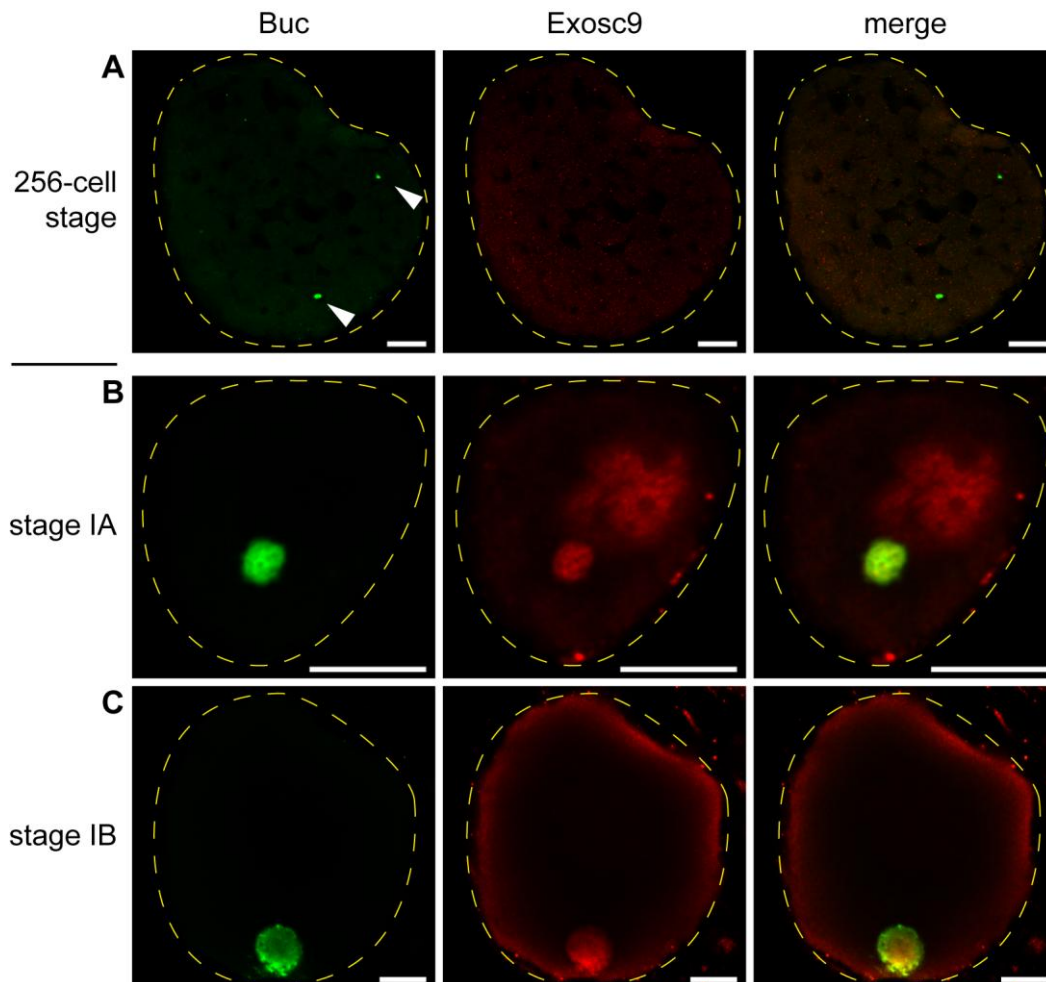


Figure 25: Endogenous Exosc9 co-localizes with Buc in the oocyte. Wild type 256-cell stage embryo (A) and stage IA (B) and IB (C) oocytes immunostained for Buc (green) and Exosc9 (red) and imaged by confocal fluorescence microscopy. No co-localization with the germ plasm (arrowheads) was detected in the embryo. Embryo section is shown in an animal view. Oocytes are shown in lateral view, animal pole to the top. Embryo and oocytes are outlined by a yellow dashed line. Scale bars represent 50 μm (embryo) and 10 μm (oocytes).

3.3.3 Endogenous p-Myl12.2 co-localizes continuously with Buc

As the exosome is involved in RNA degradation it is unclear how it is involved in the localization of Buc protein. Cytoskeletal proteins are more likely to be involved in the dynamic localization of Buc protein. The analyzed cytoskeletal element Sept2 did not show co-localization with BucLoc (Figure 24). Hence, the last candidate among the eight selected proteins, myosin light chain 12, was further analyzed.

3.3.3.1 Non-muscle myosin II components are BucLoc interactors

Myosin light chain 12, genome duplicate 2 (*myl12.2*) is a regulatory light chain of non-muscle myosin II (NMII) that was identified among the mass spectrometry proteins (Table 12; Appendix, Table 16). Non-muscle myosins are essential for cytokinesis and are involved in cell adhesion and polarity (Mabuchi and Okuno, 1977; Vicente-Manzanares et al., 2009). They form a superfamily of ATP-dependent motor proteins, responsible for actin-based motility and are composed of two heavy and two regulatory as well as two essential light chains (Vicente-Manzanares et al., 2009).

Interestingly, Myl12.2 and other proteins of the non-muscle myosin II complex were strongly enriched in the BucLoc Co-IP sample, but not in the Buc-GFP sample (Table 14).

Table 14: Components of non-muscle myosins II complex identified by mass spectrometry analysis. Fold enrichment for Buc11 88-eGFP as well as Buc-eGFP in comparison to eGFP is given for each candidate. Detailed information is presented in the appendix (Table 16).

Name	Gene	Human homolog	Fold enrichment in	
			BucLoc-eGFP	Buc-eGFP
myosin-9	myh9a	MYH9	14.9	1.2
myosin, light chain 12, genome duplicate 2	myl12.2	MYL12A	23.1	2.5
PREDICTED: myosin, light chain 6, alkali, smooth muscle and non-muscle isoform X2	myl6	MYL6	5.5	2.5

3.3.3.2 p-My12.2 co-localizes with Buc in 2-cell stage embryos

To investigate if non-muscle myosins co-localize with Buc *in vivo*, a commercial antibody was applied, which was raised against the phosphorylated human homolog of zebrafish Myl12.2. The phosphorylation of regulatory light chains leads to their activation and the formation of a functional NMII complex (Vicente-Manzanares et al., 2009). Previous reports have shown that phosphorylated non-muscle myosin II (p-NMII) co-localizes with germ plasm mRNAs at the cleavage furrow of 2-cell stage zebrafish embryos (Nair et al., 2013). To investigate if endogenous Buc co-localizes with active phosphorylated non-muscle myosin II regulatory light chain Myl12.2, 2-cell stage wild type embryos were immunostained for Buc as well as p-My12.2 and analyzed by confocal fluorescence microscopy. Indeed, endogenous Buc co-localized with p-My12.2 in a rod-like structure at the cleavage furrow (Figure 26A). A more detailed analysis revealed that the rod-like structure consists of small granules, lined up along the distal part of the cleavage furrow like on a ‘string of pearls’ (Figure 26B).

This data suggests that Buc is transported in small granules to the first cleavage furrow at 2-cell stage and that active non-muscle myosin II might be involved in this transport.

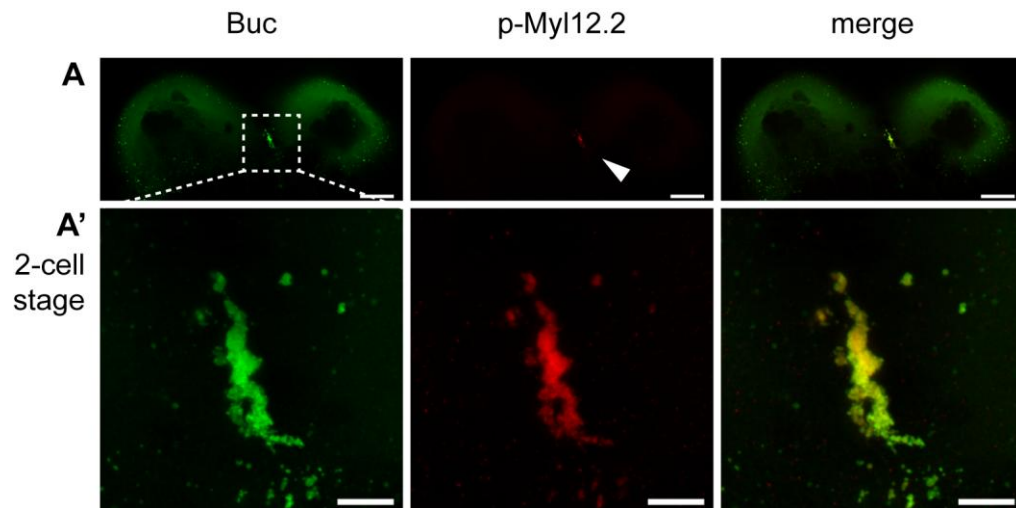


Figure 26: p-My112.2 co-localizes with Buc at the 2-cell stage cleavage furrow. Wild type 2-cell stage embryo immunostained for Buc and p-My112.2 and imaged by confocal fluorescence microscopy. Note that single granules are lined up like on a ‘string of pearls’ and together form a rod-like structure (arrowhead). Blastomeres on top of the yolk sac are shown in a lateral view, animal pole to the top. Magnification images of cleavage furrow (A’) are z-stack projections. Scale bars represent 50 μm (A) and 10 μm (A’).

3.3.3.3 p-My112.2 permanently co-localizes with Buc during oogenesis and embryogenesis

Localization of phosphorylated non-muscle myosin II in zebrafish was so far described for 2-, 4- and 8-cell stage. In these stages p-NMII localizes in a rod-like structure to the cleavage furrows and in a granular structures to the cortical region of the embryo, similar to Buc-GFP in the transgenic line (Figure 12) (Eno and Pelegri, 2013). If p-My112.2 was permanently involved in Buc localization, it would consistently co-localize with Buc.

To test this hypothesis, wild type 256-cell stage embryos and stage IB oocytes were immunostained for Buc as well as p-My112.2 and analyzed by confocal fluorescence microscopy. In 256-cell stage embryos, Buc and p-My112.2 co-localized in germ plasm aggregates, which is consistent with the identification of My112.2 by mass spectrometry analysis (Figure 27A, A’). Furthermore, p-My112.2 was localized together with Buc to the Balbiani body already during early stage IB oocytes (Figure 27B). Similarly, in later stage IB oocytes Buc and p-My112.2 were both relocated to the cortical region and spread along the cortex of the vegetal pole (Figure 27C). In this stage, p-My112.2 was additionally localized in granules within the germinal vesicle.

These results show that p-My112.2 consistently co-localizes with Buc from early oogenesis until early embryogenesis. This permanent co-localization supports a role of non-muscle myosin II in Buc localization. Furthermore, this is the first time that a protein directly associated with the cytoskeleton has been described to constantly localize to the germ plasm during zebrafish oogenesis and embryogenesis. Such a permanent protein localization to the germ plasm has so far only been described for Buc (this study).

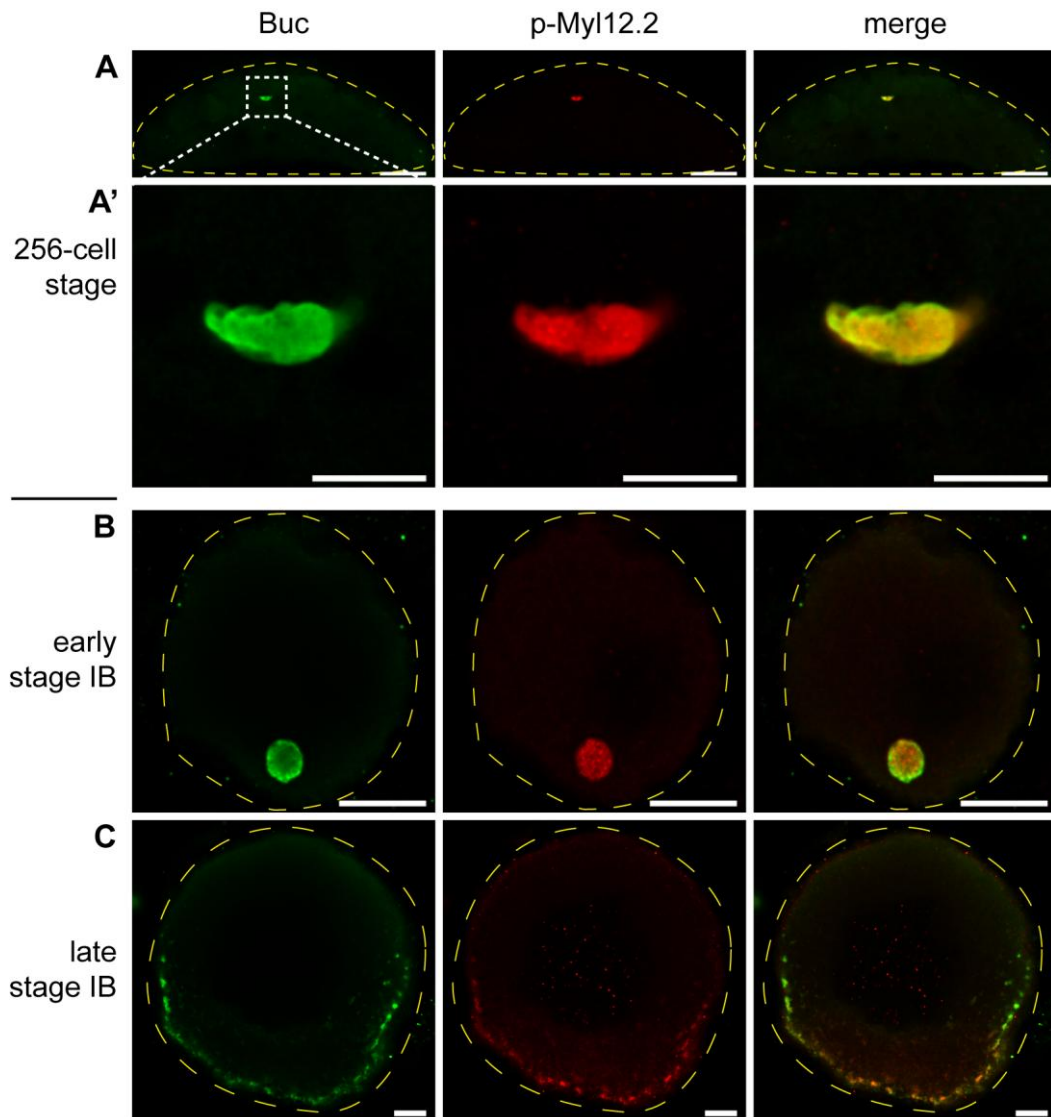


Figure 27: p-My12.2 co-localizes with Buc in oogenesis as well as embryogenesis. Wild type 256-cell stage embryo (A, magnified A') and stage IB oocytes (B, C) immunostained for Buc and p-My12.2 and imaged by confocal fluorescence microscopy. Embryo and oocytes, outlined by a yellow dashed line, are shown in lateral view, animal pole to the top. Scale bars represent 50 μm (A) and 10 μm (A', B, C).

In summary, the interaction with BucLoc and the localization analysis of non-muscle myosins suggests a role of the NMII-complex, composed of Myh9a, Myl12.2 and Myl6, in the localization of Buc to the germ plasm in zebrafish oogenesis as well as early embryogenesis.

4 Discussion

Buc has been recently identified in zebrafish as the first vertebrate protein that is necessary for germ plasm formation and sufficient for the formation of primordial germ cells (Bontems et al., 2009). Since proper germ plasm localization is a critical step in germ cell development, the localization of the germ plasm regulator Buc is of special interest. Therefore, the aim of this study was to characterize the localization of Buc protein in zebrafish and to analyze the underlying localization mechanism that ensures proper localization of Buc.

Buc was identified in this study as a permanent germ plasm component during zebrafish oogenesis and embryogenesis up to 48 hpf. Buc localization is established by the newly identified BucLoc localization domain in the zebrafish embryo. Using this domain, 213 proteins were identified that specifically interact with the Buc localization domain by Co-IP and subsequent mass spectrometry analysis. Further analysis of the interaction candidates led to the identification of Exocs9 as a germ plasm component in zebrafish oocytes. Moreover, consistent co-localization of Buc with the interacting non-muscle myosin II component Myl12.2 suggests a role of non-muscle myosin II in Buc localization.

4.1 Localization of endogenous Buc to the germ plasm and its functional relevance

Despite the unique function, the localization of endogenous Buc protein has not been characterized before this study. Therefore, the spatial and temporal requirement of the germ plasm organizing activity of Buc was not defined so far.

4.1.1 Buc localizes to the germ plasm during germ plasm aggregation and localization in oogenesis

The *buc* mutant phenotype shows a defect in germ plasm aggregation already during early oogenesis (Bontems et al., 2009). Hence, the protein was expected to be present in this early stage. Indeed, the analysis of endogenous Buc localization by immunostaining uncovered Buc protein as a permanent component of the germ plasm in oocytes (Figure 8, Figure 28). This observation is consistent with the localization of overexpressed Buc-GFP (Bontems et al., 2009). In addition, *buc* mRNA localizes to the Balbiani body in early oocytes (Bontems et al., 2009). Furthermore, Buc protein was recently detected in the Balbiani body by immunostaining with a polyclonal antibody directed against the very N-terminus of Buc (Heim et al., 2014). Likewise, the *Xenopus* homolog of Buc, Xvelo, has recently been shown to localize to the Balbiani body in early oocytes (Nijjar and Woodland, 2013).

Buc localization in oocytes suggests that Buc protein activity is essential in oogenesis starting at stage IA. A previous finding shows that other germ plasm mRNAs such as *vasa*, *dazl* and *nanos* are no longer localized in *buc* mutant oocytes (Bontems et al., 2009; Marlow and Mullins, 2008). Together with the early localization of Buc to the Balbiani body, this finding indicates an upstream role of Buc in the aggregation and localization of germ plasm components. Since no known functional domains could be identified in the Buc sequence, the protein might act as a scaffolding protein and serve as a platform for the aggregation of other germ plasm components.

In addition, Buc localization accompanies the disassembly of the Balbiani body and Buc moves with the germ plasm aggregates to the vegetal cortex in stage IB oocytes (Figure 8, Figure 28). This pattern of localization resembles the localization of previously described germ plasm mRNAs as well as *buc* mRNA and the germ plasm protein Rbpms2 (Bontems, 2009; Kosaka et al., 2007). Therefore, Buc localization suggests the permanent necessity of its activity in the germ plasm. One could speculate that the protein is involved in the maintenance of the germ plasm aggregates or that Buc is involved in their localization to the vegetal pole or both.

Furthermore, Buc mirrors the localization of *vasa* mRNA in late stage II oocytes, indicating that Buc co-localizes with the germ plasm throughout oogenesis (Figure 8, Figure 28) (Kosaka et al., 2007). Buc is the only germ plasm protein that has been described during these late stages. During late oogenesis at stage III Buc is no longer detected (Figure 8G). Nevertheless, the presence of Buc right after fertilization strongly suggests that Buc is present during late oogenesis (Figure 11). The accumulation of yolk globules during late oogenesis and their autofluorescence make it difficult to detect a comparatively minor signal in the huge oocyte.

Interestingly, *buc* mRNA changes its localization in oogenesis between stage II and III from vegetal to animal (Bontems et al., 2009). This indicates the presence of various pathways for germ plasm localization during late zebrafish oogenesis. *Vasa* mRNA spreads along the vegetal cortex, *dazl* mRNA localizes strictly to the vegetal cortex, while *nanos3* is vegetally localized and is no longer detected during stage III (Kosaka et al., 2007). Since Buc protein spreads along the vegetal cortex similar to *vasa* mRNA, both germ plasm components seem to share the same localization pathway during late oogenesis. At the same time, this indicates that *buc* mRNA and Buc protein are localized by separate pathways in late oogenesis.

The detailed analysis of Buc localization identified Buc as permanent germ plasm component during zebrafish oogenesis. Hence, Buc can be used as the first permanent germ plasm marker on the protein level during zebrafish oogenesis. Moreover, the permanent Buc localization suggests the necessity of Buc activity throughout zebrafish oogenesis. Together with previous findings, this indicates a role of Buc in the aggregation of germ plasm. Buc might be additionally involved in the dynamic localization of these aggregates to the Balbiani body and the vegetal cortex.

4.1.2 Buc is a stable germ plasm component during germ cell specification in early embryogenesis

The previous finding that *buc* mRNA does not localize to the germ plasm during early zebrafish embryogenesis, raised the question of Buc localization during germ cell specification (Bontems et al., 2009). The presence of endogenous Buc during early cleavage stages and the localization to the germ plasm indicates a role of Buc in germ cell specification during early embryogenesis (Figure 13, Figure 28). This result is in line with the detection of transgenic Buc-GFP, which shows an identical localization pattern as endogenous Buc (Figure 13). Similar to Buc, the previously described germ plasm proteins Brul and Ziwi localize to the first and second cleavage furrow at 4-cell stage (Hashimoto et al., 2006; Houwing et al., 2007). Other germ plasm RNAs such as *vasa*, *nanos3*, *dazl* or *brul* mRNA also localize to the

distal end of the cleavage furrows (Hashimoto et al., 2004). The situation that mRNA is not localized, while the corresponding protein localizes to the germ plasm as it is the case for *buc*, has already been described for other germ plasm components, such as *Drosophila vasa* transcripts (Hay et al., 1988).

The *buc* mutant embryo does not initiate cleavage after fertilization (Dosch et al., 2004). Therefore, it is difficult to address whether Buc activity is essential during early embryogenesis. All maternally contributed germ plasm components together are required for zebrafish germ cell formation at 4-cell stage (Hashimoto et al., 2004). Since this also includes Buc, an essential role of the protein in germ cell formation in the embryo cannot be ruled out. In addition, overexpression of Buc in 1-cell stage induces the specification of additional primordial germ cells (Bontems et al., 2009). Since this takes place without inducing *de novo* formation of other germ plasm components, a model was suggested, in which Buc accumulates redundant germ plasm components and by this induces the formation of additional primordial germ cells (Bontems et al., 2009). This model is in accordance with the observed localization of Buc to the germ plasm (Figure 13, Figure 28). Moreover, decreasing levels of transgenic Buc-GFP localized at the cleavage furrows are observed after each cell cleavage (Figure 12). This observation is in line with the recent finding that the amount of germ plasm at the cleavage furrows is approximately halved with every cell cleavage (Eno and Pelegri, 2013). Decreasing localization of Buc to the cleavage furrows together with the previously identified role of Buc in germ cell induction suggests that Buc might be a limiting factor in germ plasm aggregation. Hence, germ plasm aggregation might limit the localization of germ plasm to the cleavage furrows.

To directly address the question if Buc is essential for primordial germ cell specification during zebrafish embryogenesis, a knockdown of the maternally provided protein would be necessary during the first cleavage stages. Unfortunately, no methods are available to specifically knock down an already expressed endogenous protein in a temporally controlled manner. To overcome these methodical constraints, the transgenic *buc-gfp* line could be of use. The GFP-tagged protein could be eliminated at the 4-cell stage by laser ablation of the protein or bleaching with high laser intensity. In addition, the protein knockdown system deGradFP, which directly targets GFP fusion proteins for degradation, could be used to eliminate Buc-GFP in the transgenic line (Caussinus et al., 2012). In that case, mRNA encoding deGradFP would have to be injected already in oocytes to ensure the presence of the protein at the beginning of embryonic development. Injection in oocytes would also be necessary to observe an early effect after overexpression of a dominant negative construct, such as BucLoc. However, such an approach would only be promising if the interaction is dynamic and BucLoc can replace Buc.

Buc permanently localizes to the germ plasm during early zebrafish embryogenesis, which indicates that Buc activity might be required for germ cell specification from fertilization up to blastula stage. Due to the permanent germ plasm localization, Buc can be used as a protein germ plasm marker in future studies.

4.1.3 Buc localizes to germinal granules in primordial germ cells

Buc mRNA is expressed throughout oogenesis and early embryogenesis until 3 hpf at constant levels. These mRNA levels decrease during midblastula transition at 4 hpf and are no longer detected at 7 hpf (Bontems et al., 2009). In contrast to *buc* mRNA, the protein is expressed during embryogenesis and is still detected in co-localization with Vasa at 48 hpf in primordial germ cells (Figure 14, Figure 28). In accordance, transgenic Buc-GFP continuously localizes to the primordial germ cells until 72 hpf (own observation). These results indicate that Buc activity might be required in primordial germ cells during late embryogenesis. A possible role of Buc might be to maintain the structure of the germ plasm granules and properly localize them in the perinuclear region. Using the transgenic *buc-gfp* line and the described protein knockdown methods (Chapter 4.1.2), Buc protein can be specifically eliminated in primordial germ cells. Subsequently, the resulting phenotype might be analyzed in terms of germ plasm localization and survival of primordial germ cells.

Since the zygotic *buc* mRNA expression starts late in females past juvenile stage (42 dpf) (Bontems et al., 2009), the detected Buc protein is most likely of maternal origin. This indicates that Buc protein is highly stabilized once it reaches the primordial germ cells. Interestingly, the maternally provided germ plasm components Vasa and Brul are expressed at stable levels throughout embryogenesis up to 24 hpf (Hashimoto et al., 2006; Knaut et al., 2000). Hence, it is likely that also maternal Buc protein is stabilized up to 24 hpf. Furthermore, *vasa* transcripts levels drop at 6 hpf. Thus, the maternal Vasa protein is most likely stabilized during early embryogenesis, similar to Buc, although additional protein might come from zygotically expressed *vasa* mRNA (Knaut et al., 2000; Wolke et al., 2002). Together with the localization analysis, this suggests that maternal Buc might be continuously expressed during early embryogenesis. To test this hypothesis, the expression levels of endogenous protein during embryogenesis have to be analyzed by immunoblotting.

Despite the unknown role of Buc in primordial germ cells, the localization to germinal granules suggests that Buc activity might be required for germ cell maintenance beyond 48 hpf. Nevertheless, the late function of Buc remains to be discovered.

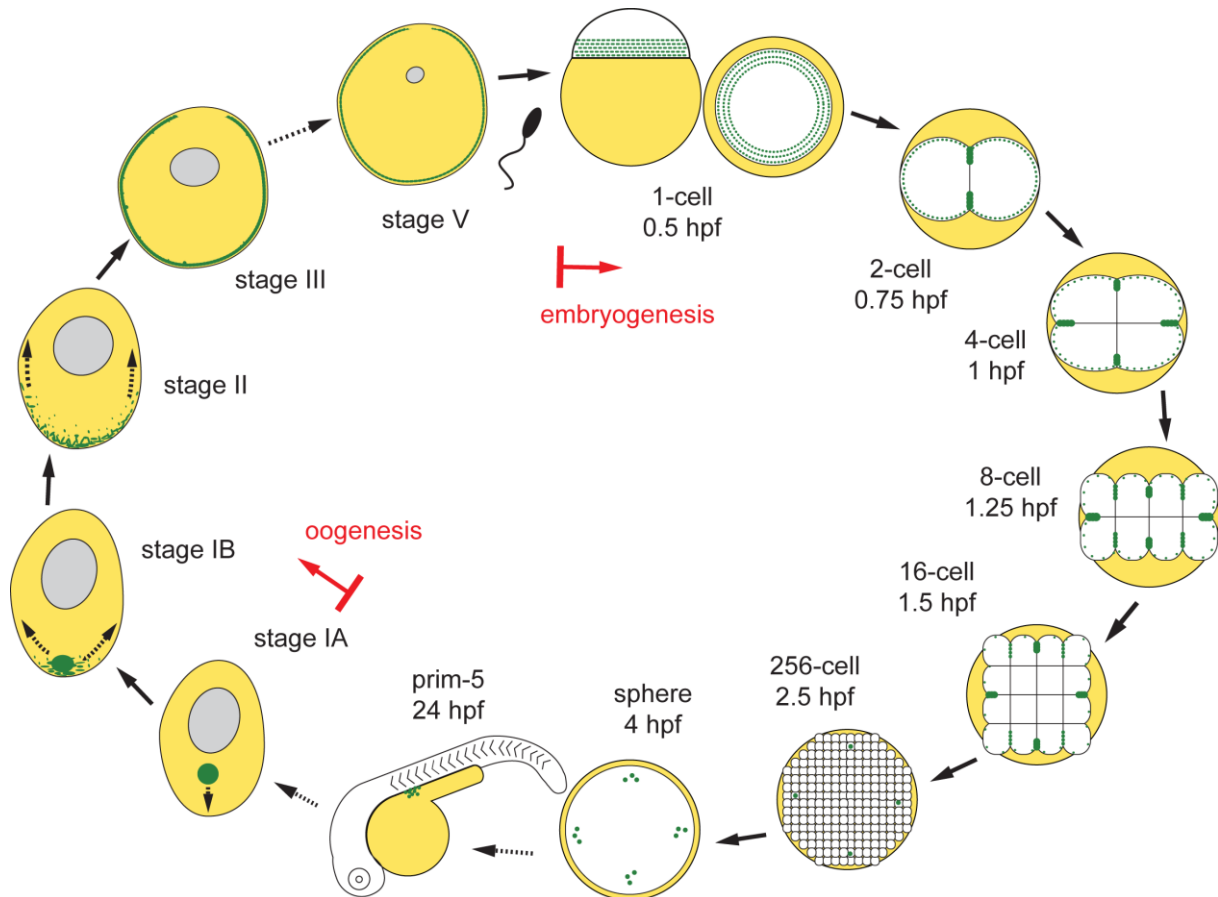


Figure 28: Schematic representation of endogenous Buc protein localization during zebrafish oogenesis and embryogenesis. Schematic drawings show the localization of Buc (green) during different stages of oogenesis and embryogenesis. Note that not all stages are depicted. Missing stages are indicated by a dashed arrow. Germ plasm localization is described in detail in the text. A 1-cell stage embryo is shown in lateral and animal view. Prim-5 stage embryo is presented in lateral view. Other embryonic stages are shown in animal view with the yolk (yellow) beneath the cells (white). Oocytes are displayed in lateral view, animal pole to the top. Embryos and oocytes are not drawn to scale.

In summary, Buc is the first protein described in zebrafish that is consistently localized to the germ plasm from oogenesis till embryogenesis. This not only makes it a valuable, universal marker of the germ plasm at all stages, but also raises the question of its function during this developmental period. The common theme of germ plasm aggregation and localization in all the stages of localized Buc and the previously obtained functional data, indicate a consistent role for Buc in germ plasm aggregation, localization and maintenance.

4.2 Transgenic Buc-GFP marks the germ plasm *in vivo*

Integration of *buc-gfp* into the *buc^{p106}* mutant background rescues the mutant phenotype (Bontems, 2009). Furthermore, transgenic Buc-GFP mimics the endogenous Buc localization to the germ plasm during oogenesis as well as embryogenesis (Figure 13, Figure 10). Thus, transgenic Buc-GFP not only mirrors the activity of endogenous Buc, but also reflects its spatial and temporal expression. This makes the transgenic *buc-gfp* zebrafish line a valuable tool to continuously analyze the germ plasm localization in the developing organism. In addition, the line is homozygous for the *buc-gfp* transgene. Therefore, new generations do not have to be genotyped, making it easy to propagate the line.

The detailed analysis of Buc-GFP in the transgenic line revealed that Buc localizes to the first, second and third cleavage furrows (Figure 12). A significant localization of Buc could not be detected at the fourth cleavage furrows. Interestingly, the amount of localized protein, judged by the fluorescence signal, decreases from one cleavage furrow to the next (Figure 12). This might be the reason that localization of Buc to the third cleavage furrows is not maintained and suggests a concentration-dependent maintenance of germ plasm at the cleavage furrow. Most likely, germ plasm is degraded as the local concentration falls below a certain threshold. Such an instability of germ plasm aggregations at the third cleavage furrows has recently been described using *vasa* mRNA as germ plasm marker (Eno and Pelegri, 2013). Moreover, Eno and colleagues found that the number of localized granules is approximately halved with every cell cleavage. They suggest a correlation between the bisection of germ plasm granules and the bisection of the cortical cell surface each cell cleavage (Eno and Pelegri, 2013). Since Buc-GFP is also localized to the granules at the cortex (Figure 12), the transgenic line can be used to characterize these dynamics and to identify parameters involved in this process. Furthermore, tracking of single granules would help to investigate the process of germ plasm aggregation in detail within the blastodisc and the cleaving embryo. This would also allow investigating the lack of phenotype after the depletion of germ plasm in the cleavage furrow at 2-cell stage (Hashimoto et al., 2004). The aggregation of cortical germ plasm granules to the second cleavage furrow at 4-cell stage might be sufficient to prevent loss of primordial germ cells.

Strong reduction in the number of cortical Buc-GFP positive granules indicates that if they do not aggregate at the cleavage furrow, they are rapidly degraded (Figure 12). This would be consistent with previous results that *vasa* mRNA positive granules at the cortex are strongly reduced in number during early cleavage stages and *vasa* mRNA is rapidly degraded in somatic cells (Wolke et al., 2002). Also in *C. elegans*, germ plasm, which is not properly localized to the presumptive primordial germ cells, becomes degraded (DeRenzo et al., 2003; Zhang et al., 2009). Further detailed analysis of Buc-GFP aggregations in presumptive primordial germ cells at sphere stage revealed the existence of small inclusions (Figure 21). With their size of 0.5-1 μm , it might be that these inclusions are mitochondria, which are a known component of germ plasm (Kloc et al., 2004).

The transgenic *buc-gfp* line will not only be helpful for characterizing the function of Buc in early and late embryogenesis (Chapters 4.1.2 and 4.1.3), but also for other experiments, in which it is essential to follow germ plasm dynamics *in vivo* at a high spatial and temporal resolution.

In transgenic *buc-gfp* embryos, the inheritance of germ plasm and the subsequent migration of primordial germ cells can be tracked right off the first cell. Hence, with new imaging techniques, such as light-sheet microscopy, germ plasm dynamics can be analyzed from 1-cell stage on in high temporal and spatial resolution. In contrast to microinjection of mRNA encoded germ plasm markers such as *gfp-3'UTR-nanos*, the protein dynamics can be analyzed right after fertilization without any delay or manipulations of the embryo (Kopranner et al., 2001). In addition, fluorescence recovery after photobleaching (FRAP) experiments can provide insight into the dynamics of the germ plasm structure at the embryonic stage of choice. Moreover, the transgenic *buc-gfp* line can be crossed to any other transgenic zebrafish marker line that labels for example a specific cell compartment. This would allow the *in vivo*

detection of localized germ plasm in relation to a cellular compartment. Effects on germ plasm can likewise be analyzed in the transgenic *buc-gfp* line by gene overexpression through RNA microinjection or drug treatments. Additionally, the transgenic *buc-gfp* line will be of use for isolation, transplantation, culturing and any *in vitro* manipulations of primordial germ cells.

To sum up, the transgenic *buc-gfp* line is the first zebrafish line, labeling the germ plasm throughout oogenesis and embryogenesis. Therefore, it will be an effective tool for numerous experimental approaches to characterize the dynamics of germ plasm and to mark primordial germ cells.

4.3 Buc and Osk have distinct localization mechanisms

The stable localization of Buc to the germ plasm throughout early embryogenesis and its essential function in germ plasm aggregation raised the question of how this localization is established and what the underlying mechanisms are (Bontems et al., 2009). Zebrafish Buc and *Drosophila* Osk are both important regulators in germ plasm formation (Bontems et al., 2009; Ephrussi and Lehmann, 1992). Furthermore, Buc and Osk both show a specific localization pattern and are restricted to the vegetal / posterior pole in the embryo (Figure 11) (Bontems, 2009; Markussen et al., 1995). As *Drosophila* Osk is additionally able to induce the formation of ectopic germ cells in zebrafish (Bontems, 2009), the localization of Buc was addressed in a cross-species approach.

Intensive comparison and analysis of Buc and Osk protein sequences did not reveal any shared domains (Figure 15). Thus, it is unlikely that Buc and Osk are homologs, deriving from a common ancestor. In fact, this finding supports the theory that germ plasm evolved divergently in different species (Johnson et al., 2011). Nevertheless, the functional analogy in zebrafish might also extend to a similar localization mechanism (Bontems, 2009).

Localization analysis of Buc and Osk in zebrafish as well as in *Drosophila* revealed distinct localization patterns of both proteins (Figure 16, Figure 18). The condensed anchoring of Osk-eGFP to the anterior pole is in contrast to the more widely distributed Buc-eGFP in *Drosophila* (Figure 16). Tight localization of Osk-eGFP targeted by the *bicoid* 3'UTR to the anterior cortex resembles the condensed localization previously observed for endogenous Osk at the posterior pole (Breitwieser et al., 1996).

In addition, the analysis of the embryonic phenotype of the transgenic of *osk-egfp* flies indicates that this localization is sufficient for the previously described activity in anterior posterior patterning (Figure 17) (Ephrussi and Lehmann, 1992). The previously described phenotype of ectopic germ cell formation in transgenic *osk-bcd3'UTR* flies was not observed in the transgenic *osk-egfp-bcd3'UTR* flies of this study (Ephrussi and Lehmann, 1992; Suyama et al., 2009). Hence, it might be that the eGFP-tag hinders Osk to interact with proteins essential for the induction of germ cell formation. Transgenic *buc-egfp-bcd3'UTR* flies do not show any phenotype, which indicates that the difference in localization to Osk is of functional relevance and that Osk contains a localization signal that is not present in Buc (Figure 17). So far, a domain sufficient for Osk interaction with the actin-binding protein Lasp has been described *in vitro* (Suyama et al., 2009). However, it is unclear whether this domain is also necessary to localize Osk *in vivo*.

In zebrafish, Buc-eGFP shows a specific localization pattern in zebrafish while Osk-eGFP does not (Figure 18). A signal in Osk protein, essential for its localization, has not been described so far. This finding indicates that the previously observed ability of Osk to induce the formation of additional primordial germ cells is based on an artificial localization of the protein caused by overexpression. Moreover, an *osk* transgene was not able to rescue the mutant (Bontems, 2009). Although the localization of the protein was not analyzed, it is likely that also in this case, Osk did not properly localize to the germ plasm.

The cross-species approach highlights the importance of proper localization of a protein for its functional activity, but did not lead to new insights into the localization mechanisms of Buc.

4.4 Identification of BucLoc and other conserved domains in Buc protein

4.4.1 BucLoc identified as the first protein germ plasm localization domain

Buc transcripts are restricted to the germ plasm during early oogenesis, but are no longer localized during embryogenesis (Bontems et al., 2009). Thus, Buc protein itself has to contain a signal that is essential for its proper localization to the germ plasm. This localization signal was identified at the N-terminus in an extensive systematic Buc deletion analysis and is encoded by amino acids 11-88 (Figure 20). BucLoc is necessary and sufficient for localization of Buc protein to the germ plasm (Figure 20, Figure 21). This is the first time that a protein domain has been identified in a metazoan that exhibits these characteristics.

Interestingly, the localization domain BucLoc overlaps with the N-terminal domain (aa 24-84) conserved in other vertebrate Buc homologs (Figure 15B). This suggests that the localization domain is not only essential in zebrafish Buc, but might as well be functionally relevant in other vertebrate homologs. Lately, this hypothesis was supported by the identification of a localization domain in Xvelo, the *Xenopus* homolog of Buc. In Xvelo, the first 114 N-terminal amino acids are sufficient to localize a GFP fusion to the germ plasm in *Xenopus* oocytes (Nijjar and Woodland, 2013). Hence, the BucLoc localization might be conserved in other Buc vertebrate homologs.

In addition, the finding that the Xvelo localizes by an overlapping localization domain in oocytes, suggests that BucLoc might as well be responsible for germ plasm localization of Buc in oocytes (Nijjar and Woodland, 2013). BucLoc is present in the predicted *buc*^{p43} and *buc*^{p106} mutant proteins. Therefore, the expressed protein should localize in mutant oocytes. Nevertheless, Buc protein was not detected in immunostainings (Figure 9B). This suggests that the mutant proteins are not expressed or rapidly degraded after expression. An additional localization domain, involved in localization of Buc protein in the oocyte, cannot be excluded. However, it is unlikely that the non-conserved C-terminal part, missing in predicted Buc^{p106} protein, encodes a localization domain (Figure 19). Immunoblots of early oocyte protein lysates would conclusively address the question whether the *buc* mutants are protein null alleles.

Surprisingly, analysis of the amino acid composition of BucLoc revealed that proline and aromatic amino acids are strongly enriched (Figure 22). Additionally, a SH3-domain binding site was predicted at the C-terminal end of BucLoc (Figure 22). Since Buc48-88 contains the predicted SH3-domain binding site and does not localize, it is unlikely that localization exclusively depends on this site (Figure 20). Site directed mutagenesis of the predicted SH3-domain binding site would shed light on its functional relevance. Interestingly, the

interaction of Osk with the actin-binding protein Lasp depends on the SH3-domain of Lasp. Nevertheless, Osk does not contain a perfect SH3-domain binding site in the region that is sufficient to interact with Lasp (Suyama et al., 2009).

In addition, proline-rich regions are known to form stiff structures that can bind rapidly and non-specifically to other proteins, thus acting as a “sticky arm” (Williamson, 1994). Hence, the N-terminus of Buc might bind to other proteins based on such a fast, non-specific interaction. However, an unspecific binding contradicts the specific localization observed for Buc. In this case, only if the mRNA is localized in the first place, the expressed protein could be specifically targeted to its interaction partners. As *buc* mRNA is localized to the germ plasm in the early oocyte, Buc might bind other germ plasm proteins unspecifically and serve as germ plasm scaffolding protein persistently during oogenesis and embryogenesis.

Besides its role in localization of Buc to the germ plasm, BucLoc can be exploited as unidirectional molecular shuttle to the germ plasm. So far, only RNA can be targeted to primordial germ cells by injection of the RNA, tagged with the 3'UTR of *nanos3* (Kopranner et al., 2001; Saito et al., 2006). However, after translation of the RNA in the primordial germ cells, the protein does not necessarily have to localize specifically to the germ plasm. With the Buc localization domain at hand, proteins of choice can be tagged with BucLoc and are then specifically transported and anchored to the germ plasm. By this, the germ plasm can, for instance, be labeled with fluorescent proteins. Additionally, BucLoc might be used to target RNA guided nucleases, such as Cas9, specifically to the primordial germ cells, thereby enhancing mutagenesis rates (Harrison et al., 2014). Furthermore, such a mutagenesis approach would allow the targeted induction of germline specific mutations in a vertebrate. Such germline clones would be valuable to study the role of otherwise zygotic lethal mutations in the germline and are so far only available in *Drosophila* (Perrimon, 1998). Moreover, the BucLoc localization domain would allow screening specifically for proteins that interfere with germ plasm maintenance or with specification of primordial germ cells. In the long run, such a BucLoc fusion protein might be interesting for medical applications to induce sterility in vertebrate animals already during embryogenesis.

The outlined findings show that BucLoc not only provides insight into the localization mechanism of Buc, but will also find its application as a molecular shuttle to the germ plasm.

4.4.2 Additional protein domains in Buc

The identification of BucLoc as the sole localization domain proofed the assumption wrong that the very C-terminus, lost in the predicted Buc^{p106} mutant protein, is involved in localization. Although, the 38 C-terminal amino acids are not conserved, they are essential for Buc activity as they are missing in the *buc*^{p106} mutant (Figure 15). The lack of conservation indicates that the C-terminus does not encode a specific motif, but might, if lost, change the secondary structure of Buc in a way that access to other domains is impeded. Such a domain might be the newly identified and highly conserved domain in the center of Buc (aa 372-394) (Figure 15). An essential role in Buc localization can be excluded for the central domain, as BucLoc on its own is sufficient as well as essential to localize the protein. Nevertheless, the high conservation of the central domain in Buc vertebrate homologs suggests an important function of this domain. Therefore, systematic Buc deletion constructs could be analyzed for

their potential to induce the formation of additional germ cells using a previously described assay (Bontems, 2009).

Overexpression of Buc^{p43}-eGFP or Buc-eGFP in *Drosophila* embryos leads to a granular localization of the protein (Figure 16). The formation of granules in *Drosophila* indicates that the protein interacts with other proteins or with itself. Recent data of Xvelo, the Buc homolog in *Xenopus*, support the idea of Buc self-interaction. Bimolecular fluorescence complementation experiments of Xvelo indicate self-interaction, which is lost in a splice variant, lacking C-terminal two thirds of Xvelo (aa 270-779) (Nijjar and Woodland, 2013). As Buc^{p43} lacks the C-terminal half of Buc, a presumptive self-interaction domain might be encoded in the N-terminal half (aa 1-361). Therefore, a potential Buc self-interaction domain might exist in the C-terminal end of Buc^{p43} (aa 270-361), which would exclude the conserved central domain in Buc (Figure 19). Overexpression of Buc and Buc deletion constructs in cell culture, would determine whether Buc or specific Buc domains self-interact and whether Buc is intrinsically capable of granule formation.

Besides the localization domain BucLoc, being necessary and sufficient to localize Buc as well as other proteins to zebrafish germ plasm, also other functional domains might be hidden in Buc and are awaiting their discovery. Particularly the highly conserved central domain is a promising candidate to encode a functional Buc domain.

4.5 Analysis of the BucLoc interactome

4.5.1 Identification of BucLoc interacting proteins by Co-IP and mass spectrometry analysis

With the identification of BucLoc, Buc interacting proteins involved specifically in its localization could be identified in living embryos. The protein was purified by immunoprecipitation when it was localized to the germ plasm in the presumptive primordial germ cells. Hence, Co-IP of *in vivo* proteins with subsequent mass spectrometry analysis is a powerful tool to identify biologically relevant protein interaction partners.

BucLoc Co-IP and subsequent mass spectrometry analysis revealed 213 potential interaction partners (Figure 23). Not all proteins could be annotated to different molecular pathways, most likely due to the incomplete annotation of zebrafish proteins to the KEGG database. Interestingly, 8% of the annotated proteins are involved in mRNA transport, surveillance and degradation (Figure 23). This is in line with a suggested role of germ plasm in mRNA processing (Strome and Lehmann, 2007). Since these proteins are unlikely to be involved in the localization of Buc, it might be that also secondary bound germ plasm proteins were co-immunoprecipitated.

Two of eight analyzed BucLoc were identified to co-localize with Buc on the endogenous level in the germ plasm. This indicates that the BucLoc Co-IP and subsequent mass spectrometry reached its goal and enriched for proteins specifically interacting with the BucLoc localization domain *in vivo*. On the other side, the other six proteins are most likely false positive interactions. One reason for these false positives might be that during lysis of the embryo, proteins of different cells and different compartments can interact that otherwise would never come in contact. Hence, the number of false positives might be reduced in advance by enrichment of primordial germ cells using fluorescence-activated cell sorting, although this method has not been used so far in these early stages (Fan et al., 2008). In

addition, Buc Δ 11-88-eGFP, which was not available at the time when the Co-IP experiments were done, can be used as negative control for future experiments.

Unexpectedly, Buc was only moderately enriched in the Buc-GFP Co-IP sample (2-fold) and the counts in BucLoc-eGFP Co-IP sample were lower as in the negative control (Appendix, Table 16). This might be due to problems with the Co-IP or with the identification of Buc in the mass spectrometry. Surprisingly, the sequenced Buc peptides that were identified in mass spectrometry, never covered the first 88 amino acids of Buc. Overall 45 % of the Buc sequence were covered by sequenced peptides. The reason for the lack of sequenced peptides at the Buc N-terminus might have technical reasons, but remains unclear. Hence, the lack of sequenced peptides for BucLoc in the mass spectrometry analysis is most likely the reason why Buc was not detected enriched in the BucLoc-eGFP Co-IP sample.

The BucLoc-eGFP Co-IP combined with subsequent mass spectrometry analysis identified interacting proteins involved in localization of Buc *in vivo*. Nevertheless, the method can be improved to lower the level of false positives by enrichment of the germ plasm containing cells prior to the Co-IP or by use of newly available controls.

4.5.2 Further promising proteins among the 213 BucLoc interaction candidates

Besides the eight proteins that have been analyzed for co-localization with BucLoc, also other proteins among the 213 interaction candidates are worth being discussed (Table 12; Appendix, Table 17).

The amino acid analysis of BucLoc revealed a strong enrichment of prolines (Figure 22). In this context, it is remarkable that three out of four proteins classified as proline-rich coiled-coil proteins were strongly enriched in the BucLoc Co-IP sample. The functions of PRRC2C (*prrc2c*), PRRC2B isoform X4 (*prrc2b*) and large proline-rich protein BAT2 (*prrc2a*) are unknown. In addition, KEGG analysis revealed six nuclear pore proteins among the 213 interaction candidates with the highest counts for Nup133. This is interesting in the context of previous results, which describe the close association of germ plasm components with nuclear pores in zebrafish as well as *C. elegans* (Knaut et al., 2000; Updike et al., 2011).

In the same screen, in which *buc* was identified, another maternal effect mutant, called *p6cv*, was identified with the same phenotype as the *buc* mutant (Dosch et al., 2004). The mutated gene encodes for microtubule-actin crosslinking factor 1 (*macfla*), which belongs to the highly conserved spectraplakins family of cytoskeletal linker proteins (Bontems et al., 2011; Gupta et al., 2010). In the *macfla* mutation oocyte polarity is disrupted, the oocyte nucleus is mislocalized and the Balbiani body enlarged as well as not properly localized (Gupta et al., 2010). These findings indicate that the proper localization of germ plasm depends on cytoskeletal elements in oocytes. Moreover, analysis of zebrafish hair cells suggested a role of Macfla in the integration of actin and tubulin cytoskeletal networks (Antonellis et al., 2014). Interestingly, Macfla was strongly enriched in BucLoc-eGFP and Buc-GFP Co-IP samples (Appendix, Table 17). This indicates, that Macfla is not only involved in germ plasm aggregation in the oocyte, but might additionally have a role in embryonic germ plasm. Despite this interesting phenotype and the strong enrichment in the mass spectrometry analysis, *macfla* was not pursued further as an interaction candidate since it encodes a huge 899 kDa protein, which would be very time-consuming to clone. Besides Macfla and non-muscle myosin II, another cytoskeletal element was strongly enriched only in the

BucLoc-eGFP Co-IP sample: dynein heavy chain, a component of the motor protein dynein, which is involved in cargo transportation along cytoskeletal microtubules (Appendix, Table 16). This additionally suggests a close association of the microtubular cytoskeleton with the localization of Buc.

Most germ plasm proteins, identified so far in zebrafish, are involved in RNA binding and were therefore not expected to be among the interaction candidates. Nevertheless, the zebrafish RNA-binding protein Rbpms2 was recently identified to interact with the N-terminus of Buc (aa 1-52 and 117-251) in a yeast two-hybrid analysis. Moreover, Rbpms2 co-immunoprecipitates with GFP-Buc after overexpression in human embryonic kidney cells (Heim et al., 2014). In addition, the *Xenopus* germ plasm component Hermes, homolog of zebrafish Rbpms2, interacts with Xvelo, the *Xenopus* homolog of Buc, in yeast two-hybrid screens. Furthermore, *in vitro* translated Xvelo co-immunoprecipitates with Hermes (Nijjar and Woodland, 2013). Contrasting these results, Rbpms2 was not identified among the potential interaction candidates of BucLoc. The reason might be that BucLoc only partially overlaps with the two proposed zebrafish Rbpms2 interaction domains. However, also among the Buc-GFP interacting proteins Rbpms2 was not identified. This suggests that the interaction identified *in vitro* is not relevant *in vivo* during early zebrafish embryogenesis. As expected, other known germ plasm RNA-binding proteins, such as Brul or Ziwi, were not identified as significant interaction candidates of Buc or BucLoc as well. In contrast, Vasa was more than threefold enriched in the Buc-GFP Co-IP sample, but not in BucLoc (Appendix, Table 16). This suggests that Vasa might interact with Buc outside the localization domain and thus might be involved in another functional interaction.

In summary, besides the analyzed BucLoc interaction candidates, further proteins, identified in the mass spectrometry analysis, are promising candidates to be involved in Buc interactions and need to be further investigated.

4.6 Exosome complex newly identified in germ plasm

Seven potential BucLoc interaction candidates were analyzed by overexpression for co-localization with BucLoc in zebrafish embryos. Overexpressed Exosc9-eGFP co-localized with BucLoc-mCherry in the germ plasm in embryos at 2.5 hpf and thereby fulfilled a prerequisite for functional *in vivo* interaction (Figure 24). Exosc9 is a component of an essential multi-subunit ribonuclease complex called exosome, which is involved in processing and degradation of many classes of RNAs (Januszyk and Lima, 2014). Together with five other proteins, Exosc9 forms the barrel-like core structure of the exosome, which associates three more cap proteins and a distinct exonuclease depending on its localization in the cytoplasm or in the nucleus (Lykke-Andersen et al., 2011).

Interestingly, nine out of ten components of the cytoplasmic exosome, but no nuclear exosomal exonuclease, were identified in the mass spectrometry analysis to be significantly enriched in Buc as well as in BucLoc (Table 13). Hence, it seems like the whole cytoplasmic complex was co-immunoprecipitated with BucLoc and may be a component of the germ plasm. Lack of the exclusively nuclear localized exonuclease Exosc10 is in accordance with the observed cytoplasmic localization of Buc and the germ plasm. The localization of Exosc9 to the germ plasm could be confirmed at the endogenous level in early oocytes, but not in early embryos at 2.5 hpf (Figure 25). Exosc9 localizes as well to the germinal vesicle in the

early oocyte, which indicates that in early oogenesis regulation of RNAs is additionally required in the nucleus (Figure 25). These findings suggest for the first time that Exosc9, and most likely the whole cytoplasmic exosome, is a component of the germ plasm in early oocytes. However, the interaction with the germ plasm might be only transient in early stages or the exosome is not as strongly enriched as in the oocyte and therefore not detected by immunostaining. Immunostaining of further exosomal proteins would reveal if the whole exosomal complex is present in the germ plasm.

The role of the newly identified germ plasm exosome might be to regulate expression of germ plasm mRNAs, degrade mislocalized mRNAs of somatic genes or regulate the levels of other classes of RNAs. Thus, a role of exosomal proteins in the localization of Buc is unlikely. On the contrary, an interaction of Buc with exosomal proteins to regulate the activity of the exosome in the germ plasm is conceivable. Whether the interaction of Buc and Exosc9 is direct, has to be analyzed by Co-IP experiments with *in vitro* translated proteins.

In short, the exosomal protein Exosc9 has been described for the first time to be a component of the germ plasm. Still, the functional importance of the Buc-Exosc9 interaction has to be characterized.

4.7 Potential role of non-muscle myosin II in germ plasm localization

As Exosc9 is part of a molecular machinery that is involved in RNA processing or degradation, it is unlikely that Exosc9 is responsible for the specific localization of Buc. In fact, cytoskeletal proteins are more likely to be involved in Buc localization. From the promising candidates Dynein, Macf1a and Myl12.2, Myl12.2 was chosen to be further analyzed, as previous data indicated localization of non-muscle myosin II to the germ plasm in zebrafish (Nair et al., 2013).

4.7.1 Buc co-localizes with p-Myl12.2 throughout oogenesis and early embryogenesis

Non-muscle myosins describe a superfamily of ATP-dependent motor proteins, responsible for actin-based motility (Vicente-Manzanares et al., 2009). Myosins are present in all non-muscle eukaryotic cells and most of them belong to the class II (non-muscle myosins II, NMII). NMII molecules have a hexameric composition consisting of two heavy chain subunits, two essential light chain subunits (or alkali light chains) and two regulatory light chain subunits (Vicente-Manzanares et al., 2009). Interestingly, non-muscle myosins are essential for cytokinesis and are involved in cell adhesion and polarity (Mabuchi and Okuno, 1977; Vicente-Manzanares et al., 2009). In mouse fibroblasts the regulatory light chains Myl12a/b are essential to maintain the stability of the heavy chain Myh9 as well as the essential light chain Myl6, indicating that they form a non-muscle myosin II complex (Park et al., 2011). Interestingly, the zebrafish homologs of Myh12a/b, Myh9 and Myl6 were identified to be highly enriched in the BucLoc-eGFP Co-IP sample (Table 14).

To investigate if Myl12.2 co-localizes with Buc *in vivo*, an antibody was applied that has been previously used to detect phosphorylated, hence active, zebrafish non-muscle myosin II (Nair et al., 2013). This commercial antibody was raised against a synthetic phosphopeptide corresponding to residues surrounding Ser19 of human myosin light chain II. The human reference protein is highly homologous to Myl9b, Myl12.2 and its paralog Myl12.1, which

was also highly enriched in the BucLoc-eGFP Co-IP sample (Appendix, Table 16). Hence, it cannot be excluded that besides Myl12.2, other zebrafish homologs are detected by this antibody.

Phosphorylated and hence active Myl12.2 co-localizes with Buc at the cleavage furrow in 2-cell stage embryos indicating that both co-localize in the germ plasm (Figure 26). In accordance with this result, p-Myl12.2 co-localizes with the germ plasm components *dazl*, *dead end* and *vasa* mRNA to the germ plasm at 2-cell stage (Nair et al., 2013). Interestingly, a detailed analysis of the localization of Buc and p-Myl12.2 at the cleavage furrow revealed that the rod-like structure actually consists of small granules that line up like on a ‘string of pearls’ (Figure 26). This is consistent with the idea that Buc-positive germ plasm granules aggregate in advance and are recruited to the cleavage furrow to specify the future primordial germ cells. The ‘string of pearls’-like structure of Buc and p-Myl12.2-positive granules is in line with observations of *vasa* mRNA granules lining up at the first, second and third cleavage furrows (Eno and Pelegri, 2013). Interestingly, cell cleavage is defective, cortical β -catenin recruitment is disturbed and NMII localization is significantly reduced upon specific inhibition of NMII by blebbistatin (Urven et al., 2006). This suggests an important role of NMII in cytoskeletal rearrangements and recruitment of furrow components during the first cleavages in zebrafish embryos.

So far, the localization of non-muscle myosin II has been described only from 2-cell until 8-cell stage (Eno and Pelegri, 2013). Though it was surprising to see that, in addition to 2-cell stage, Buc co-localizes permanently with p-Myl12.2 throughout oogenesis and early embryogenesis (Figure 27). This suggests a robust interaction of Buc and p-Myl12.2 during germ plasm aggregation in the oocyte and germ cell specification in the embryo. In the BucLoc Co-IP sample the whole non-muscle myosin complex consisting of Myh9a, Myl12.2 and Myl6 was identified. To investigate the directly interacting non-muscle myosin II component, Buc Co-IP experiments with *in vitro* translated proteins have to be carried out.

Together with the strong enrichment of the other components of the non-muscle myosin II complex in the BucLoc-eGFP Co-IP sample, this suggests a consistent role of p-Myl12.2 and the non-muscle myosin II complex in the localization of Buc.

4.7.2 Mechanistic trailer truck model of Buc localization and function during germ cell specification

The consistent co-localization of p-Myl12.2 with Buc suggests a permanent role of NMII in the localization of the germ plasm organizer Buc. These findings together with the loss-of-function phenotype in oocytes and the gain-of-function phenotype in embryos led to the following model.

In stage IA oocytes, Buc directly localizes to the Balbiani body (Figure 8). As also *buc* mRNA localizes the same at this early stage, it can be speculated that the mRNA might be involved in the localized translation of Buc (Bontems, 2009). Other germ plasm components also become localized to the Balbiani body and might be aggregated and compacted with Buc serving as a scaffolding platform. Additionally, Buc can interact via its localization domain BucLoc with non-muscle myosin II. By this, germ plasm granules might assemble with Buc as a scaffolding protein, which at the same time connects the granules to actin microfilaments via

NMII (Figure 29). Similar to germ plasm segregation in early embryogenesis, microtubular structures might be involved in the transport of the actin-NMII-Buc-germ plasm complex to the vegetal pole (Lindeman and Pelegri, 2010). Such a role of microtubules is suggested by analysis of the *macf1a* mutants, in which defective localization of stable microtubules to the cortex leads to the mislocalization of the Balbiani body and the deregulation of its size (Gupta et al., 2010). Subsequent anchoring to the vegetal cortex and spreading at the cortex might be dependent on the actin cytoskeleton, similar to the actin-dependent anchoring of germ plasm mRNAs to the vegetal cortex in *Xenopus* (Kloc and Etkin, 1995). In this phase, germ plasm granules might be still maintained by Buc and be transported via NMII along the cortical actin cytoskeleton to reach close to the animal pole during late stage oogenesis. The germ plasm-free animal pole of the blastomere upon fertilization suggests that in the oocyte, granules do not cover the whole cortex (Figure 11, Figure 28). Rather granules might be excluded from the animal most part of the oocyte by some unknown mechanism.

The pericleavage actin filaments, with NMII-Buc-germ plasm granules attached to it, might subsequently be recruited to the forming cleavage furrow by astral microtubules, similar to what has been described previously (Figure 5, Figure 29) (Lindeman and Pelegri, 2010; Urven et al., 2006). Throughout this process, Buc is supposed to be responsible for the maintenance of the germ plasm granules and the connection to the cytoskeleton via interaction of BucLoc with the actin-based motor protein NMII. NMII might further be responsible for the compaction of the germ plasm by moving the Buc-germ plasm granules towards the distal end, as judged by lack of compaction after treatment with the NMII specific inhibitor blebbistatin (Figure 29) (Urven et al., 2006). The germ plasm granules are lined up in a 'string of pearls'-like fashion at the first cleavage furrows (Figure 26). Most likely due to a concentration-dependent mechanism, these aggregations are only stable at the first and second cleavage furrow (Figure 12) (Eno and Pelegri, 2013).

The remaining four germ plasm clusters are inherited by the prospective primordial germ cells (Figure 14). Buc might still serve as a scaffold in the primordial germ cells, thus connecting the germ plasm with the actin cytoskeleton via NMII and by this ensuring proper germ plasm localization (Figure 29). Since Buc is still localized to primordial germ cells at 48 hpf, Buc is likely to be continuously required for the maintenance of germ plasm integrity (Figure 14). Whether or not Buc continues to interact with NMII in primordial germ cells, is not known. Treatments with the microtubule inhibitor nocodazole indicate that microtubular structures are involved in the maintenance of germ plasm granule structure, associated with the nucleus in primordial germ cells at 11 (Strasser et al., 2008). Hence, at later stages a similar mechanism to early cleavage stages is conceivable. The NMII-Buc-germ plasm granules might be associated with actin filaments, which in turn are positioned in a microtubule-dependent manner.

In short, Buc might act as a trailer, loaded with germ plasm components and attached by BucLoc, serving as a trailer hitch, to the NMII truck, which brings the trailer to its destination. Together, hundreds of these trailer trucks, sometimes driving solo, sometimes driving in a convoy, ensure proper specification of primordial germ cells.

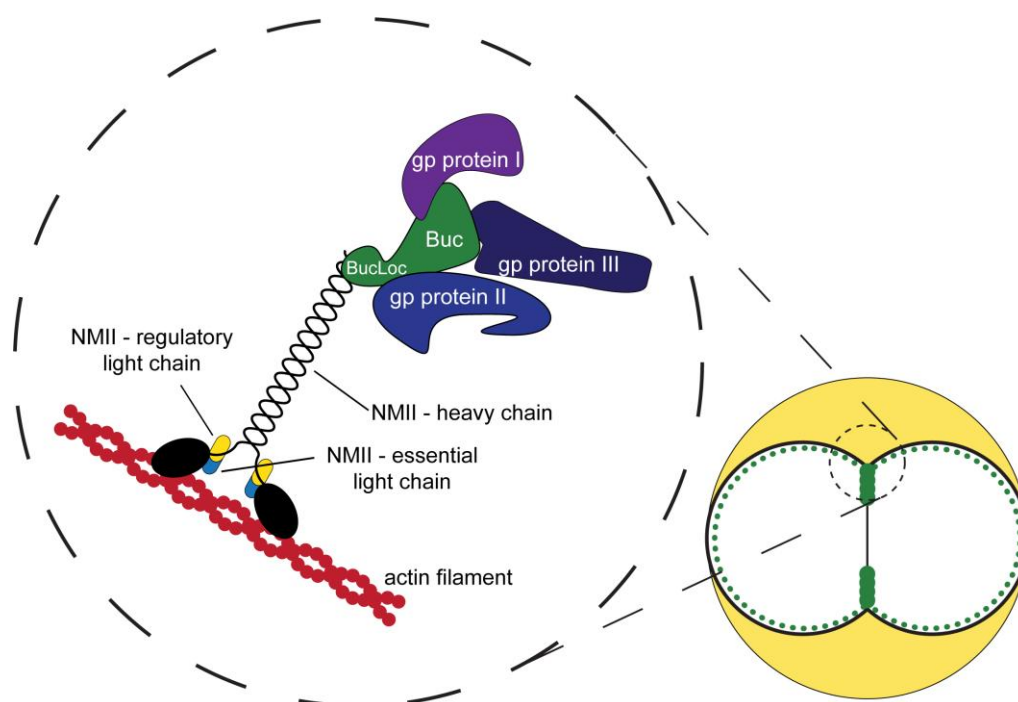


Figure 29: Hypothetical trailer truck model of Buc localization. Schematic drawing of protein interactions involved in Buc localization, exemplary shown for a 2-cell stage embryo. Buc (“trailer”) binds via its BucLoc localization domain (“trailer hitch”) to the non-muscle myosin II complex (“truck”) and thereby couples Buc to actin filaments. Buc possibly serves as a scaffold for other germ plasm proteins. Hence, this localization mechanism might be involved in proper localization of germ plasm granules. Schematic 2-cell stage embryo is drawn in animal view.

This hypothetical model of the Buc localization and functional mechanism, based on the Buc localization and interaction analysis, remains to be validated by experimental data.

The direct interaction between Buc and components of non-muscle myosin II has to be analyzed. Subsequently, the functional relevance of such an interaction has to be investigated. This will be a challenging task as both proteins are maternally provided and in addition non-muscle myosin II inhibition by blebbistatin affects furrow maturation during early zebrafish cleavage stages (Urven et al., 2006). Moreover, functional analysis of Buc in embryonic stages will only be possible after the establishment of a maternal protein knockdown method. To overcome this limitation, the Buc-GFP transgenic line will be helpful in experimental approaches such as protein ablation by bleaching or deGradFP mediated knockdown (Chapter 4.2).

The results of this study suggest a mechanism, in which the newly identified specific Buc localization during oogenesis and early embryogenesis is established by the continuous interaction of the mapped BucLoc localization domain with the non-muscle myosin II complex.

5 Conclusion

Zebrafish Buc is an important factor in germ cell specification in zebrafish and has been previously identified as the first germ plasm organizer in vertebrates. However, neither the localization nor the temporal requirement of Buc was known.

In this study, the characterization of Buc localization identified endogenous Buc as the first protein continuously localizing to the germ plasm during zebrafish oogenesis and early embryogenesis. This suggests that Buc function is necessary during germ plasm aggregation, germ cell specification and primordial germ cell maintenance. In addition, loss of Buc localization in mutant oocytes shows the functional importance of proper Buc localization during germ plasm aggregation.

This specific localization of Buc to the germ plasm during early embryogenesis is established by the newly identified, conserved BucLoc localization domain. BucLoc is the first protein localization domain in a metazoan that has been shown to be necessary and sufficient for localization to the germ plasm. Hence, it not only gives insight into how Buc is localized to the germ plasm in zebrafish, but additionally allows targeting of the germ plasm on the protein level for the first time.

Immunoprecipitation of BucLoc out of living embryos and subsequent mass spectrometry analysis identified 213 potential interacting proteins. Surprisingly, subsequent analyses of interacting proteins led to the identification of Exosc9, part of the exosome, as novel germ plasm component. Furthermore, non-muscle myosin II, co-immunoprecipitating with BucLoc, co-localizes with Buc to the germ plasm throughout oogenesis and early embryogenesis. This suggests a potential localization mechanism, described in the trailer truck model, by which Buc is localized to the actin cytoskeleton, mediated by Non-muscle myosin II. This model of Buc localization is in line with the current models of germ plasm segregation during early embryogenesis.

In further functional studies on Buc-non-muscle myosin II interaction, the established transgenic *buc-gfp* line, reflecting the endogenous Buc localization *in vivo*, will be of great value. In addition, this line will be of use for other researchers in the field to investigate the dynamics of germ plasm in different stages or to study the migration of primordial germ cells. Moreover, it would be interesting to see whether the BucLoc localization domain can be used as a molecular shuttle to the germ plasm in other vertebrates.

The characterization of endogenous Buc localization, the identification of the essential BucLoc localization domain and the interaction as well as co-localization of Buc with non-muscle myosin II, provides insight into the localization mechanism of an important regulator of germ plasm aggregation in the process of germ cell specification.

6 Bibliography

- Ahringer, J., 2003. Control of cell polarity and mitotic spindle positioning in animal cells. *Curr Opin Cell Biol.* 15, 73-81.
- Ahuja, A. and Extavour, C.G., 2014. Patterns of molecular evolution of the germ line specification gene *oskar* suggest that a novel domain may contribute to functional divergence in *Drosophila*. *Dev Genes Evol.* 224, 65-77.
- Albamonte, M.I., Albamonte, M.S., Stella, I., Zuccardi, L. and Vitullo, A.D., 2013. The infant and pubertal human ovary: Balbiani's body-associated VASA expression, immunohistochemical detection of apoptosis-related BCL2 and BAX proteins, and DNA fragmentation. *Hum Reprod.* 28, 698-706.
- Anne, J., 2010. Targeting and anchoring Tudor in the pole plasm of the *Drosophila* oocyte. *PLoS One.* 5, e14362.
- Antonellis, P.J., Pollock, L.M., Chou, S.W., Hassan, A., Geng, R., Chen, X., Fuchs, E., Alagramam, K.N., Auer, M. and McDermott, B.M., Jr., 2014. ACF7 is a hair-bundle antecedent, positioned to integrate cuticular plate actin and somatic tubulin. *J Neurosci.* 34, 305-12.
- Babu, K., Cai, Y., Bahri, S., Yang, X. and Chia, W., 2004. Roles of Bifocal, Homer, and F-actin in anchoring Oskar to the posterior cortex of *Drosophila* oocytes. *Genes Dev.* 18, 138-43.
- Beer, R.L. and Draper, B.W., 2013. *nanos3* maintains germline stem cells and expression of the conserved germline stem cell gene *nanos2* in the zebrafish ovary. *Dev Biol.* 374, 308-18.
- Bischof, J., Maeda, R.K., Hediger, M., Karch, F. and Basler, K., 2007. An optimized transgenesis system for *Drosophila* using germ-line-specific ϕ C31 integrases. *Proc Natl Acad Sci U S A.* 104, 3312-7.
- Bontems, F., 2009. The Role of Bucky Ball in Germ Plasm Assembly in Zebrafish. Thesis, University of Geneva, Geneva, Switzerland.
- Bontems, F., Baerlocher, L., Mehenni, S., Bahechar, I., Farinelli, L. and Dosch, R., 2011. Efficient mutation identification in zebrafish by microarray capturing and next generation sequencing. *Biochem Biophys Res Commun.* 405, 373-6.
- Bontems, F., Stein, A., Marlow, F., Lyautey, J., Gupta, T., Mullins, M.C. and Dosch, R., 2009. Bucky ball organizes germ plasm assembly in zebrafish. *Curr Biol.* 19, 414-22.
- Bounoure, L., 1934. Recherches sur la lignée germinale chez la grenouille rousse aux premiers stades du développement. *Ann. Sci. Nat.*, 67-248.
- Boveri, T., 1910. Die Potenzen der *Ascaris*-Blastomeren bei abgeanderter Furchung. *Festschrift für R. Hertwig, III, Vol. 3, Fischer, Jena*, pp. 131-214.

- Braat, A.K., van de Water, S., Goos, H., Bogerd, J. and Zivkovic, D., 2000. Vasa protein expression and localization in the zebrafish. *Mech Dev.* 95, 271-4.
- Braat, A.K., van de Water, S., Korving, J. and Zivkovic, D., 2001. A zebrafish vasa morphant abolishes vasa protein but does not affect the establishment of the germline. *Genesis.* 30, 183-5.
- Braat, A.K., Zandbergen, T., van de Water, S., Goos, H.J. and Zivkovic, D., 1999. Characterization of zebrafish primordial germ cells: morphology and early distribution of vasa RNA. *Dev Dyn.* 216, 153-67.
- Brand, A.H. and Perrimon, N., 1993. Targeted gene expression as a means of altering cell fates and generating dominant phenotypes. *Development.* 118, 401-15.
- Breitwieser, W., Markussen, F.H., Horstmann, H. and Ephrussi, A., 1996. Oskar protein interaction with Vasa represents an essential step in polar granule assembly. *Genes Dev.* 10, 2179-88.
- Brendza, R.P., Serbus, L.R., Duffy, J.B. and Saxton, W.M., 2000. A function for kinesin I in the posterior transport of oskar mRNA and Staufen protein. *Science.* 289, 2120-2.
- Buehr, M.L. and Blackler, A.W., 1970. Sterility and partial sterility in the South African clawed toad following the pricking of the egg. *J Embryol Exp Morphol.* 23, 375-84.
- Callebaut, I. and Mornon, J.P., 2010. LOTUS, a new domain associated with small RNA pathways in the germline. *Bioinformatics.* 26, 1140-4.
- Castagnetti, S. and Ephrussi, A., 2003. Orb and a long poly(A) tail are required for efficient oskar translation at the posterior pole of the *Drosophila* oocyte. *Development.* 130, 835-43.
- Caussinus, E., Kanca, O. and Affolter, M., 2012. Fluorescent fusion protein knockout mediated by anti-GFP nanobody. *Nat Struct Mol Biol.* 19, 117-21.
- Chekulaeva, M., Hentze, M.W. and Ephrussi, A., 2006. Bruno acts as a dual repressor of oskar translation, promoting mRNA oligomerization and formation of silencing particles. *Cell.* 124, 521-33.
- Cinalli, R.M., Rangan, P. and Lehmann, R., 2008. Germ cells are forever. *Cell.* 132, 559-62.
- Claussen, M. and Pieler, T., 2004. Xvelo1 uses a novel 75-nucleotide signal sequence that drives vegetal localization along the late pathway in *Xenopus* oocytes. *Dev Biol.* 266, 270-84.
- Cox, R.T. and Spradling, A.C., 2003. A Balbiani body and the fusome mediate mitochondrial inheritance during *Drosophila* oogenesis. *Development.* 130, 1579-90.
- Crow, J.F., 1994. Advantages of sexual reproduction. *Dev Genet.* 15, 205-13.
- Curtis, D., Apfeld, J. and Lehmann, R., 1995. nanos is an evolutionarily conserved organizer of anterior-posterior polarity. *Development.* 121, 1899-910.

- DeRenzo, C., Reese, K.J. and Seydoux, G., 2003. Exclusion of germ plasm proteins from somatic lineages by cullin-dependent degradation. *Nature*. 424, 685-9.
- Dosch, R., Wagner, D.S., Mintzer, K.A., Runke, G., Wiemelt, A.P. and Mullins, M.C., 2004. Maternal control of vertebrate development before the midblastula transition: mutants from the zebrafish I. *Dev Cell*. 6, 771-80.
- Draper, B.W., McCallum, C.M. and Moens, C.B., 2007. *nanos1* is required to maintain oocyte production in adult zebrafish. *Dev Biol*. 305, 589-98.
- Eberhart, C.G., Maines, J.Z. and Wasserman, S.A., 1996. Meiotic cell cycle requirement for a fly homologue of human Deleted in Azoospermia. *Nature*. 381, 783-5.
- Eno, C. and Pelegri, F., 2013. Gradual recruitment and selective clearing generate germ plasm aggregates in the zebrafish embryo. *Bioarchitecture*. 3, 125-32.
- Ephrussi, A., Dickinson, L.K. and Lehmann, R., 1991. Oskar organizes the germ plasm and directs localization of the posterior determinant *nanos*. *Cell*. 66, 37-50.
- Ephrussi, A. and Lehmann, R., 1992. Induction of germ cell formation by *oskar*. *Nature*. 358, 387-92.
- Evans, T., Wade, C.M., Chapman, F.A., Johnson, A.D. and Loose, M., 2014. Acquisition of germ plasm accelerates vertebrate evolution. *Science*. 344, 200-3.
- Ewen-Campen, B., Srouji, J.R., Schwager, E.E. and Extavour, C.G., 2012. Oskar predates the evolution of germ plasm in insects. *Curr Biol*. 22, 2278-83.
- Extavour, C.G. and Akam, M., 2003. Mechanisms of germ cell specification across the metazoans: epigenesis and preformation. *Development*. 130, 5869-84.
- Fan, L., Moon, J., Wong, T.T., Crodian, J. and Collodi, P., 2008. Zebrafish primordial germ cell cultures derived from *vasa::RFP* transgenic embryos. *Stem Cells Dev*. 17, 585-97.
- Ferraro, E., Peluso, D., Via, A., Ausiello, G. and Helmer-Citterich, M., 2007. SH3-Hunter: discovery of SH3 domain interaction sites in proteins. *Nucleic Acids Res*. 35, W451-4.
- Finn, R.D., Clements, J. and Eddy, S.R., 2011. HMMER web server: interactive sequence similarity searching. *Nucleic Acids Res*. 39, W29-37.
- Gasteiger, E., Gattiker, A., Hoogland, C., Ivanyi, I., Appel, R.D. and Bairoch, A., 2003. ExPASy: The proteomics server for in-depth protein knowledge and analysis. *Nucleic Acids Res*. 31, 3784-8.
- Gavis, E.R. and Lehmann, R., 1994. Translational regulation of *nanos* by RNA localization. *Nature*. 369, 315-8.
- Gilboa, L. and Lehmann, R., 2004. Repression of primordial germ cell differentiation parallels germ line stem cell maintenance. *Curr Biol*. 14, 981-6.

- Giraldez, A.J., Mishima, Y., Rihel, J., Grocock, R.J., Van Dongen, S., Inoue, K., Enright, A.J. and Schier, A.F., 2006. Zebrafish MiR-430 promotes deadenylation and clearance of maternal mRNAs. *Science*. 312, 75-9.
- Gonzalez-Mariscal, L., Betanzos, A. and Avila-Flores, A., 2000. MAGUK proteins: structure and role in the tight junction. *Semin Cell Dev Biol*. 11, 315-24.
- Groth, A.C., Fish, M., Nusse, R. and Calos, M.P., 2004. Construction of transgenic *Drosophila* by using the site-specific integrase from phage phiC31. *Genetics*. 166, 1775-82.
- Gruidl, M.E., Smith, P.A., Kuznicki, K.A., McCrone, J.S., Kirchner, J., Roussell, D.L., Strome, S. and Bennett, K.L., 1996. Multiple potential germ-line helicases are components of the germ-line-specific P granules of *Caenorhabditis elegans*. *Proc Natl Acad Sci U S A*. 93, 13837-42.
- Gupta, T., Marlow, F.L., Ferriola, D., Mackiewicz, K., Dapprich, J., Monos, D. and Mullins, M.C., 2010. Microtubule actin crosslinking factor 1 regulates the Balbiani body and animal-vegetal polarity of the zebrafish oocyte. *PLoS Genet*. 6, e1001073.
- Guraya, S.S., 1979. Recent advances in the morphology, cytochemistry, and function of Balbiani's vitelline body in animal oocytes. *Int Rev Cytol*. 59, 249-321.
- Harrison, M.M., Jenkins, B.V., O'Connor-Giles, K.M. and Wildonger, J., 2014. A CRISPR view of development. *Genes Dev*. 28, 1859-1872.
- Hashimoto, Y., Maegawa, S., Nagai, T., Yamaha, E., Suzuki, H., Yasuda, K. and Inoue, K., 2004. Localized maternal factors are required for zebrafish germ cell formation. *Dev Biol*. 268, 152-61.
- Hashimoto, Y., Suzuki, H., Kageyama, Y., Yasuda, K. and Inoue, K., 2006. Bruno-like protein is localized to zebrafish germ plasm during the early cleavage stages. *Gene Expr Patterns*. 6, 201-5.
- Hay, B., Jan, L.Y. and Jan, Y.N., 1988. A protein component of *Drosophila* polar granules is encoded by vasa and has extensive sequence similarity to ATP-dependent helicases. *Cell*. 55, 577-87.
- Hayashi, K., de Sousa Lopes, S.M. and Surani, M.A., 2007. Germ cell specification in mice. *Science*. 316, 394-6.
- Heasman, J., Quarmby, J. and Wylie, C.C., 1984. The mitochondrial cloud of *Xenopus* oocytes: the source of germinal granule material. *Dev Biol*. 105, 458-69.
- Heim, A.E., Hartung, O., Rothhamel, S., Ferreira, E., Jenny, A. and Marlow, F.L., 2014. Oocyte polarity requires a Bucky ball-dependent feedback amplification loop. *Development*. 141, 842-54.
- Houston, D.W., Zhang, J., Maines, J.Z., Wasserman, S.A. and King, M.L., 1998. A *Xenopus* DAZ-like gene encodes an RNA component of germ plasm and is a functional homologue of *Drosophila* boule. *Development*. 125, 171-80.

- Houwing, S., Kamminga, L.M., Berezikov, E., Cronembold, D., Girard, A., van den Elst, H., Filippov, D.V., Blaser, H., Raz, E., Moens, C.B., Plasterk, R.H., Hannon, G.J., Draper, B.W. and Ketting, R.F., 2007. A role for Piwi and piRNAs in germ cell maintenance and transposon silencing in Zebrafish. *Cell*. 129, 69-82.
- Howley, C. and Ho, R.K., 2000. mRNA localization patterns in zebrafish oocytes. *Mech Dev*. 92, 305-9.
- Ikenishi, K. and Nieuwkoop, P.D., 1978. Location and Ultrastructure of Primordial Germ-Cells (Pgcs) in *Ambystoma-Mexicanum*. *Development Growth & Differentiation*. 20, 1-9.
- Ikenishi, K., Tanaka, T.S. and Komiya, T., 1996. Spatio-temporal distribution of the protein of *Xenopus vasa* homologue (*Xenopus vasa*-like gene 1, *XVLG1*) in embryos. *Development Growth & Differentiation*. 38, 527-535.
- Illmensee, K. and Mahowald, A.P., 1974. Transplantation of posterior polar plasm in *Drosophila*. Induction of germ cells at the anterior pole of the egg. *Proc Natl Acad Sci U S A*. 71, 1016-20.
- Januszyk, K. and Lima, C.D., 2014. The eukaryotic RNA exosome. *Curr Opin Struct Biol*. 24C, 132-140.
- Johnson, A.D., Richardson, E., Bachvarova, R.F. and Crother, B.I., 2011. Evolution of the germ line-soma relationship in vertebrate embryos. *Reproduction*. 141, 291-300.
- Juhn, J. and James, A.A., 2006. oskar gene expression in the vector mosquitoes, *Anopheles gambiae* and *Aedes aegypti*. *Insect Mol Biol*. 15, 363-72.
- Kane, D.A. and Kimmel, C.B., 1993. The zebrafish midblastula transition. *Development*. 119, 447-56.
- Kane, D.A., Warga, R.M. and Kimmel, C.B., 1992. Mitotic domains in the early embryo of the zebrafish. *Nature*. 360, 735-7.
- Kay, B.K., Williamson, M.P. and Sudol, M., 2000. The importance of being proline: the interaction of proline-rich motifs in signaling proteins with their cognate domains. *FASEB J*. 14, 231-41.
- Kim-Ha, J., Kerr, K. and Macdonald, P.M., 1995. Translational regulation of oskar mRNA by bruno, an ovarian RNA-binding protein, is essential. *Cell*. 81, 403-12.
- Kim-Ha, J., Smith, J.L. and Macdonald, P.M., 1991. oskar mRNA is localized to the posterior pole of the *Drosophila* oocyte. *Cell*. 66, 23-35.
- Kimmel, C.B., Ballard, W.W., Kimmel, S.R., Ullmann, B. and Schilling, T.F., 1995. Stages of embryonic development of the zebrafish. *Dev Dyn*. 203, 253-310.
- King, M.L., Zhou, Y. and Bubunencko, M., 1999. Polarizing genetic information in the egg: RNA localization in the frog oocyte. *Bioessays*. 21, 546-57.

- Kloc, M., Bilinski, S. and Etkin, L.D., 2004. The Balbiani body and germ cell determinants: 150 years later. *Curr Top Dev Biol.* 59, 1-36.
- Kloc, M. and Etkin, L.D., 1995. Two distinct pathways for the localization of RNAs at the vegetal cortex in *Xenopus* oocytes. *Development.* 121, 287-97.
- Knaut, H., Pelegri, F., Bohmann, K., Schwarz, H. and Nusslein-Volhard, C., 2000. Zebrafish vasa RNA but not its protein is a component of the germ plasm and segregates asymmetrically before germline specification. *J Cell Biol.* 149, 875-88.
- Knaut, H., Steinbeisser, H., Schwarz, H. and Nusslein-Volhard, C., 2002. An evolutionary conserved region in the vasa 3'UTR targets RNA translation to the germ cells in the zebrafish. *Curr Biol.* 12, 454-66.
- Kobayashi, S., Yamada, M., Asaoka, M. and Kitamura, T., 1996. Essential role of the posterior morphogen nanos for germline development in *Drosophila*. *Nature.* 380, 708-11.
- Koprunner, M., Thisse, C., Thisse, B. and Raz, E., 2001. A zebrafish nanos-related gene is essential for the development of primordial germ cells. *Genes Dev.* 15, 2877-85.
- Kosaka, K., Kawakami, K., Sakamoto, H. and Inoue, K., 2007. Spatiotemporal localization of germ plasm RNAs during zebrafish oogenesis. *Mech Dev.* 124, 279-89.
- Kugler, J.M. and Lasko, P., 2009. Localization, anchoring and translational control of oskar, gurken, bicoid and nanos mRNA during *Drosophila* oogenesis. *Fly (Austin).* 3, 15-28.
- Kuznicki, K.A., Smith, P.A., Leung-Chiu, W.M., Estevez, A.O., Scott, H.C. and Bennett, K.L., 2000. Combinatorial RNA interference indicates GLH-4 can compensate for GLH-1; these two P granule components are critical for fertility in *C. elegans*. *Development.* 127, 2907-16.
- Laemmli, U.K., 1970. Cleavage of structural proteins during the assembly of the head of bacteriophage T4. *Nature.* 227, 680-5.
- Lai, F. and King, M.L., 2013. Repressive translational control in germ cells. *Mol Reprod Dev.* 80, 665-76.
- Lasko, P.F. and Ashburner, M., 1990. Posterior localization of vasa protein correlates with, but is not sufficient for, pole cell development. *Genes Dev.* 4, 905-21.
- Laupsien, P., 2013. Die Funktion von slow-as-molasses (slam) während der Zellularisierung von *Drosophila melanogaster*. Thesis, University of Heidelberg, Heidelberg.
- Lawson, K.A., Dunn, N.R., Roelen, B.A., Zeinstra, L.M., Davis, A.M., Wright, C.V., Korving, J.P. and Hogan, B.L., 1999. Bmp4 is required for the generation of primordial germ cells in the mouse embryo. *Genes Dev.* 13, 424-36.
- Lehmann, R. and Nusslein-Volhard, C., 1986. Abdominal segmentation, pole cell formation, and embryonic polarity require the localized activity of oskar, a maternal gene in *Drosophila*. *Cell.* 47, 141-52.

- Lehmann, R. and Nusslein-Volhard, C., 1991. The maternal gene nanos has a central role in posterior pattern formation of the *Drosophila* embryo. *Development*. 112, 679-91.
- Lindeman, R.E. and Pelegri, F., 2010. Vertebrate maternal-effect genes: Insights into fertilization, early cleavage divisions, and germ cell determinant localization from studies in the zebrafish. *Mol Reprod Dev*. 77, 299-313.
- Link, V., Shevchenko, A. and Heisenberg, C.P., 2006. Proteomics of early zebrafish embryos. *BMC Dev Biol*. 6, 1.
- Lykke-Andersen, S., Tomecki, R., Jensen, T.H. and Dziembowski, A., 2011. The eukaryotic RNA exosome: same scaffold but variable catalytic subunits. *RNA Biol*. 8, 61-6.
- Lynch, J.A., Ozuak, O., Khila, A., Abouheif, E., Desplan, C. and Roth, S., 2011. The phylogenetic origin of oskar coincided with the origin of maternally provisioned germ plasm and pole cells at the base of the Holometabola. *PLoS Genet*. 7, e1002029.
- Mabuchi, I. and Okuno, M., 1977. The effect of myosin antibody on the division of starfish blastomeres. *J Cell Biol*. 74, 251-63.
- Maegawa, S., Yamashita, M., Yasuda, K. and Inoue, K., 2002. Zebrafish DAZ-like protein controls translation via the sequence 'GUUC'. *Genes Cells*. 7, 971-84.
- Maegawa, S., Yasuda, K. and Inoue, K., 1999. Maternal mRNA localization of zebrafish DAZ-like gene. *Mech Dev*. 81, 223-6.
- Mahowald, A.P., 1971. Polar granules of *Drosophila*. 3. The continuity of polar granules during the life cycle of *Drosophila*. *J Exp Zool*. 176, 329-43.
- Marinos, E. and Billett, F.S., 1981. Mitochondrial number, cytochrome oxidase and succinic dehydrogenase activity in *Xenopus laevis* oocytes. *J Embryol Exp Morphol*. 62, 395-409.
- Markussen, F.H., Michon, A.M., Breitwieser, W. and Ephrussi, A., 1995. Translational control of oskar generates short OSK, the isoform that induces pole plasma assembly. *Development*. 121, 3723-32.
- Marlow, F.L. and Mullins, M.C., 2008. Bucky ball functions in Balbiani body assembly and animal-vegetal polarity in the oocyte and follicle cell layer in zebrafish. *Dev Biol*. 321, 40-50.
- McWilliam, H., Li, W., Uludag, M., Squizzato, S., Park, Y.M., Buso, N., Cowley, A.P. and Lopez, R., 2013. Analysis Tool Web Services from the EMBL-EBI. *Nucleic Acids Res*. 41, W597-600.
- Micklem, D.R., Dasgupta, R., Elliott, H., Gergely, F., Davidson, C., Brand, A., Gonzalez-Reyes, A. and St Johnston, D., 1997. The mago nashi gene is required for the polarisation of the oocyte and the formation of perpendicular axes in *Drosophila*. *Curr Biol*. 7, 468-78.

- Mosquera, L., Forristall, C., Zhou, Y. and King, M.L., 1993. A mRNA localized to the vegetal cortex of *Xenopus* oocytes encodes a protein with a nanos-like zinc finger domain. *Development*. 117, 377-86.
- Mostowy, S. and Cossart, P., 2012. Septins: the fourth component of the cytoskeleton. *Nat Rev Mol Cell Biol*. 13, 183-94.
- Mullis, K., Faloona, F., Scharf, S., Saiki, R., Horn, G. and Erlich, H., 1986. Specific enzymatic amplification of DNA in vitro: the polymerase chain reaction. *Cold Spring Harb Symp Quant Biol*. 51 Pt 1, 263-73.
- Nair, S., Marlow, F., Abrams, E., Kapp, L., Mullins, M.C. and Pelegri, F., 2013. The chromosomal passenger protein birc5b organizes microfilaments and germ plasm in the zebrafish embryo. *PLoS Genet*. 9, e1003448.
- Nakamura, A., Sato, K. and Hanyu-Nakamura, K., 2004. *Drosophila* cup is an eIF4E binding protein that associates with Bruno and regulates oskar mRNA translation in oogenesis. *Dev Cell*. 6, 69-78.
- Nakamura, A. and Seydoux, G., 2008. Less is more: specification of the germline by transcriptional repression. *Development*. 135, 3817-3827.
- Nakamura, A., Shirae-Kurabayashi, M. and Hanyu-Nakamura, K., 2010. Repression of early zygotic transcription in the germline. *Curr Opin Cell Biol*. 22, 709-14.
- Newmark, P.A. and Boswell, R.E., 1994. The mago nashi locus encodes an essential product required for germ plasm assembly in *Drosophila*. *Development*. 120, 1303-13.
- Nijjar, S. and Woodland, H.R., 2013. Protein interactions in *Xenopus* germ plasm RNP particles. *PLoS One*. 8, e80077.
- Nüsslein-Volhard, C. and Dahm, R., 2002. *Zebrafish: a practical approach*. New York: Oxford University Press.
- Ohinata, Y., Payer, B., O'Carroll, D., Ancelin, K., Ono, Y., Sano, M., Barton, S.C., Obukhanych, T., Nussenzweig, M., Tarakhovsky, A., Saitou, M. and Surani, M.A., 2005. Blimp1 is a critical determinant of the germ cell lineage in mice. *Nature*. 436, 207-13.
- Olsen, L.C., Aasland, R. and Fjose, A., 1997. A vasa-like gene in zebrafish identifies putative primordial germ cells. *Mech Dev*. 66, 95-105.
- Park, I., Han, C., Jin, S., Lee, B., Choi, H., Kwon, J.T., Kim, D., Kim, J., Lifirsu, E., Park, W.J., Park, Z.Y., Kim do, H. and Cho, C., 2011. Myosin regulatory light chains are required to maintain the stability of myosin II and cellular integrity. *Biochem J*. 434, 171-80.
- Pelegri, F., 2003. Maternal factors in zebrafish development. *Dev Dyn*. 228, 535-54.

- Pelegri, F., Knaut, H., Maischein, H.M., Schulte-Merker, S. and Nusslein-Volhard, C., 1999. A mutation in the zebrafish maternal-effect gene *nebel* affects furrow formation and *vasa* RNA localization. *Curr Biol.* 9, 1431-40.
- Pepling, M.E., Wilhelm, J.E., O'Hara, A.L., Gephardt, G.W. and Spradling, A.C., 2007. Mouse oocytes within germ cell cysts and primordial follicles contain a Balbiani body. *Proc Natl Acad Sci U S A.* 104, 187-92.
- Perrimon, N., 1998. Creating mosaics in *Drosophila*. *Int J Dev Biol.* 42, 243-7.
- Raz, E., 2003. Primordial germ-cell development: the zebrafish perspective. *Nat Rev Genet.* 4, 690-700.
- Reijo, R., Lee, T.Y., Salo, P., Alagappan, R., Brown, L.G., Rosenberg, M., Rozen, S., Jaffe, T., Straus, D., Hovatta, O. and et al., 1995. Diverse spermatogenic defects in humans caused by Y chromosome deletions encompassing a novel RNA-binding protein gene. *Nat Genet.* 10, 383-93.
- Rongo, C., Gavis, E.R. and Lehmann, R., 1995. Localization of *oskar* RNA regulates *oskar* translation and requires *Oskar* protein. *Development.* 121, 2737-46.
- Ruggiu, M., Speed, R., Taggart, M., McKay, S.J., Kilanowski, F., Saunders, P., Dorin, J. and Cooke, H.J., 1997. The mouse *Dazl* gene encodes a cytoplasmic protein essential for gametogenesis. *Nature.* 389, 73-7.
- Rupp, R.A., Snider, L. and Weintraub, H., 1994. *Xenopus* embryos regulate the nuclear localization of *XMyoD*. *Genes Dev.* 8, 1311-23.
- Saito, T., Fujimoto, T., Maegawa, S., Inoue, K., Tanaka, M., Arai, K. and Yamaha, E., 2006. Visualization of primordial germ cells in vivo using GFP-*nos1* 3'UTR mRNA. *Int J Dev Biol.* 50, 691-9.
- Sambrook, J. and Russel, D.W., 2001. *Molecular Cloning: a laboratory manual*. Third Edition. Cold Spring Harbour Laboratory Press, Cold Spring Harbour, New York.
- Sanger, F., Nicklen, S. and Coulson, A.R., 1977. DNA sequencing with chain-terminating inhibitors. *Proc Natl Acad Sci U S A.* 74, 5463-7.
- Santos, A.C. and Lehmann, R., 2004. Germ cell specification and migration in *Drosophila* and beyond. *Curr Biol.* 14, R578-89.
- Schupbach, T. and Wieschaus, E., 1986. Germline autonomy of maternal-effect mutations altering the embryonic body pattern of *Drosophila*. *Dev Biol.* 113, 443-8.
- Selman, K., Wallace, R.A., Sarka, A. and Qi, X.P., 1993. Stages of Oocyte Development in the Zebrafish, *Brachydanio-Rerio*. *Journal of Morphology.* 218, 203-224.
- Seydoux, G. and Braun, R.E., 2006. Pathway to totipotency: lessons from germ cells. *Cell.* 127, 891-904.

- Sharp, P.A., Sugden, B. and Sambrook, J., 1973. Detection of two restriction endonuclease activities in *Haemophilus parainfluenzae* using analytical agarose-ethidium bromide electrophoresis. *Biochemistry*. 12, 3055-63.
- Smith, L.D., 1966. The role of a "germinal plasm" in the formation of primordial germ cells in *Rana pipiens*. *Dev Biol*. 14, 330-47.
- Smorag, L., Xu, X., Engel, W. and Pantakani, D.V., 2014. The roles of DAZL in RNA biology and development. *Wiley Interdiscip Rev RNA*.
- Strasser, M.J., Mackenzie, N.C., Dumstrei, K., Nakkrasae, L.I., Stebler, J. and Raz, E., 2008. Control over the morphology and segregation of Zebrafish germ cell granules during embryonic development. *BMC Dev Biol*. 8, 58.
- Strome, S., 2005. Specification of the germ line. *WormBook*, ed. The *C. elegans* Research Community, *WormBook*, doi/10.1895/wormbook.1.9.1, <http://www.wormbook.org>.
- Strome, S. and Lehmann, R., 2007. Germ versus soma decisions: lessons from flies and worms. *Science*. 316, 392-3.
- Strome, S. and Wood, W.B., 1983. Generation of asymmetry and segregation of germ-line granules in early *C. elegans* embryos. *Cell*. 35, 15-25.
- Styhler, S., Nakamura, A., Swan, A., Suter, B. and Lasko, P., 1998. *vasa* is required for GURKEN accumulation in the oocyte, and is involved in oocyte differentiation and germline cyst development. *Development*. 125, 1569-78.
- Suyama, R., Jenny, A., Curado, S., Pellis-van Berkel, W. and Ephrussi, A., 2009. The actin-binding protein Lasp promotes Oskar accumulation at the posterior pole of the *Drosophila* embryo. *Development*. 136, 95-105.
- Suzuki, H., Maegawa, S., Nishibu, T., Sugiyama, T., Yasuda, K. and Inoue, K., 2000. Vegetal localization of the maternal mRNA encoding an EDEN-BP/Bruno-like protein in zebrafish. *Mech Dev*. 93, 205-9.
- Tada, H., Mochii, M., Orii, H. and Watanabe, K., 2012. Ectopic formation of primordial germ cells by transplantation of the germ plasm: direct evidence for germ cell determinant in *Xenopus*. *Dev Biol*. 371, 86-93.
- Takeda, Y., Mishima, Y., Fujiwara, T., Sakamoto, H. and Inoue, K., 2009. DAZL relieves miRNA-mediated repression of germline mRNAs by controlling poly(A) tail length in zebrafish. *PLoS One*. 4, e7513.
- Tanaka, S.S., Toyooka, Y., Akasu, R., Katoh-Fukui, Y., Nakahara, Y., Suzuki, R., Yokoyama, M. and Noce, T., 2000. The mouse homolog of *Drosophila Vasa* is required for the development of male germ cells. *Genes Dev*. 14, 841-53.
- Tanaka, T. and Nakamura, A., 2008. The endocytic pathway acts downstream of Oskar in *Drosophila* germ plasm assembly. *Development*. 135, 1107-17.

- Theusch, E.V., Brown, K.J. and Pelegri, F., 2006. Separate pathways of RNA recruitment lead to the compartmentalization of the zebrafish germ plasm. *Dev Biol.* 292, 129-41.
- Towbin, H., Staehelin, T. and Gordon, J., 1979. Electrophoretic transfer of proteins from polyacrylamide gels to nitrocellulose sheets: procedure and some applications. *Proc Natl Acad Sci U S A.* 76, 4350-4.
- Toyooka, Y., Tsunekawa, N., Takahashi, Y., Matsui, Y., Satoh, M. and Noce, T., 2000. Expression and intracellular localization of mouse Vasa-homologue protein during germ cell development. *Mech Dev.* 93, 139-49.
- Tsigkari, K.K., Acevedo, S.F. and Skoulakis, E.M., 2012. 14-3-3epsilon Is required for germ cell migration in *Drosophila*. *PLoS One.* 7, e36702.
- Updike, D.L., Hachey, S.J., Kreher, J. and Strome, S., 2011. P granules extend the nuclear pore complex environment in the *C. elegans* germ line. *J Cell Biol.* 192, 939-48.
- Urven, L.E., Yabe, T. and Pelegri, F., 2006. A role for non-muscle myosin II function in furrow maturation in the early zebrafish embryo. *J Cell Sci.* 119, 4342-52.
- van der Waal, M.S., Hengeveld, R.C., van der Horst, A. and Lens, S.M., 2012. Cell division control by the Chromosomal Passenger Complex. *Exp Cell Res.* 318, 1407-20.
- Vanzo, N.F. and Ephrussi, A., 2002. Oskar anchoring restricts pole plasm formation to the posterior of the *Drosophila* oocyte. *Development.* 129, 3705-14.
- Vicente-Manzanares, M., Ma, X., Adelstein, R.S. and Horwitz, A.R., 2009. Non-muscle myosin II takes centre stage in cell adhesion and migration. *Nat Rev Mol Cell Biol.* 10, 778-90.
- von Wittich, W.H., 1845. *Dissertatio Sistens Observationes Quaedam De Araneis Ex Ovo Evolutione.* Halis Saxonum, Halle, Germany.
- Wakahara, M., 1977. Partial characterization of "primordial germ cell-forming activity" localized in vegetal pole cytoplasm in anuran eggs. *J Embryol Exp Morphol.* 39, 221-33.
- Wang, J.T. and Seydoux, G., 2013. Germ Cell Specification. *Germ Cell Development in C. Elegans.* 757, 17-39.
- Weidinger, G., Wolke, U., Kopranner, M., Klinger, M. and Raz, E., 1999. Identification of tissues and patterning events required for distinct steps in early migration of zebrafish primordial germ cells. *Development.* 126, 5295-307.
- Weismann, A., 1893. *The Germ-plasm: A Theory of Heredity.* Charles Scribner's Sons
- Westerfield, M., 2000. *The zebrafish book. A guide for the laboratory use of zebrafish (Danio rerio).* 4th ed., Univ. of Oregon Press, Eugene.
- Whittington, P.M. and Dixon, K.E., 1975. Quantitative studies of germ plasm and germ cells during early embryogenesis of *Xenopus laevis*. *J Embryol Exp Morphol.* 33, 57-74.

- Wieschaus, E. and Nüsslein-Volhard, C., 1986. Looking at embryos, pp. 199–227 in *Drosophila: A Practical Approach*, edited by Roberts D. B. IRL Press, Oxford.
- Williamson, M.P., 1994. The structure and function of proline-rich regions in proteins. *Biochem J.* 297 (Pt 2), 249-60.
- Wilson, J.E., Connell, J.E. and Macdonald, P.M., 1996. aubergine enhances oskar translation in the *Drosophila* ovary. *Development.* 122, 1631-9.
- Wolke, U., Weidinger, G., Kopranner, M. and Raz, E., 2002. Multiple levels of posttranscriptional control lead to germ line-specific gene expression in the zebrafish. *Curr Biol.* 12, 289-94.
- Wylie, C.C. and Heasman, J., 1976. Formation of Gonadal Ridge in *Xenopus-Laevis* .1. Light and Transmission Electron-Microscope Study. *J Embryol Exp Morphol.* 35, 125-138.
- Xiol, J., Spinelli, P., Laussmann, M.A., Homolka, D., Yang, Z., Cora, E., Coute, Y., Conn, S., Kadlec, J., Sachidanandam, R., Kaksonen, M., Cusack, S., Ephrussi, A. and Pillai, R.S., 2014. RNA Clamping by Vasa Assembles a piRNA Amplifier Complex on Transposon Transcripts. *Cell.* 157, 1698-711.
- Xu, E.Y., Moore, F.L. and Pera, R.A., 2001. A gene family required for human germ cell development evolved from an ancient meiotic gene conserved in metazoans. *Proc Natl Acad Sci U S A.* 98, 7414-9.
- Yabe, T., Ge, X., Lindeman, R., Nair, S., Runke, G., Mullins, M.C. and Pelegri, F., 2009. The maternal-effect gene cellular island encodes aurora B kinase and is essential for furrow formation in the early zebrafish embryo. *PLoS Genet.* 5, e1000518.
- Yabe, T., Ge, X. and Pelegri, F., 2007. The zebrafish maternal-effect gene cellular atoll encodes the centriolar component sas-6 and defects in its paternal function promote whole genome duplication. *Dev Biol.* 312, 44-60.
- Yoon, C., Kawakami, K. and Hopkins, N., 1997. Zebrafish vasa homologue RNA is localized to the cleavage planes of 2- and 4-cell-stage embryos and is expressed in the primordial germ cells. *Development.* 124, 3157-65.
- Zhang, Y., Yan, L., Zhou, Z., Yang, P., Tian, E., Zhang, K., Zhao, Y., Li, Z., Song, B., Han, J., Miao, L. and Zhang, H., 2009. SEPA-1 mediates the specific recognition and degradation of P granule components by autophagy in *C. elegans*. *Cell.* 136, 308-21.
- Zhu, J.L., Lin, S.L., Li, M., Ouyang, Y.C., Hou, Y., Schatten, H. and Sun, Q.Y., 2010. Septin2 is modified by SUMOylation and required for chromosome congression in mouse oocytes. *Cell Cycle.* 9, 1607-16.
- Zimyanin, V.L., Belaya, K., Pecreaux, J., Gilchrist, M.J., Clark, A., Davis, I. and St Johnston, D., 2008. In vivo imaging of oskar mRNA transport reveals the mechanism of posterior localization. *Cell.* 134, 843-53.

List of Figures

Figure 1: Formation of the Balbiani body and distribution along the vegetal cortex during <i>Xenopus</i> oogenesis.	16
Figure 2: Early germ cell development in <i>Drosophila</i> , <i>C. elegans</i> and <i>Xenopus</i>	17
Figure 3: Schematic representation of germ plasm localization during zebrafish oogenesis. ...	20
Figure 4: Schematic representation of germ plasm localization during zebrafish embryogenesis.	22
Figure 5: Germ plasm segregation during early zebrafish embryogenesis.	28
Figure 6: <i>buc</i> mutants show a defect in the embryonic animal-vegetal polarity.	29
Figure 7: Construct used to make a transgenic <i>buc-gfp</i> zebrafish line.	30
Figure 8: Endogenous Buc localizes to the Balbiani body and spreads along the vegetal cortex during oogenesis.	52
Figure 9: Buc does not localize to the Balbiani body in <i>buc</i> mutant oocytes.	53
Figure 10: Transgenic Buc-GFP reflects the localization of endogenous Buc in oocytes.	54
Figure 11: Buc-GFP localizes to the germ plasm during early embryogenesis.	55
Figure 12: Buc-GFP is stable only in four condensed rod-like aggregates during early embryogenesis.	56
Figure 13: Endogenous Buc and transgenic Buc-GFP are localized to the germ plasm in early embryos.	57
Figure 14: Endogenous Buc is localized to the perinuclear region of primordial germ cells during early embryogenesis.	58
Figure 15: Zebrafish Buc and <i>Drosophila</i> Osk are divergent in sequence and show sequence homologies to other proteins.	60
Figure 16: Buc-eGFP shows a different localization pattern in <i>Drosophila</i> compared to Osk-eGFP.	61
Figure 17: <i>osk-egfp</i> transgenic embryos show defects in anterior-posterior patterning.	62
Figure 18: Osk-eGFP does not resemble the localization pattern of Buc-eGFP in zebrafish. ...	63

Figure 19: Buc ^{p43} sequence contains conserved N-terminal domains.	64
Figure 20: Buc11-88 is necessary and sufficient for Buc localization in embryos.....	65
Figure 21: BucLoc-mCherry co-localizes with transgenic Buc-GFP to the germ plasm.	66
Figure 22: BucLoc is highly enriched in proline and aromatic amino acids and SH3 binding sites are predicted.....	67
Figure 23: 213 specific interaction partners of BucLoc are involved in diverse molecular pathways.	69
Figure 24: Exosc9-eGFP co-localizes with BucLoc-mCherry.....	72
Figure 25: Endogenous Exosc9 co-localizes with Buc in the oocyte.	74
Figure 26: p-Myl12.2 co-localizes with Buc at the 2-cell stage cleavage furrow.....	76
Figure 27: p-Myl12.2 co-localizes with Buc in oogenesis as well as embryogenesis.....	77
Figure 28: Schematic representation of endogenous Buc protein localization during zebrafish oogenesis and embryogenesis.	82
Figure 29: Hypothetical trailer truck model of Buc localization.	93

List of Tables

Table 1: Primers used for genotyping of zebrafish.	33
Table 2: <i>Drosophila</i> lines used to make transgenic flies.....	35
Table 3: Cloned vector constructs used to generate transgenic flies.	37
Table 4: Cloned expression plasmids used for <i>in vitro</i> transcription of Buc deletion constructs or Buc interaction candidates.....	38
Table 5: Standard PCR program for DNA amplification with Phusion polymerase.	40
Table 6: Primers used for conventional restriction enzyme cloning and gateway cloning.....	40
Table 7: Colony PCR program.....	42
Table 8: Sequencing PCR program.....	45
Table 9: Primers used for sequencing.	45
Table 10: Antibodies used for western blotting.	47
Table 11: Antibodies used for immunostaining.	49
Table 12: BucLoc interaction candidates selected for further analysis.....	71
Table 13: Exosomal proteins identified by mass spectrometry analysis.....	73
Table 14: Components of non-muscle myosins II complex identified by mass spectrometry analysis.....	75
Table 15: Hidden Markov model analysis of Buc and Oskar in the respective organism database.....	110
Table 16: Further Buc interacting proteins.	111
Table 17: 213 BucLoc interaction candidates selected from 3464 proteins identified by mass spectrometry analysis.....	112

7 Appendix

7.1 Hidden Markov model analysis of Buc and Osk

To detect potential distantly related domains in Buc and Osk, hidden Markov models (HMMs) of Buc and Osk were used to search within the respective other protein database (Table 15, Figure 15).

Table 15: Hidden Markov model analysis of Buc and Oskar in the respective organism database. Hits of the used HMM in the indicated databases are shown with their corresponding E-value. HMMER analysis were done in collaboration with Dr. Thomas Lingner

Used Hidden-Markov-Model	Searched NCBI organism database	Significant hits	E-Value of aligned domain
Buc-HMM	<i>Danio rerio</i>	Bucky ball	9.4e-223
		zDazl	0.022
	<i>Drosophila melanogaster</i>	-	-
Osk-HMM	<i>Danio rerio</i>	Trd7A	1.4e-11
		Trd7A, isoform 1	3.2e-11
		Tdrd5	2.4e-07
		Trd7B	1e-06
		Her13	0.017
	<i>Drosophila melanogaster</i>	Oskar; isoform A	2.8e-223
		Oskar; isoform C	1.1e-205
		RE24380p	8.8e-198
		CG8920, isoform D / E / RE10852p	1.9e-07
		CG8920, isoform B / C	2.8e-07
		CG34007	0.00015
Tejas / FI02030p	0.0048		
IP20666p	0.016		

7.2 Further proteins of the BucLoc interactome

Further BucLoc interacting proteins, not included in the list of 213 proteins, are interesting potential Buc interaction partners.

Table 16: Further Buc interacting proteins. List is an excerpt of the full list with 3464 proteins identified by mass spectrometry analysis (Core Facility of Proteome Analysis, UMG, Goettingen).

Identified Protein	Accession Number	eGFP Co-IP	Buc-GFP Co-IP	BucLoc-eGFP Co-IP
3'-5' exoribonuclease CSL4 homolog	gi 224495967	0	21.2	4.4
Exosome complex exonuclease RRP40	gi 71480074	0	10.2	4.5
Exosome complex exonuclease RRP41	gi 41152247	0	12.4	4.5
Exosome component 5	gi 112419436 (+1)	0	14.1	3.7
Cluster of myosin-9	gi 319655760 [7]	53.8	54.3	866.1
Cluster of myosin, light chain 12, genome duplicate 2	gi 194578861 [2]	0	2.5	27.3
Myosin regulatory light chain 12B	gi 47550703	0	0	22.4
PREDICTED: myosin, light chain 6, alkali, smooth muscle and non-muscle isoform X2	gi 528482978	4.3	10.7	23.6
Bucky ball	gi 377550362	60.1	118.6	33.8
Cluster of PREDICTED: probable ATP-dependent RNA helicase DDX4 isoform X1	gi 528491414 [3]	159.3	542.7	136.2
Cytoplasmic dynein 1 heavy chain 1	gi 112363126	0	0	1296.9

7.3 213 BucLoc interaction candidates

213 BucLoc interaction candidates selected from the total list of 3464 proteins by applying selection criteria (Chapter 3.3.1.1).

Table 17: 213 BucLoc interaction candidates selected from 3464 proteins identified by mass spectrometry analysis. Candidates were chosen according to the indicated criteria (Chapter 3.3.1.1). Proteins are sorted by descending counts in BucLoc-eGFP. Mass spectrometry analysis was done at the Core Facility of Proteome Analysis, UMG, Goettingen.

Identified Protein	Accession Number	eGFP Co-IP	Buc-GFP Co-IP	BucLoc-eGFP Co-IP
PREDICTED: protein PRRC2C [Danio rerio]	gi 528511146	79.6	1278.6	817.9
PREDICTED: zinc finger protein 318-like isoform X1 [Danio rerio]	gi 528497145	12.4	666.7	512.8
Cluster of PREDICTED: protein PRRC2B isoform X4 [Danio rerio] (gi 528481247)	gi 528481247 [2]	22.6	480.1	320.0
large proline-rich protein BAT2 [Danio rerio]	gi 319738640 (+2)	71.6	362.1	280.0
PREDICTED: msx2-interacting protein isoform X1 [Danio rerio]	gi 326678004 (+2)	63.3	434.0	257.4
PREDICTED: microtubule-actin cross-linking factor 1, isoforms 1/2/3/5 isoform X1 [Danio rerio]	gi 528510265	0.0	546.5	218.8
uncharacterized protein LOC792544 [Danio rerio]	gi 194353937	15.8	83.1	201.9
Cluster of PREDICTED: OTU domain-containing protein 4 isoformX1 [Danio rerio] (gi 528518829)	gi 528518829 [2]	83.8	417.6	189.9
PREDICTED: YLP motif-containing protein 1 isoform X2 [Danio rerio]	gi 528511017	36.9	232.6	185.5
PREDICTED: symplekin isoform X2 [Danio rerio]	gi 326668188 (+1)	52.9	218.7	184.5
PREDICTED: microtubule-associated protein futsch-like [Danio rerio]	gi 528497151	1.7	123.8	181.0
retinoblastoma-binding protein 6 isoform 1 [Danio rerio]	gi 302632528 (+4)	13.0	75.0	159.1
Cluster of PREDICTED: membrane-associated guanylate kinase, WW and PDZ domain-containing protein 1 [Danio rerio] (gi 528488944)	gi 528488944 [4]	62.6	191.7	157.7
guanine nucleotide-binding protein subunit beta-2-like 1 [Danio rerio]	gi 18859301	53.1	208.3	149.1
PREDICTED: uncharacterized protein LOC767754 isoform X1 [Danio rerio]	gi 528467168 (+2)	45.1	104.3	134.7
Cluster of eukaryotic translation initiation factor 4A, isoform 1A [Danio rerio] (gi 38198643)	gi 38198643 [3]	43.2	230.2	127.8
PERQ amino acid-rich with GYF domain-containing protein 2 [Danio rerio]	gi 71834468	55.0	261.2	123.5
Cluster of zinc finger CCCH domain-containing protein 13 [Danio rerio] (gi 319738618)	gi 319738618	39.2	118.6	120.6
Cluster of PREDICTED: cell cycle associated protein 1b isoform X1 [Danio rerio] (gi 528508316)	gi 528508316 [3]	39.1	262.3	117.6
Cluster of PREDICTED: eukaryotic	gi 528482894 [2]	6.5	204.5	114.7

translation initiation factor 4E transporter isoform X1 [Danio rerio] (gi 528482894)				
PREDICTED: cytoskeleton-associated protein 5 isoform X1 [Danio rerio]	gi 528520895	2.9	71.0	110.6
regulation of nuclear pre-mRNA domain containing 2a [Danio rerio]	gi 41053979	0.0	65.7	96.8
Cluster of LIM domain only 7b [Danio rerio] (gi 319996634)	gi 319996634 [2]	5.5	182.2	89.9
GPI-anchored membrane protein 1 [Danio rerio]	gi 51011059	17.0	206.9	89.8
PREDICTED: trinucleotide repeat-containing gene 6B protein [Danio rerio]	gi 528495941	0.0	130.1	84.6
Cluster of glutathione S-transferase pi [Danio rerio] (gi 18858197)	gi 18858197	7.1	32.3	82.7
Cluster of PREDICTED: pyrroline-5-carboxylate reductase isoform X1 [Danio rerio] (gi 528495079)	gi 528495079 [2]	28.1	108.1	81.0
ATP synthase subunit O, mitochondrial [Danio rerio]	gi 51467909	4.7	21.0	76.8
pre-mRNA cleavage complex 2 protein Pcf11 [Danio rerio]	gi 55925534	0.9	100.4	75.3
PREDICTED: DNA-directed RNA polymerase II subunit RPB1 isoform X2 [Danio rerio]	gi 528496057 (+1)	0.0	58.5	72.8
Cluster of ataxin-2 [Danio rerio] (gi 190358425)	gi 190358425 [2]	30.9	149.0	70.6
5'-3' exoribonuclease 1 [Danio rerio]	gi 289577074 (+1)	1.4	114.6	65.5
voltage-dependent anion-selective channel protein 2 [Danio rerio]	gi 41054601 (+1)	16.5	33.7	65.5
Cluster of splicing factor 45 [Danio rerio] (gi 41055474)	gi 41055474 [2]	13.5	132.2	57.6
voltage-dependent anion-selective channel protein 1 [Danio rerio]	gi 47777306	17.5	42.1	57.0
PREDICTED: protein FAM208A [Danio rerio]	gi 528517763	1.9	70.5	54.5
single-stranded DNA-binding protein, mitochondrial [Danio rerio]	gi 62955585	11.5	24.0	54.4
PREDICTED: tyrosine 3-monooxygenase/tryptophan 5-monooxygenase activation protein, zeta polypeptide isoform X1 [Danio rerio]	gi 528509453	3.6	13.6	53.7
non-POU domain-containing octamer-binding protein [Danio rerio]	gi 42415509	23.4	96.3	52.9
Cluster of PREDICTED: fish-egg lectin isoform X1 [Danio rerio] (gi 528491480)	gi 528491480 [5]	7.2	64.2	52.2
alpha-2-macroglobulin-like precursor [Danio rerio]	gi 320118891	0.0	17.3	50.3
Cluster of PREDICTED: chromodomain helicase DNA binding protein 4 isoform X1 [Danio rerio] (gi 528509046)	gi 528509046 [4]	1.7	30.1	49.5
14-3-3 protein epsilon [Danio rerio]	gi 47086819	4.6	12.4	47.8
Cluster of uncharacterized protein LOC100141336 precursor [Danio rerio] (gi 168823478)	gi 168823478 [5]	11.2	41.2	47.5
PREDICTED: protein SCAF11 isoform X1 [Danio rerio]	gi 528475676 (+2)	0.9	52.1	45.5

PREDICTED: cytoplasmic dynein 2 heavy chain 1-like, partial [Danio rerio]	gi 528502710	20.8	42.4	44.2
Cluster of PREDICTED: pericentriolar material 1 protein isoform X7 [Danio rerio] (gi 528467744)	gi 528467744 [3]	1.7	12.9	44.1
alpha-2-macroglobulin-like [Danio rerio]	gi 319655740 (+2)	2.9	18.7	43.1
PREDICTED: ubiquitin carboxyl-terminal hydrolase 10 isoformX1 [Danio rerio]	gi 326669691	1.0	138.2	42.9
PREDICTED: cleavage stimulation factor subunit 2-like isoform X1 [Danio rerio]	gi 326673799	11.3	86.7	40.3
Cluster of PREDICTED: alpha-2-macroglobulin isoformX1 [Danio rerio] (gi 326665588)	gi 326665588 [2]	8.9	60.0	39.8
PREDICTED: eukaryotic translation initiation factor 4 gamma 3 [Danio rerio]	gi 528517986	3.0	151.5	39.8
Ndufa9 protein [Danio rerio]	gi 157423514 (+2)	9.6	22.4	39.6
Zgc:158157 protein [Danio rerio]	gi 55250357	0.0	63.4	39.5
Cluster of myosin light chain alkali, smooth-muscle isoform [Danio rerio] (gi 47174755)	gi 47174755 [6]	8.7	17.3	39.1
Cluster of PREDICTED: uncharacterized protein LOC100000125 isoform X2 [Danio rerio] (gi 528510415)	gi 528510415 [3]	6.1	103.3	38.8
signal-induced proliferation-associated 1-like protein 1 [Danio rerio]	gi 529250122	2.8	31.4	38.7
eukaryotic translation initiation factor 4E-1B [Danio rerio]	gi 18858611	11.8	92.6	37.4
Cycl1 protein [Danio rerio]	gi 51327354 (+1)	11.5	32.9	35.8
complement component 1 Q subcomponent-binding protein, mitochondrial [Danio rerio]	gi 324021711 (+1)	9.0	19.2	35.8
LOC449616 protein [Danio rerio]	gi 213624848 (+2)	0.0	92.5	35.8
PREDICTED: cyclin-dependent kinase 13 [Danio rerio]	gi 326679472	5.8	67.7	33.7
Cluster of CWF19-like protein 2 [Danio rerio] (gi 76253886)	gi 76253886 [2]	0.0	28.5	32.6
nanog homeobox [Danio rerio]	gi 528505177 (+1)	3.9	60.8	32.4
PREDICTED: zinc finger CCCH domain-containing protein 4-like isoform X1 [Danio rerio]	gi 528501822	0.0	18.3	31.6
Cluster of PREDICTED: unconventional myosin-Va [Danio rerio] (gi 326680074)	gi 326680074 [4]	3.7	20.9	31.4
PREDICTED: protein FAM208A-like [Danio rerio]	gi 528516938	0.0	23.0	31.2
glutamate dehydrogenase 1b [Danio rerio]	gi 41282194	0.0	27.4	31.0
S-phase kinase-associated protein 1 [Danio rerio]	gi 41152201	14.5	29.8	30.8
PREDICTED: tyrosine-protein phosphatase non-receptor type 13 isoform X1 [Danio rerio]	gi 528513092 (+4)	6.4	107.4	30.7
Cluster of ADP-ribosylation factor 1 like [Danio rerio] (gi 41393117)	gi 41393117 [2]	0.0	11.2	30.1

Si:dkey-16k6.1 protein [Danio rerio]	gi 45767805 (+1)	2.4	7.8	29.8
Cluster of ras homolog gene family, member Ad [Danio rerio] (gi 50539958)	gi 50539958 [3]	1.2	16.1	29.4
tight junction protein ZO-2 isoform 1 [Danio rerio]	gi 320118869 (+2)	0.0	13.5	29.2
Cluster of uncharacterized protein LOC569235 precursor [Danio rerio] (gi 350536793)	gi 350536793 [3]	13.0	42.7	29.2
ATP-dependent RNA helicase DDX42 [Danio rerio]	gi 302318882	0.0	73.3	27.9
Cluster of PREDICTED: hypothetical protein LOC565404 [Danio rerio] (gi 189517232)	gi 189517232 [5]	6.7	58.2	27.5
PREDICTED: telomerase-binding protein EST1A-like isoform X1 [Danio rerio]	gi 326671361 (+1)	0.0	90.3	27.4
PREDICTED: ATP synthase subunit b, mitochondrial isoform X1 [Danio rerio]	gi 528487650 (+1)	3.5	9.1	27.1
mitochondrial import inner membrane translocase subunit Tim13 [Danio rerio]	gi 50539998	0.0	10.2	26.9
PREDICTED: RNA-binding protein 27 isoform X2 [Danio rerio]	gi 528491090 (+1)	5.8	32.9	26.7
PREDICTED: nudC domain-containing protein 1 isoform X1 [Danio rerio]	gi 528509803	2.7	11.2	26.6
regulation of nuclear pre-mRNA domain-containing protein 1B [Danio rerio]	gi 41054665 (+3)	0.0	63.3	25.4
nuclear pore complex protein Nup133 [Danio rerio]	gi 47087231	0.0	8.9	25.1
PREDICTED: RNA-binding protein 6 isoform X1 [Danio rerio]	gi 528483145	0.0	25.4	24.6
Cluster of PREDICTED: RNA-binding protein 26 [Danio rerio] (gi 528481486)	gi 528481486 [2]	2.5	30.2	24.6
glutamate dehydrogenase 1a [Danio rerio]	gi 47086875	0.0	11.1	24.5
Cluster of Bub3 protein [Danio rerio] (gi 53734038)	gi 53734038 [2]	3.2	16.2	23.8
Cluster of PREDICTED: cat eye syndrome critical region protein 2 isoform X2 [Danio rerio] (gi 528521383)	gi 528521383 [2]	0.0	46.3	23.6
LYR motif-containing protein 4 [Danio rerio]	gi 256000753	0.0	7.7	23.4
mitochondrial inner membrane protein [Danio rerio]	gi 47777298 (+1)	3.5	15.4	22.5
Abcf2 protein [Danio rerio]	gi 42542861 (+1)	7.3	27.2	22.5
DNA-directed RNA polymerase II subunit RPB2 [Danio rerio]	gi 302488402	0.0	33.2	22.5
Cluster of SNW domain-containing protein 1 [Danio rerio] (gi 50838798)	gi 50838798	7.9	39.3	22.4
PREDICTED: NFX1-type zinc finger-containing protein 1-like [Danio rerio]	gi 528483584	5.8	39.3	22.4
periphilin-1 [Danio rerio]	gi 121583944 (+1)	1.4	33.7	22.3
PREDICTED: unconventional myosin-IXa isoform X1 [Danio rerio]	gi 528486090 (+1)	0.0	56.0	22.2
PREDICTED: histone-lysine N-methyltransferase SETD1A isoform X1 [Danio rerio]	gi 326666050	0.0	38.1	21.9
PREDICTED: death-inducer obliterator	gi 528516988	0.0	59.7	21.9

1-like [Danio rerio]				
Cluster of LOC100000597 protein [Danio rerio] (gi 66910514)	gi 66910514 [5]	0.0	10.2	21.7
dolichyl-diphosphooligosaccharide--protein glycosyltransferase subunit DAD1 [Danio rerio]	gi 154426290	0.0	10.2	21.1
protein QIL1 [Danio rerio]	gi 113678245	4.2	10.2	21.1
PREDICTED: E3 ubiquitin-protein ligase TTC3 isoform X2 [Danio rerio]	gi 528491184	2.8	70.6	21.0
serine/threonine-protein phosphatase 2A 56 kDa regulatory subunit delta isoform [Danio rerio]	gi 50726892	0.0	5.5	20.9
cytochrome b-c1 complex subunit Rieske, mitochondrial [Danio rerio]	gi 157073897	0.0	6.1	20.7
Cluster of Protein regulator of cytokinesis 1 [Danio rerio] (gi 28279644)	gi 28279644 [2]	7.5	61.7	20.4
PREDICTED: E3 ubiquitin-protein ligase HERC2, partial [Danio rerio]	gi 528483182	0.0	8.5	20.0
Cluster of LOC563225 protein [Danio rerio] (gi 115292012)	gi 115292012 [2]	7.9	17.8	19.7
Cluster of eukaryotic translation initiation factor 4B [Danio rerio] (gi 47550837)	gi 47550837 [6]	0.0	41.9	19.6
high mobility group protein B2 [Danio rerio]	gi 82658290	0.9	5.7	19.4
IcIn protein [Danio rerio]	gi 44890532 (+2)	7.6	23.6	19.3
nuclear pore complex protein Nup160 [Danio rerio]	gi 41054908	0.0	5.3	19.3
Cluster of TNF receptor-associated protein 1 [Danio rerio] (gi 165972373)	gi 165972373 [2]	0.0	71.3	18.8
Cluster of PREDICTED: microtubule-associated serine/threonine-protein kinase 3-like [Danio rerio] (gi 528470977)	gi 528470977 [2]	0.0	25.5	18.8
M-phase phosphoprotein 8 [Danio rerio]	gi 187607764	2.4	42.2	18.7
PREDICTED: PHD finger protein 3 isoform X1 [Danio rerio]	gi 528498598 (+1)	0.0	18.4	18.5
PREDICTED: sideroflexin-3 isoform X1 [Danio rerio]	gi 528497698	1.9	7.2	18.2
Cluster of Epithelial cell adhesion molecule [Danio rerio] (gi 44890710)	gi 44890710 [2]	1.8	13.9	18.0
Sept2 protein [Danio rerio]	gi 115313325 (+3)	0.0	13.3	17.6
Cluster of PREDICTED: regulation of nuclear pre-mRNA domain-containing protein 2 isoform X1 [Danio rerio] (gi 528502856)	gi 528502856 [2]	0.0	12.6	17.5
Zgc:77560 protein [Danio rerio]	gi 42542976 (+1)	2.4	66.6	17.4
Cluster of PREDICTED: nucleolar pre-ribosomal-associated protein 1-like [Danio rerio] (gi 528501168)	gi 528501168 [2]	2.9	20.9	17.3
ras-related protein Rab-14 [Danio rerio]	gi 41393147	0.0	5.1	16.8
NADH dehydrogenase [ubiquinone] 1 beta subcomplex subunit 10 [Danio rerio]	gi 41152268	3.5	17.2	16.8
Cluster of oxoglutarate (alpha-ketoglutarate) dehydrogenase (lipoamide) [Danio rerio]	gi 254028264 [2]	0.0	5.6	16.6

(gi 254028264)				
Pard3 protein [Danio rerio]	gi 190339230 (+4)	0.9	32.3	16.6
DNA-directed RNA polymerase II subunit RPB3 [Danio rerio]	gi 269784633	0.0	22.8	16.3
RecName: Full=Protein CASC3; AltName: Full=Cancer susceptibility candidate gene 3 protein homolog; AltName: Full=Metastatic lymph node protein 51 homolog; Short=DrMLN51; Short=Protein MLN 51 homolog	gi 123886565 (+1)	6.3	28.9	16.1
Cluster of serine/threonine kinase 36 (fused homolog, Drosophila) [Danio rerio] (gi 320043268)	gi 320043268	6.0	13.9	16.0
cytotoxic granule-associated RNA binding protein 1 [Danio rerio]	gi 47086779	6.4	16.9	16.0
Cluster of PREDICTED: uncharacterized protein LOC393431 isoform X1 [Danio rerio] (gi 528486792)	gi 528486792	0.0	9.1	16.0
Cluster of nuclear receptor corepressor 2 [Danio rerio] (gi 380420327)	gi 380420327 [4]	0.0	57.7	15.9
Cas-Br-M (murine) ecotropic retroviral transforming sequence-like 1 [Danio rerio]	gi 41055074	3.3	20.8	15.7
PREDICTED: polyribonucleotide 5'-hydroxyl-kinase Clp1-like [Danio rerio]	gi 189528302	0.0	53.2	15.4
uncharacterized protein LOC556124 [Danio rerio]	gi 157909776	1.4	30.5	15.2
succinate dehydrogenase [ubiquinone] iron-sulfur subunit, mitochondrial precursor [Danio rerio]	gi 148922926	5.4	11.3	14.9
Cluster of cAMP-dependent protein kinase catalytic subunit alpha [Danio rerio] (gi 130493522)	gi 130493522 [3]	0.0	8.8	14.9
serine/threonine-protein kinase 3 [Danio rerio]	gi 41054445 (+1)	3.6	49.0	14.8
uncharacterized protein LOC541537 [Danio rerio]	gi 62122901	0.0	7.4	14.6
chromodomain-helicase-DNA-binding protein 8 [Danio rerio]	gi 320461545 (+2)	0.0	22.7	14.6
PREDICTED: splicing factor, arginine/serine-rich 15 [Danio rerio]	gi 528492333	0.0	20.4	14.4
zinc finger HIT domain-containing protein 3 [Danio rerio]	gi 41053670	3.5	33.1	14.0
eukaryotic translation initiation factor 6 [Danio rerio]	gi 41055624 (+2)	0.0	9.1	13.9
PREDICTED: nuclear pore complex protein Nup153 isoform X1 [Danio rerio]	gi 528510621	0.0	17.5	13.7
PREDICTED: uncharacterized protein LOC436879 isoform X4 [Danio rerio]	gi 528517594	0.0	11.1	13.3
Zgc:111960 protein [Danio rerio]	gi 166796880	0.0	11.6	13.2
very low-density lipoprotein receptor precursor [Danio rerio]	gi 169646705 (+4)	0.0	5.1	13.0
C-terminal binding protein 1 [Danio rerio]	gi 40254690	3.3	11.6	12.9
claudin-like protein ZF-A89 [Danio rerio]	gi 30725822	0.0	5.2	12.8
Cluster of PREDICTED: C2 domain-	gi 528501432	0.0	9.2	12.7

containing protein 3 [Danio rerio] (gi 528501432)				
PREDICTED: histone deacetylase 1 isoform X1 [Danio rerio]	gi 528510099	2.6	29.6	12.0
peptidyl-prolyl cis-trans isomerase-like 1 [Danio rerio]	gi 77683061	1.9	18.6	11.9
Cluster of ras-related C3 botulinum toxin substrate 1 [Danio rerio] (gi 54792776)	gi 54792776 [2]	3.5	11.7	11.9
PREDICTED: uncharacterized protein KIAA0556-like [Danio rerio]	gi 528520519	0.0	14.9	11.8
PREDICTED: trinucleotide repeat-containing gene 6B protein-like isoform X2 [Danio rerio]	gi 528472879 (+1)	0.0	23.4	11.7
nuclear pore complex protein Nup107 [Danio rerio]	gi 71834480	1.8	6.9	11.3
Cluster of PREDICTED: tight junction protein ZO-1-like [Danio rerio] (gi 528521995)	gi 528521995	0.0	12.5	11.3
DIS3-like exonuclease 1 [Danio rerio]	gi 160333118	0.0	32.6	11.3
PREDICTED: PAB-dependent poly(A)-specific ribonuclease subunit 2-like isoform X2 [Danio rerio]	gi 528518391 (+1)	0.0	13.3	11.2
Cluster of PREDICTED: PERQ amino acid-rich with GYF domain-containing protein 1-like isoform X1 [Danio rerio] (gi 528492127)	gi 528492127 [2]	0.0	13.3	11.2
uncharacterized protein LOC550263 [Danio rerio]	gi 62955177	0.0	14.9	11.2
Cluster of PREDICTED: serine/threonine-protein kinase TAO2-like [Danio rerio] (gi 125812164)	gi 125812164	0.0	17.9	10.7
PREDICTED: uncharacterized protein LOC503771 isoform X3 [Danio rerio]	gi 528519733	0.0	17.1	10.6
Cluster of LOC559853 protein, partial [Danio rerio] (gi 79151969)	gi 79151969 [2]	0.0	38.9	10.4
PREDICTED: serine/threonine-protein kinase LATS1 isoform X1 [Danio rerio]	gi 528510786	0.0	20.4	10.2
PREDICTED: cyclin-dependent kinase 12 [Danio rerio]	gi 528509066	0.9	29.5	10.0
poly(rC)-binding protein 2 [Danio rerio]	gi 41055221	0.0	12.7	9.9
nanog homeobox [Danio rerio]	gi 148357118	0.0	28.5	9.9
Cluster of TIA1 cytotoxic granule-associated RNA binding protein [Danio rerio] (gi 37681959)	gi 37681959 [4]	4.8	33.1	9.9
protein mago nashi homolog [Danio rerio]	gi 62955377	3.8	15.8	9.8
nucleoporin 98 [Danio rerio]	gi 320118905 (+1)	0.0	7.5	9.7
uncharacterized protein LOC100126100 precursor [Danio rerio]	gi 157954446 (+1)	2.9	22.5	9.7
N-acetyltransferase 10 [Danio rerio]	gi 41055301	4.7	15.0	9.7
OCIA domain-containing protein 1 [Danio rerio]	gi 41053513 (+1)	0.0	5.8	9.5
cytochrome c oxidase subunit II [Danio rerio]	gi 8395615	2.4	5.1	9.5
PREDICTED: transcription factor 19 [Danio rerio]	gi 292624089	0.0	17.6	9.4
signal recognition particle 9 [Danio rerio]	gi 41055367	0.0	5.1	9.4

actin related protein 2/3 complex subunit 4 [Danio rerio]	gi 45387521	0.0	7.4	9.1
PREDICTED: lysine-specific demethylase 6A isoform X1 [Danio rerio]	gi 528490350 (+1)	0.0	26.6	8.8
exosome complex exonuclease RRP4 [Danio rerio]	gi 339717151	2.9	22.8	8.8
PREDICTED: bromodomain adjacent to zinc finger domain, 2A isoform X1 [Danio rerio]	gi 528517226 (+1)	0.0	8.0	8.7
PREDICTED: AF4/FMR2 family member 4 isoform X1 [Danio rerio]	gi 528514500 (+3)	2.6	13.3	8.6
Cluster of PREDICTED: kinesin family member 13A [Danio rerio] (gi 528505240)	gi 528505240 [5]	0.0	5.4	8.4
exosome complex exonuclease RRP45 [Danio rerio]	gi 54400656	0.0	20.2	8.4
exosome complex component MTR3 [Danio rerio]	gi 66472734	1.0	14.4	8.1
MGC174638 protein [Danio rerio]	gi 156230391 (+2)	0.0	7.8	8.0
Cluster of cyclin-L1 [Danio rerio] (gi 41054323)	gi 41054323	3.6	13.3	7.7
Xrcc5 protein [Danio rerio]	gi 133777834	0.0	12.9	7.7
sorting and assembly machinery component 50 homolog B [Danio rerio]	gi 55925219	0.0	5.2	7.4
Cluster of PREDICTED: rho GTPase-activating protein 21 isoform X1 [Danio rerio] (gi 528470502)	gi 528470502 [2]	0.0	10.9	7.4
60S ribosomal protein L29 [Danio rerio]	gi 51010951	2.9	11.6	7.1
immediate early response 3-interacting protein 1 precursor [Danio rerio]	gi 356991159	0.0	5.1	7.0
transmembrane and coiled-coil domains 1 [Danio rerio]	gi 50540216 (+1)	1.9	8.7	7.0
PREDICTED: wu:fc48e01 [Danio rerio]	gi 125820176	0.0	18.4	6.8
Zgc:123096 protein, partial [Danio rerio]	gi 50417024 (+1)	0.0	6.1	6.6
PREDICTED: protein TANC1-like isoform X2 [Danio rerio]	gi 528481904 (+1)	0.0	9.1	6.4
Centrin2 [Danio rerio]	gi 161213715 (+1)	1.9	14.9	6.3
PREDICTED: dehydrogenase/reductase SDR family member 7B isoform X1 [Danio rerio]	gi 528473478	0.0	10.8	6.3
cyclin T2b [Danio rerio]	gi 47086855	2.7	16.8	6.3
U4/U6.U5 tri-snRNP-associated protein 1 [Danio rerio]	gi 50540414	0.0	15.6	5.9
PREDICTED: uveal autoantigen with coiled-coil domains and ankyrin repeats [Danio rerio]	gi 292616084 (+1)	0.0	6.6	5.9
C-Myc-binding protein [Danio rerio]	gi 91176306	0.0	15.4	5.9
transcription elongation factor B polypeptide 1 [Danio rerio]	gi 52219182 (+1)	0.0	7.7	5.9
Cluster of cytochrome c oxidase assembly factor 5 [Danio rerio] (gi 238859533)	gi 238859533	0.0	5.1	5.9
PREDICTED: uncharacterized protein DKFZp762I1415-like [Danio rerio]	gi 68399071	0.0	5.1	5.9
Ku70 autoantigen [Danio rerio]	gi 114215700 (+2)	1.6	7.4	5.7

uncharacterized protein LOC100216070 [Xenopus (Silurana) tropicalis]	gi 213983243 (+1)	0.0	11.3	5.6
RNA-binding protein 8A [Danio rerio]	gi 61651846	2.4	9.0	5.6
G kinase anchoring protein 1 [Danio rerio]	gi 32451811 (+3)	0.0	17.8	5.6
PREDICTED: nuclear receptor coactivator 3 [Danio rerio]	gi 326671802	0.0	14.8	5.3
Cluster of PREDICTED: mps one binder kinase activator-like 1B-like [Danio rerio] (gi 292614396)	gi 292614396 [5]	0.0	9.1	5.1
coiled-coil-helix-coiled-coil-helix domain-containing protein 2, mitochondrial [Danio rerio]	gi 41152140	0.0	8.1	5.1
store-operated calcium entry-associated regulatory factor precursor [Danio rerio]	gi 115495791 (+2)	0.0	13.2	5.0

7.4 Digital appendix

For a full list of the 3464 proteins identified by mass spectrometry analysis please open the Excel file on the CD (Table 17). For the time lapse movie of transgenic buc gfp embryo, corresponding to Figure 12, please open the avi file on the CD (Figure 30).

Curriculum Vitae

Personal details

Name: Stephan Riemer
Day of birth: August 24th, 1983
Place of birth: Kirchheim unter Teck, Germany
Address: Arndtstr. 7, 37075 Göttingen, Germany
Email: stephan.riemer@med.uni-goettingen.de

Education

- 04/2011 – 10/2014 Doctoral studies, Department of Developmental Biochemistry,
Georg August University Göttingen
Title of PhD thesis: Analyzing the molecular mechanism of Bucky ball
localization during germ cell specification in zebrafish
Supervisor: Dr. Roland Dosch
GGNB Genes and Development
- 10/2004 – 12/2010 Studies of Technical Biology, University Stuttgart
Main Focus: Biochemistry, Molecular Biology, Technical Biochemistry
Diploma thesis, Institute of Microbiology, University Stuttgart
Title of diploma thesis: Installation of an alternative glycerol pathway
in Escherichia coli via the glycerol dehydrogenase GldA and the
dihydroxyacetone kinase DhaK_{Eb} of Escherichia blattae
Supervisor: Prof. Dr. Georg Sprenger
- 08/2003 – 05/2004 Civilian service, AMSEL, Wernau
- 09/1994 – 08/2003 Abitur, Schloßgymnasium, Kirchheim unter Teck

